

BSIM-CMG 106.0.0

Multi-Gate MOSFET Compact Model

Technical Manual

Authors:
Sriramkumar V., Navid Paydavosi,
Darsen Lu, Chung-Hsun Lin,
Mohan Dunga, Shijing Yao, Tanvir Morshed,
Ali Niknejad, and Chenming Hu

Project Director:
Prof. Ali Niknejad and Prof. Chenming Hu

**Department of Electrical Engineering and Computer Sciences
University of California, Berkeley, CA 94720**

**Copyright 2012
The Regents of University of California
All Right Reserved**

Nondisclosure Statement

The content of BSIM-CMG model (including source code, manual, technical note, and equation list) is currently distributed by BSIM Group, a research group at EECS Department, University of California at Berkeley, to designated Receiving Parties only.

The content of BSIM-CMG model can not be distributed by Receiving Party to any third party without written agreement by BSIM Group.

Contents

1	Introduction	5
2	Model Description	5
3	BSIM-CMG 106.0.0 Model Equations	7
3.1	Bias Independent Calculations	7
3.2	Terminal Voltages	16
3.3	Short Channel Effects	16
3.4	Surface Potential Calculation	17
3.5	Drain Saturation Voltage	24
3.6	Average Potential, Charge and Related Variables	27
3.7	Quantum Mechanical Effects	27
3.8	Mobility degradation and series resistance	29
3.9	Output Conductance	30
3.10	Velocity Saturation	31
3.11	Drain Current Model	32
3.12	Intrinsic Capacitance Model	33
3.13	Parasitic resistances and capacitance models	36
3.14	Impact Ionization and GIDL/GISL Model	51
3.15	Gate Tunneling Current	53
3.16	Non Quasi-static Models	56
3.17	Generation-recombination Component	60
3.18	Junction Current and capacitances	60
3.19	Self-heating model	68
3.20	Noise Models	69
4	Simulation Outputs	72

5 Parameter Extraction Procedure	73
5.1 Global Parameter Extraction	73
5.1.1 Basic Device Parameter List	73
5.1.2 Parameter Initialization	75
5.1.3 Linear region	78
5.1.4 Saturation region	82
5.1.5 Other Parameters representing important physical effects	83
5.1.6 Smoothing between Linear and Saturation regions	83
5.1.7 Other Effects	84
6 Complete Parameter List	86
6.1 Instance Parameters	86
6.2 Model Controllers and Process Parameters	87
6.3 Basic Model Parameters	91
6.4 Parameters for geometry-dependent parasitics	100
6.5 Parameters for Temperature Dependence and Self-heating	102
6.6 Parameters for Variability Modeling	104
7 History of BSIM-MG Models	105

1 Introduction

The continuous evolution and enhancement of planar bulk CMOS technology has fueled the growth of the microelectronics industry for the past several decades. When we reach the end of the technology roadmap for the classical CMOS, multiple gate MOSFETs (MuGFETs) will likely take up the baton. We have developed a multiple gate MOSFET compact model for technology/circuits development in the short term and for product design in the longer term [1].

Several different MuGFET structures and two different modes of operation are being pursued in the industry today. In the case of horizontal double gate (DG), the two gates will likely be asymmetric— having different work functions and underlying dielectric thicknesses, complicating the compact model. Also, the two gates are likely to be biased at two different voltages, known as independent gates. In the other double, triple, or all-around gate cases, the gates are biased at the same voltage, known as the common gate. Some designs will use lightly doped body to maximize mobility, others will use very high doping concentrations in thin body to obtain sufficient V_t adjustment.

BSIM-CMG has been developed to model the electrical characteristics of MG structures. The details of the model will be described in this document. It will serve the needs of all circuit designer/ technology developers by providing versatility without compromising ease of use and computational efficiency. The model currently addresses common gate devices. A separate model BSIM-IMG addresses independent gate devices [2].

2 Model Description

BSIM-CMG is implemented in Verilog-A. Physical surface-potential-based formulations are derived for both intrinsic and extrinsic models with finite body doping. The surface potentials at the source and drain ends are solved analytically with poly-depletion and quantum mechanical effects. The effect of finite body doping is captured through a perturbation approach. The analytic surface potential solution agrees with 2-D device simulation results well. If the channel doping concentration is low enough to be neglected, computational efficiency can be further improved by setting COREMOD = 1.

All the important MG transistor behaviors are captured by this model. Volume inversion is included in the solution of the Poisson's equation, hence the subsequent I-V

formulation automatically captures the volume inversion effect. Analysis of the electrostatic potential in the body of MG MOSFETs provided the model equation for the short channel effects (SCE). The extra electrostatic control from the end-gates (top/bottom gates) (triple or quadruple-gate) is also captured in the short channel model.

Users can specify the MG structure of interest via a geometry mode selector (GE-OMOD, DG = 0, TG = 1, QG = 2, CG = 3). Hybrid-surface-orientation mobility, corner-induced effective width reduction, and end-channel-enhanced electrostatic control are considered to address the physics of tri-gate (TG) and quadruple-gate (QG) devices.

BSIM-CMG provides the flexibility to model devices with novel materials. This includes parameters for non-silicon channel devices and High-K/ Metal-gate stack.

Other important effects, such as, mobility degradation, velocity saturation, velocity overshoot, series resistance, channel length modulation, quantum mechanical effects, gate tunneling current, gate-induced-drain-leakage, temperature effects, channel thermal noise, flicker noise, noise associated with device parasitics, and parasitic capacitance, are also incorporated in the model.

BSIM-CMG has been verified with industrial experimental data. The model is continuous and symmetric at $V_{ds} = 0$. This physics-based model is scalable and predictive over a wide range of device parameters.

3 BSIM-CMG 106.0.0 Model Equations

3.1 Bias Independent Calculations

Physical Constants

Physical quantities in BSIM-CMG are in M.K.S units unless specified otherwise.

$$q = 1.6 \times 10^{-19} \quad (3.1)$$

$$\epsilon_0 = 8.8542 \times 10^{-12} \quad (3.2)$$

$$\hbar = 1.05457 \times 10^{-34} \quad (3.3)$$

$$m_e = 9.11 \times 10^{-31} \quad (3.4)$$

$$k = 1.3787 \times 10^{-23} \quad (3.5)$$

$$\epsilon_{sub} = EPSRSUB \cdot \epsilon_0 \quad (3.6)$$

$$\epsilon_{ox} = EPSROX \cdot \epsilon_0 \quad (3.7)$$

$$C_{ox} = \frac{3.9 \cdot \epsilon_0}{EOT} \quad (3.8)$$

$$C_{si} = \frac{\epsilon_{sub}}{TFIN} \quad (3.9)$$

$$\epsilon_{ratio} = \frac{EPSRSUB}{3.9} \quad (3.10)$$

Effective Channel Width, Channel Length and Fin Number

$$\Delta L = LINT + \frac{LL}{(L + XL)^{LLN}} \quad (3.11)$$

$$\Delta L_{CV} = DLC + \frac{LLC}{(L + XL)^{LLN}} \quad (3.12)$$

$$L_{eff} = L + XL - 2\Delta L \quad (3.13)$$

$$L_{eff,CV} = L + XL - 2\Delta L_{CV} \quad (3.14)$$

If $GEOMOD = 0$ then

$$W_{eff0} = 2 \cdot HFIN - DELTAW \quad (3.15)$$

$$W_{eff,CV0} = 2 \cdot HFIN - DELTAWCV \quad (3.16)$$

If $GEOMOD = 1$ then

$$W_{eff0} = 2 \cdot HFIN + FECH \cdot TFIN - DELTAW \quad (3.17)$$

$$W_{eff,CV0} = 2 \cdot HFIN + FECH \cdot TFIN - DELTAWCV \quad (3.18)$$

If $GEOMOD = 2$ then

$$W_{eff0} = 2 \cdot HFIN + 2 \cdot FECH \cdot TFIN - DELTAW \quad (3.19)$$

$$W_{eff,CV0} = 2 \cdot HFIN + 2 \cdot FECH \cdot TFIN - DELTAWCV \quad (3.20)$$

If $GEOMOD = 3$ then

$$R = \frac{D}{2} \quad (3.21)$$

$$W_{eff0} = \pi \cdot D - DELTAW \quad (3.22)$$

$$W_{eff,CV0} = \pi \cdot D - DELTAWCV \quad (3.23)$$

$$NFIN_{total} = NFIN \times NF \quad (3.24)$$

Geometry-dependent source/drain resistance

Please refer to section 3.13.

Quantum Mechanical Effects

The following bias-independent calculations are for the threshold voltage shift and bias dependence of inversion charge centroid due to quantum mechanical confinement. See section on 'Surface Potential Calculation' and 'Quantum Mechanical Effects' for more details.

$$m_x = 0.916 \cdot m_e \quad (3.25)$$

$$m'_x = 0.190 \cdot m_e \quad (3.26)$$

$$m_d = 0.190 \cdot m_e \quad (3.27)$$

$$m'_d = 0.417 \cdot m_e \quad (3.28)$$

$$g' = 4.0 \quad (3.29)$$

$$g = 2.0 \quad (3.30)$$

If $GEOMOD = 0$ then

$$MTcen = 1 + AQMTCEN \cdot \exp\left(-\frac{TFIN}{BQMTCEN}\right) \quad (3.31)$$

If $GEOMOD = 1$ then

$$MTcen = 1 + AQMTCEN \cdot \exp\left(-\frac{\min(HFIN, TFIN)}{BQMTCEN}\right) \quad (3.32)$$

If $GEOMOD = 2$ then

$$MTcen = 1 + AQMTCEN \cdot \exp\left(-\frac{\min(HFIN, TFIN)}{BQMTCEN}\right) \quad (3.33)$$

If $GEOMOD = 3$ then

$$MTcen = 1 + AQMTCEN \cdot \exp\left(-\frac{R}{BQMTCEN}\right) \quad (3.34)$$

Binning Calculations

The optional binning methodology [3] is adopted in BSIM-MG.

For a given L, NFIN, each model parameter $PARAM_i$ is calculate as a function of PARAM, a length dependent term, LPARAM, a number of fin per finger(NFIN) dependent term, NPARAM and a product $L \times NFIN$ term, PPARAM:

$$\begin{aligned} PARAM_i = & PARAM + \frac{10^{-6}}{L_{eff} + DLBIN} \cdot LPARAM + \frac{1.0}{NFIN} \cdot NPARAM + \\ & \frac{10^{-6}}{NFIN \cdot (L_{eff} + DLBIN)} \cdot PPARAM \end{aligned} \quad (3.35)$$

For the list of binable parameters, please refer to the complete parameter list in the end of this technical note.

Length scaling equations

$$U0[L] = \begin{cases} U0_i \cdot [1 - UP_i \cdot L_{eff}^{-LPA}] & LPA > 0 \\ U0_i \cdot [1 - UP_i] & \text{Otherwise} \end{cases} \quad (3.36)$$

$$MEXP[L] = MEXP_i + AMEXP \cdot L_{eff}^{-BMEXP} \quad (3.37)$$

$$PCLM[L] = PCLM_i + APCLM \cdot \exp\left(-\frac{L_{eff}}{BPCLM}\right) \quad (3.38)$$

$$UA[L] = UA_i + AUA \cdot \exp\left(-\frac{L_{eff}}{BUA}\right) \quad (3.39)$$

$$UD[L] = UD_i + AUD \cdot \exp\left(-\frac{L_{eff}}{BUD}\right) \quad (3.40)$$

(3.41)

If $RDSMOD = 0$ then

$$RDSW[L] = RDSW_i + ARDSW \cdot \exp\left(-\frac{L_{eff}}{BRDSW}\right) \quad (3.42)$$

If $RDSMOD = 1$ then

$$RSW[L] = RSW_i + ARSW \cdot \exp\left(-\frac{L_{eff}}{BRSW}\right) \quad (3.43)$$

$$RDW[L] = RDW_i + ARDW \cdot \exp\left(-\frac{L_{eff}}{BRDW}\right) \quad (3.44)$$

$$PTWG[L] = PTWG_i + APTWG \cdot \exp\left(-\frac{L_{eff}}{BPTWG}\right) \quad (3.45)$$

$$VSAT[L] = VSAT_i + AVSAT \cdot \exp\left(-\frac{L_{eff}}{BVSAT}\right) \quad (3.46)$$

$$VSAT1[L] = VSAT1_i + AVSAT1 \cdot \exp\left(-\frac{L_{eff}}{BVSAT1}\right) \quad (3.47)$$

Temperature Effects

$$T = \$temperature + DTEMP \quad (3.48)$$

$$E_{g,TNOM} = BG0SUB - \frac{TBGASUB \cdot TNOM^2}{TNOM + TBGBSUB} \quad (3.49)$$

$$E_g = BG0SUB - \frac{TBGASUB \cdot T^2}{T + TBGBSUB} \quad (3.50)$$

$$n_i = NI0SUB \cdot \left(\frac{T}{300.15} \right)^{\frac{3}{2}} \cdot \exp \left(\frac{BG0SUB \cdot q}{2k \cdot 300.15} - \frac{E_g \cdot q}{2k \cdot T} \right) \quad (3.51)$$

$$N_c = NC0SUB \cdot \left(\frac{T}{300.15} \right)^{\frac{3}{2}} \quad (3.52)$$

$$V_{bi} = \frac{kT}{q} \cdot \ln \left(\frac{NSD \cdot NBODY}{n_i^2} \right) \quad (3.53)$$

$$\Phi_B = V_t \cdot \ln \left(\frac{NBODY}{n_i} \right) \quad (3.54)$$

$$\Delta V_{th,temp} = \left(KT1 + \frac{KT1L}{L_{eff}} \right) \cdot \left(\frac{T}{TNOM} - 1 \right) + KT2 \cdot (V_{bgx} - \Delta \Phi_2) + KT3 \cdot V_{dsx} \quad (3.55)$$

$$\mu_0(T) = U0[L] \cdot \left(\frac{T}{TNOM} \right)^{UTE_i} \cdot [1 + UTL_i \cdot (T - TNOM)] \quad (3.56)$$

$$UA(T) = UA[L] \cdot [1 + UA1_i \cdot (T - TNOM)] \quad (3.57)$$

$$UD(T) = UD[L] \cdot \left(\frac{T}{TNOM} \right)^{UD1_i} \quad (3.58)$$

$$UCS(T) = UCS_i \cdot \left(\frac{T}{TNOM} \right)^{UCSTE_i} \quad (3.59)$$

$$(3.60)$$

$$VSAT(T) = VSAT[L] \cdot (1 - AT \cdot (T - TNOM)) \quad (3.61)$$

$$VSAT1(T) = VSAT1[L] \cdot (1 - AT \cdot (T - TNOM)) \quad (3.62)$$

$$PTWG(T) = PTWG[L] \cdot (1 - PTWGT \cdot (T - TNOM)) \quad (3.63)$$

$$MEXP(T) = MEXP[L] \cdot (1 + TMEXP \cdot (T - TNOM)) \quad (3.64)$$

$$BETA0(T) = BETA0_i \cdot \left(\frac{T}{TNOM} \right)^{IIT} \quad (3.65)$$

$$SII0(T) = SII0_i \left(1 + TII \left(\frac{T}{TNOM} - 1 \right) \right) \quad (3.66)$$

$$BGIDL(T) = BGIDL_i \cdot (1 + TGIDL \cdot (T - TNOM)) \quad (3.67)$$

$$BGISL(T) = BGISL_i \cdot (1 + TGIDL \cdot (T - TNOM)) \quad (3.68)$$

$$RDSWMIN(T) = RDSWMIN \cdot (1 + PRT \cdot (T - TNOM)) \quad (3.69)$$

$$RDSW(T) = RDSW[L] \cdot (1 + PRT \cdot (T - TNOM)) \quad (3.70)$$

$$RSWMIN(T) = RSWMIN \cdot (1 + PRT \cdot (T - TNOM)) \quad (3.71)$$

$$RDWMIN(T) = RDWMIN \cdot (1 + PRT \cdot (T - TNOM)) \quad (3.72)$$

$$RSW(T) = RSW[L] \cdot (1 + PRT \cdot (T - TNOM)) \quad (3.73)$$

$$RDW(T) = RDW[L] \cdot (1 + PRT \cdot (T - TNOM)) \quad (3.74)$$

$$R_{s,geo}(T) = R_{s,geo} \cdot (1 + PRT \cdot (T - TNOM)) \quad (3.75)$$

$$R_{d,geo}(T) = R_{d,geo} \cdot (1 + PRT \cdot (T - TNOM)) \quad (3.76)$$

$$Igtemp = \left(\frac{T}{TNOM} \right)^{IGT_i} \quad (3.77)$$

$$T_{3s} = \exp \left(\frac{\frac{qE_{g,TNOM}}{k \cdot TNOM} - \frac{qE_g}{kT} + XTIS \cdot \ln \left(\frac{T}{TNOM} \right)}{NJS} \right) \quad (3.78)$$

$$J_{ss}(T) = JSS \cdot T_{3s} \quad (3.79)$$

$$J_{ssws}(T) = JSWS \cdot T_{3s} \quad (3.80)$$

$$J_{sswgs}(T) = JSWGS \cdot T_{3s} \quad (3.81)$$

$$T_{3d} = \exp \left(\frac{\frac{qE_{g,TNOM}}{k \cdot TNOM} - \frac{qE_g}{kT} + XTID \cdot \ln \left(\frac{T}{TNOM} \right)}{NJD} \right) \quad (3.82)$$

$$J_{sd}(T) = JSD \cdot T_{3d} \quad (3.83)$$

$$J_{sswd}(T) = JSWD \cdot T_{3d} \quad (3.84)$$

$$J_{sswgd}(T) = JSWGD \cdot T_{3d} \quad (3.85)$$

$$CJS(T) = CJS \cdot [1 + TCJ \cdot (T - TNOM)] \quad (3.86)$$

$$CJD(T) = CJD \cdot [1 + TCJ \cdot (T - TNOM)] \quad (3.87)$$

$$CJSWS(T) = CJSWS \cdot [1 + TCJSW \cdot (T - TNOM)] \quad (3.88)$$

$$CJSWD(T) = CJSWD \cdot [1 + TCJSW \cdot (T - TNOM)] \quad (3.89)$$

$$CJSWGS(T) = CJSWGS \cdot [1 + TCJSWG \cdot (T - TNOM)] \quad (3.90)$$

$$CJSWGD(T) = CJSWGD \cdot [1 + TCJSWG \cdot (T - TNOM)] \quad (3.91)$$

$$PBS(T) = PBS(TNOM) - TPB \cdot (T - TNOM) \quad (3.92)$$

$$PBD(T) = PBD(TNOM) - TPB \cdot (T - TNOM) \quad (3.93)$$

$$PBSWS(T) = PBSWS(TNOM) - TPBSW \cdot (T - TNOM) \quad (3.94)$$

$$PBSWD(T) = PBSWD(TNOM) - TPBSW \cdot (T - TNOM) \quad (3.95)$$

$$PBSWGS(T) = PBSWGS(TNOM) - TPBSWG \cdot (T - TNOM) \quad (3.96)$$

$$PBSWGD(T) = PBSWGD(TNOM) - TPBSWG \cdot (T - TNOM) \quad (3.97)$$

Body Doping and Gate Workfunction

If $COREMOD = 1$ and $NBODY_i > 10^{23} m^{-3}$ then

$$n_{body} = 10^{23} m^{-3} \quad (3.98)$$

else

$$n_{body} = NBODY_i \quad (3.99)$$

If $NGATE_i > 0$ then

$$\Delta\Phi = \max(0, \frac{E_g}{2} - \frac{kT}{q} \cdot \ln(\frac{NGATE_i}{n_i})) \quad (3.100)$$

else

$$\Delta\Phi = \begin{cases} PHIG_i - EASUB & \text{for NMOS,} \\ (EASUB + E_g) - PHIG_i & \text{for PMOS.} \end{cases} \quad (3.101)$$

$$\phi_B = \frac{kT}{q} \cdot \ln(\frac{n_{body}}{n_i}) \quad (3.102)$$

$$\phi_{SD} = \min\left[\frac{E_g}{2}, \frac{kT}{q} \cdot \ln(\frac{NSD_i}{n_i})\right] \quad (3.103)$$

$$V_{fbsd} = \begin{cases} PHIG_i - (EASUB + \frac{E_g}{2} - \phi_{SD}) & \text{for NMOS,} \\ -[PHIG_i - (EASUB + \frac{E_g}{2} + \phi_{SD})] & \text{for PMOS.} \end{cases} \quad (3.104)$$

If $GEOMOD \neq 3$ then

$$\gamma_0 = \frac{\sqrt{2q \epsilon_{sub} n_{body}}}{C_{ox}} \quad (3.105)$$

$$\phi_{bulk} = \frac{1}{2} \frac{qn_{body}}{\epsilon_{sub}} \left(\frac{TFIN}{2}\right)^2 \quad (3.106)$$

$$\phi_{pert} = \min(\phi_{bulk}, 0.4) \quad (3.107)$$

$$Q_{bulk} = \sqrt{2qn_{body}\epsilon_{sub}\phi_{pert}} \quad (3.108)$$

$$t_{ox} = \begin{cases} \frac{EOT \cdot \epsilon_{ox}}{3.9} & \text{if } GEOMOD \neq 3 \\ R \cdot (\exp(\frac{EOT \cdot \epsilon_{ox}}{R \cdot 3.9}) - 1) & \text{if } GEOMOD = 3 \end{cases} \quad (3.109)$$

$$q_{bs} = \begin{cases} \frac{q \cdot n_{body} \cdot TFIN}{2 \cdot C_{ox}} & \text{if } GEOMOD \neq 3 \\ \frac{q \cdot n_{body} \cdot R}{2 \cdot C_{ox}} & \text{if } GEOMOD = 3 \end{cases} \quad (3.110)$$

Polysilicon Depletion

$$V_{poly0} = \begin{cases} \frac{1}{2} \frac{q \cdot NGATE_i \cdot \epsilon_{sub}}{C_{ox}^2} & \text{if } GEOMOD \neq 3 \\ \frac{1}{2} \frac{q \cdot NGATE_i \cdot \epsilon_{sub}}{C_{ox}^2} \cdot \left(\frac{R+t_{ox}}{R}\right)^2 & \text{if } GEOMOD = 3 \end{cases} \quad (3.111)$$

$$\chi_{poly} = \frac{1}{4 \cdot V_{poly0}} \quad (3.112)$$

$$\kappa_{poly} = 1 + 2 \cdot \chi_{poly} \cdot q_{bs} \quad (3.113)$$

Short Channel Effects

$$V_{bi} = \frac{kT}{q} \cdot \ln\left(\frac{NSD_i \cdot n_{body}}{n_i^2}\right) \quad (3.114)$$

$$H_{eff} = \sqrt{\frac{HFIN}{8} \cdot (HFIN + 2 \cdot \epsilon_{ratio} \cdot EOT)} \quad (3.115)$$

$$\lambda = \begin{cases} \sqrt{\frac{\epsilon_{ratio}}{2} \left(1 + \frac{TFIN}{4\epsilon_{ratio}EOT}\right) TFIN \cdot EOT} & \text{if } GEOMOD = 0 \\ \sqrt{\frac{1}{\frac{\epsilon_{ratio}}{2} \left(1 + \frac{TFIN}{4\epsilon_{ratio}EOT}\right) TFIN \cdot EOT} + \frac{1}{4H_{eff}^2}} & \text{if } GEOMOD = 1 \\ \sqrt{\frac{0.5}{\frac{\epsilon_{ratio}}{2} \left(1 + \frac{TFIN}{4\epsilon_{ratio}EOT}\right) TFIN \cdot EOT} + \frac{1}{4H_{eff}^2}} & \text{if } GEOMOD = 2 \\ \sqrt{\frac{\epsilon_{ratio}}{2} \left(1 + \frac{R}{2\epsilon_{ratio}EOT}\right) R \cdot EOT} & \text{if } GEOMOD = 3 \end{cases} \quad (3.116)$$

3.2 Terminal Voltages

Terminal Voltages and V_{dsx} Calculation

$$V_{gs} = V_g - V_s \quad (3.117)$$

$$V_{gd} = V_g - V_d \quad (3.118)$$

$$V_{ge} = V_g - V_e \quad (3.119)$$

$$V_{ds} = V_d - V_s \quad (3.120)$$

$$V_{dsx} = \sqrt{V_{ds}^2 + 0.01} - 0.1 \quad (3.121)$$

3.3 Short Channel Effects

Weighting Function for forward and reverse modes

$$T0 = \tanh\left(\frac{0.6 * q \cdot V_{ds}}{kT}\right) \quad \text{Use un-swapped } V_{ds} \text{ here} \quad (3.122)$$

$$T1 = 0.5 + 0.5 \cdot T0 \quad (3.123)$$

$$T2 = 0.5 - 0.5 \cdot T0 \quad (3.124)$$

Asymmetric parameters

$$CDSCD_a = CDSCD_i \cdot T1 + CDSCDR_i \cdot T2 \quad (3.125)$$

$$ETA0_a = ETA0_i \cdot T1 + ETA0R_i \cdot T2 \quad (3.126)$$

$$(3.127)$$

Vt Roll-off, DIBL, and Subthreshold Slope Degradation

$$\psi_{st} = 0.4 + PHIN_i + \Phi_B \quad (3.128)$$

$$C_{dsc} = \frac{0.5}{\cosh\left(DVT1_i \cdot \frac{L_{eff}}{\lambda}\right) - 1} \cdot (CDSC_i + CDSCD_a \cdot V_{dsx}) \quad (3.129)$$

$$n = \begin{cases} 1 + \frac{CIT_i + C_{dsc}}{(2C_{si})\|C_{ox}} & \text{if } GEOMOD \neq 3 \\ 1 + \frac{CIT_i + C_{dsc}}{C_{ox}} & \text{if } GEOMOD = 3 \end{cases} \quad (3.130)$$

$$\Delta V_{th,SCE} = -\frac{0.5 \cdot DVT0_i}{\cosh\left(DVT1_i \cdot \frac{L_{eff}}{\lambda}\right) - 1} \cdot (V_{bi} - \psi_{st}) \quad (3.131)$$

$$\Delta V_{th,DIBL} = -\frac{0.5 \cdot ET A0_a}{\cosh\left(DSUB_i \cdot \frac{L_{eff}}{\lambda}\right) - 1} \cdot V_{dsx} \quad (3.132)$$

$$\Delta V_{th,RSCE} = K1RSCE_i \cdot \left[\sqrt{1 + \frac{LPE0_i}{L_{eff}}} - 1 \right] \cdot \sqrt{\psi_{st}} \quad (3.133)$$

$$\Delta V_{th,all} = \Delta V_{th,SCE} + \Delta V_{th,DIBL} + \Delta V_{th,RSCE} + \Delta V_{th,temp} \quad (3.134)$$

$$V_{gsfb} = V_{gs} - \Delta \Phi - \Delta V_{th,all} - DVTS SHIFT \quad (3.135)$$

3.4 Surface Potential Calculation

Surface potentials at the source and drain ends are derived from the Poisson's equation with a perturbation method [4] and computed using the Householder's cubic iteration method [5, 6]. Perturbation allows accurate modeling of finite body doping.

When the body is lightly-doped, a simplified surface potential algorithm can be activated by setting *COREMOD* = 1 to enhance computational efficiency.

Constants for Surface Potential Calculation

If $GEOMOD \neq 3$ then

$$r1 = \frac{2\epsilon_{sub}}{C_{ox} \cdot TFIN} \quad (3.136)$$

$$r2 = \begin{cases} 0 & \text{if } NGATE_i = 0 \\ \frac{4 \cdot nkT \epsilon_{sub}}{q \cdot TFIN^2 \cdot NGATE_i} & \text{if } NGATE_i > 0 \end{cases} \quad (3.137)$$

$$q_0 = \frac{\left(5 \frac{kT}{q} C_{Si} + 2Q_{bulk}\right)}{C_{ox}} \quad (3.138)$$

If $GEOMOD = 3$ then

$$r1 = \frac{2\epsilon_{sub}}{R \cdot C_{ox}} \quad (3.139)$$

$$r2 = \begin{cases} 0 & \text{if } NGATE_i = 0 \\ \frac{2 \cdot nkT \cdot \chi_{poly} \cdot r1^2}{q} & \text{if } NGATE_i > 0 \end{cases} \quad (3.140)$$

$$q_0 = \frac{2 \cdot nkT \cdot r1}{q} \quad (3.141)$$

Body-Doping adjustment for $GEOMOD = 0, 1, 2$ case

If $COREMOD = 1$ then

$$V_{gsfb} = V_{gsfb} - \frac{qn_{body} \cdot TFIN}{2C_{ox}} \quad (3.142)$$

Body-Doping based calculations for $GEOMOD = 3$ case

$$T_0 = \frac{qn_{body}R}{C_{ox}} \quad (3.143)$$

$$V_{t,dop} = - \left(\frac{nkT}{q} \right) \ln \left(\frac{nkT}{q \cdot T_0} \right) - \left(\frac{nkT}{q} \right) \ln \left(1 - \exp \left(\frac{q \cdot T_0}{2 \cdot r1 \cdot nkT} \right) \right) \quad (3.144)$$

$$c_{dop} = 2 \cdot r1 \cdot \exp \left(- \frac{q \cdot V_{t,dop}}{nkT} \right) \quad (3.145)$$

$$V_{t0} = \frac{T_0}{2} + 2 \cdot n \cdot \phi_b - \left(\frac{nkT}{q} \right) \ln \left(\frac{0.5 \cdot q \cdot T_0}{nkT} \right) + V_{t,dop} \quad (3.146)$$

Quantum Mechanical Vt correction

Note: $QMFACCTOR_i$ also serves as a switch here.

If $GEOMOD \neq 3$ then

$$E_0 = \frac{\hbar^2 \pi^2}{2m_x \cdot TFIN^2} \quad (3.147)$$

$$E'_0 = \frac{\hbar^2 \pi^2}{2m'_x \cdot TFIN^2} \quad (3.148)$$

$$E_1 = 4E_0 \quad (3.149)$$

$$E'_1 = 4E'_0 \quad (3.150)$$

$$\gamma = 1 + \exp\left(\frac{E_0 - E_1}{kT}\right) + \frac{g'm'_d}{gm_d} \cdot \left[\exp\left(\frac{E_0 - E'_0}{kT}\right) + \exp\left(\frac{E_0 - E'_1}{kT}\right) \right] \quad (3.151)$$

$$\Delta V_{t,QM} = QMFACCTOR_i \cdot \left[\frac{E_0}{q} - \frac{kT}{q} \ln\left(\frac{g \cdot m_d}{\pi \hbar^2 N_c} \cdot \frac{kT}{TFIN} \cdot \gamma\right) \right] \quad (3.152)$$

If $GEOMOD = 3$ then

$$E_{0,QM} = \frac{\hbar^2 (2.4048)^2}{2m_x \cdot R^2} \quad (3.153)$$

$$\Delta V_{t,QM} = QMFACCTOR_i \cdot \frac{E_{0,QM}}{q} \quad (3.154)$$

Voltage Limiting for Accumulation

If $GEOMOD \neq 3$ then

$$T0 = -(\Delta V_{t,QM} + \left(\frac{nkT}{q} \right) \ln \left(\frac{2 \cdot L_{eff} \cdot 10^{-15}}{\mu_0(T) \cdot W_{eff} \cdot nkT \cdot N_c \cdot TFIN} \right)) \quad (3.155)$$

$$T1 = V_{gsfb} + T0 + DELVTRAND \quad (3.156)$$

$$V_{gsfbeff} = \frac{1}{2} \left[T1 + \sqrt{(T1)^2 + 4 \times 10^{-8}} \right] - T0 \quad (3.157)$$

If $GEOMOD = 3$ then

$$T0 = -(\Delta V_{t,QM} + \left(\frac{nkT}{q} \right) \ln \left(\frac{2 \cdot L_{eff} \cdot 10^{-15}}{\mu_0(T) \cdot W_{eff} \cdot nkT \cdot n_i \cdot R} \right)) \quad (3.158)$$

$$T1 = V_{gsfb} + T0 + n \cdot \Phi_B + \frac{E_g}{2} + DELVTRAND \quad (3.159)$$

$$V_{gsfbeff} = \frac{1}{2} \left[T1 + \sqrt{(T1)^2 + 4 \times 10^{-8}} \right] - T0 - V_{t0} \quad (3.160)$$

Case: $GEOMOD = 0, 1, 2$

Calculations Common to the Source and Drain Surface Potentials

$$a = e^{\frac{q\phi_{pert}}{nkT}} \quad (3.161)$$

$$b = \frac{\phi_{bulk}}{(nkT/q)^2} \quad (3.162)$$

$$c = 2nkT/q \quad (3.163)$$

$$F_1 = \ln \left(\sqrt{\frac{2\epsilon_{sub}nkT}{q^2N_c}} \frac{2}{TFIN} \right) \quad (3.164)$$

Surface Potential 2-stage Analytical Approximation ($COREMOD = 0$)

$$V_{ch} = \begin{cases} \Delta V_{t,QM} & \text{at source} \\ \Delta V_{t,QM} + V_{dseff} & \text{at drain} \end{cases} \quad (3.165)$$

$$F = \frac{q(V_{gsfbeff} - \phi_{pert} - V_{ch})}{2nkT} - F_1 \quad (3.166)$$

$$Z1 = Tan^{-1} \left(exp \left(F - r1 \cdot \sqrt{\frac{\phi_{bulk} \cdot \phi_{pert}}{n(kT/q)^2}} - r2 \cdot \frac{\phi_{bulk} \cdot \phi_{pert}}{n(kT/q)^2} \right) \right) \quad (3.167)$$

$$Z2 = Tan^{-1} \left(\frac{2ln(1 + e^F)}{r1 \cdot \pi \cdot e^{q\phi_{pert}/2nkT}} \right) \quad (3.168)$$

$$\beta = MIN(Z1, Z2) \quad (3.169)$$

$$T0 = (1 + \beta Tan\beta) \quad (3.170)$$

$$T2 = \sqrt{\beta^2 \left(\frac{a}{Cos^2\beta} - 1 \right) + b \cdot (\phi_{pert} - c \cdot ln(Cos\beta))} \quad (3.171)$$

$$T3 = -2 \cdot \beta + b \cdot c \cdot Tan(\beta) + 2a \cdot \beta \cdot Sec^2(\beta) \cdot T0 \quad (3.172)$$

$$T4 = -2 + 2a \cdot \beta^2 Sec^4(\beta) + Sec^2(\beta) (2a + b \cdot c + 8a \cdot \beta Tan(\beta) + 4a \cdot \beta^2 Tan^2(\beta)) \quad (3.173)$$

$$T5 = 2T4 \cdot Tan(\beta) + 4 (3T0 \cdot a \cdot \beta Sec^4(\beta) + Tan(\beta) + 2T0 \cdot a \cdot Sec^2(\beta) Tan(\beta)) \quad (3.174)$$

$$f0 = \ln(\beta) - \ln(Cos(\beta)) + r1 \cdot T2 - F + r2 \cdot T2^2 \quad (3.175)$$

$$f1 = \frac{1}{\beta} + Tan(\beta) + \frac{r1 \cdot T3}{2T2} + r2 \cdot T3 \quad (3.176)$$

$$f2 = -\frac{1}{\beta^2} + Sec^2(\beta) - \frac{r1 \cdot T3^2}{4T2^3} + \frac{r1 \cdot T4}{2T2} + r2 \cdot T4 \quad (3.177)$$

$$\begin{aligned} f3 = & \frac{2}{\beta^3} + 2Sec^2(\beta)Tan(\beta) + \frac{3r1 \cdot T3^3}{8T2^5} - \frac{3r1 \cdot T3 \cdot T4}{4T2^3} \\ & + \frac{r1 \cdot T5}{2T2} + r2 \cdot T5 \end{aligned} \quad (3.178)$$

$$\beta = \beta - \frac{f0}{f1} \cdot \left(1 + \frac{f0 \cdot f2}{2f1^2} + \frac{f0^2 \cdot (3f2^2 - f1 \cdot f3)}{6f1^4} \right) \quad (3.179)$$

Repeat (3.170) to (3.179).

$$\psi_0 = \frac{2nkT}{q} \cdot \ln \left(\frac{2\beta}{T_{Si}} \cdot \sqrt{\frac{2\epsilon_{sub}nkT \cdot n_{body}}{q^2 n_i^2}} \right) \quad (3.180)$$

$$\begin{cases} \psi_s = \psi_0 - \frac{2nkT}{q} \ln(Cos(\beta)) + \phi_{pert} & \text{at source} \\ \psi_d = \psi_0 - \frac{2nkT}{q} \ln(Cos(\beta)) + \phi_{pert} + V_{dseff} & \text{at drain} \end{cases} \quad (3.181)$$

Simplified Surface Potential Approximation ($COREMOD = 1$)

$$V_{ch} = \begin{cases} \Delta V_{t,QM} & \text{at source} \\ \Delta V_{t,QM} + V_{dseff} & \text{at drain} \end{cases} \quad (3.182)$$

$$F = \frac{q(V_{gsfb} - V_{ch})}{2nkT} - F_1 \quad (3.183)$$

$$Z1 = Tan^{-1}(exp(F)) \quad (3.184)$$

$$Z2 = Tan^{-1} \left(\frac{2ln(1 + e^F)}{r1 \cdot \pi} \right) \quad (3.185)$$

$$\beta = MIN(Z1, Z2) \quad (3.186)$$

$$f0 = \ln(\beta) - \ln(\cos(\beta)) + r1 \cdot \beta \cdot \tan(\beta) + r2 \cdot \beta^2 \cdot \tan^2(\beta) - F \quad (3.187)$$

$$\begin{aligned} f1 &= \frac{1}{\beta} + \beta \cdot \sec^2(\beta) [r1 + 2 \cdot r2 \cdot \beta \cdot \tan(\beta)] + \\ &\quad \tan(\beta) [1 + r1 + 2 \cdot r2 \cdot \beta \cdot \tan(\beta)] \end{aligned} \quad (3.188)$$

$$\begin{aligned} f2 &= \sec^2(\beta) \left[1 + 2 \left(r1 + r2 \cdot \beta^2 \cdot \sec^2(\beta) + r1 \cdot \beta \cdot \tan(\beta) \right. \right. \\ &\quad \left. \left. + 2 \cdot r2 \cdot (\beta^2 \tan^2(\beta) + 2\beta \cdot \tan(\beta)) \right) \right] + \frac{1}{\beta^2} [2 \cdot r2 \cdot \beta^2 \cdot \tan^2(\beta) - 1] \end{aligned} \quad (3.189)$$

$$\begin{aligned} f3 &= \frac{2}{\beta^3} + 2 \cdot \beta \cdot \sec^4(\beta) \left[r1 + 2 \cdot r2 \cdot (3 + 4\beta \tan(\beta)) \right] \\ &\quad + 2 \sec^2(\beta) \tan(\beta) \cdot \left[1 + 3 \cdot r1 \right. \\ &\quad \left. + 2 \cdot r1 \cdot \beta \cdot \tan(\beta) + 2 \cdot r2 \left(3(1 + 2 \cdot \beta \cdot \tan(\beta)) + 2 \cdot \beta^2 \cdot \tan^2(\beta) \right) \right] \end{aligned} \quad (3.190)$$

$$\beta = \beta - \frac{f0}{f1} \cdot \left(1 + \frac{f0 \cdot f2}{2f1^2} + \frac{f0^2 \cdot (3f2^2 - f1 \cdot f3)}{6f1^4} \right) \quad (3.191)$$

Repeat (3.187) to (3.191).

$$\begin{cases} \psi_s = \frac{2nkT}{q} [\ln(\beta) - \ln(\cos(\beta)) + F_1] & \text{at source} \\ \psi_d = \frac{2nkT}{q} [\ln(\beta) - \ln(\cos(\beta)) + F_1] + V_{dseff} & \text{at drain} \end{cases} \quad (3.192)$$

Case: $GEOMOD = 3$, same for both $COREMOD = 0, 1$

$$V_{ch} = \begin{cases} \Delta V_{t,QM} & \text{at source} \\ \Delta V_{t,QM} + V_{dseff} & \text{at drain} \end{cases} \quad (3.193)$$

$$F = \frac{q(V_{gsfbeff} - V_{ch})}{2nkT} \quad (3.194)$$

$$\text{If } F < -10 \quad g = \exp(2 \cdot F) \quad (3.195)$$

$$\text{Else if } F > 10 \quad g = \frac{F}{r1} \quad (3.196)$$

$$\text{Else} \quad g = \frac{\sqrt{0.25 + r1^2 \cdot (\ln(1 + \exp(F)))^2}}{r1^2} \quad (3.197)$$

$$T0 = 1 + c_{dop} \cdot g \quad (3.198)$$

$$T1 = \frac{c_{dop}}{T0} \quad (3.199)$$

$$T2 = T1^2 \quad (3.200)$$

$$f0 = 0.5 \cdot \ln(g) + 0.5 \cdot \ln(T0) + r1 \cdot g + r2 \cdot g^2 - F \quad (3.201)$$

$$f1 = 0.5 \cdot \frac{1}{g} + 0.5 \cdot T1 + r1 + 2 \cdot r2 \cdot g \quad (3.202)$$

$$f2 = -0.5 \cdot \frac{1}{g^2} - 0.5 \cdot T2 + 2 \cdot r2 \quad (3.203)$$

$$f3 = \frac{1}{g^3} + T1 \cdot T2 \quad (3.204)$$

$$g = g - \frac{f0}{f1} \cdot \left(1 + \frac{f0 \cdot f2}{2f1^2} + \frac{f0^2 \cdot (3f2^2 - f1 \cdot f3)}{6f1^4} \right) \quad (3.205)$$

Repeat (3.198) to (3.205).

Source side calculations

$$V_{polys} = 2 \cdot \frac{nkT}{q} \cdot r2 \cdot g^2 \quad (3.206)$$

$$\psi_s = V_{gsfbeff} - 2 \cdot \frac{nkT}{q} \cdot r1 \cdot g - V_{polys} \quad (3.207)$$

$$q_{is} = q_0 \cdot g \quad (3.208)$$

Drain side calculations

$$V_{polyd} = 2 \cdot \frac{nkT}{q} \cdot r2 \cdot g^2 \quad (3.209)$$

$$\psi_d = V_{gsfbeff} - 2 \cdot \frac{nkT}{q} \cdot r1 \cdot g - V_{polyd} \quad (3.210)$$

$$q_{id} = q_0 \cdot g \quad (3.211)$$

3.5 Drain Saturation Voltage

The drain saturation voltage model is calculated after the source-side surface potential (ψ_s) has been calculated. V_{dseff} is subsequently used to compute the drain-side surface potential (ψ_d).

Electric Field Calculations

Electric Field is in MV/cm

If $GEOMOD \neq 3$ then

If $NGATE_i > 0$ then

$$T_{polys} = \sqrt{1 + \frac{V_{gsfbeff} - \psi_s}{V_{poly0}}} - 1 \quad (3.212)$$

$$V_{polys} = V_{poly0} \cdot T_{polys}^2 \quad (3.213)$$

else

$$V_{polys} = 0 \quad (3.214)$$

$$q_{is} = \begin{cases} V_{gsfbeff} - \psi_s - q_{bs} - V_{polys} & \text{if } COREMOD = 0 \\ V_{gsfbeff} - \psi_s - V_{polys} & \text{if } COREMOD = 1 \end{cases} \quad (3.215)$$

$$E_{effs} = 10^{-8} \cdot \left(\frac{q_{bs} + \eta \cdot q_{is}}{\epsilon_{ratio} \cdot EOT} \right) \quad (3.216)$$

Drain Saturation Voltage (V_{dsat}) Calculations

$$D_{mobs} = 1 + UA(T) \cdot (E_{effs})^{EU} + \frac{UD(T)}{\left(\frac{1}{2} \cdot \left(1 + \frac{q_{is}}{q_{bs}}\right)\right)^{UCS(T)}} \quad (3.217)$$

$$D_{mobs} = \frac{D_{mobs}}{U0MULT} \quad (3.218)$$

If $RDSMOD = 0$ then (3.219)

$$R_{ds,s} = R_{s,geo}(T) + R_{d,geo}(T) + \quad (3.220)$$

$$\frac{1}{(W_{eff0}(\mu m))^{WR_i}} \cdot \left(RDSWMIN(T) + \frac{RDSW(T)}{1 + PRWG_i \cdot q_{is}} \right)$$

If $RDSMOD = 1$ then (3.221)

$$R_{ds,s} = 0 \quad (3.222)$$

$$E_{sat} = \frac{2 \cdot VSAT(T)}{\mu_0(T)/D_{mobs}} \quad (3.223)$$

$$E_{satL} = E_{sat} \cdot L_{eff} \quad (3.224)$$

If $R_{ds,s} = 0$ then

$$V_{dsat} = \frac{E_{satL} \cdot KSATIV_i \cdot (V_{gsfbeff} - \psi_s + 2\frac{kT}{q})}{E_{satL} + KSATIV_i \cdot (V_{gsfbeff} - \psi_s + 2\frac{kT}{q})} \quad (3.225)$$

else

$$WVC_{ox} = W_{eff0} \cdot VSAT(T) \cdot C_{ox} \quad (3.226)$$

$$T_a = 2 \cdot WVC_{ox} \cdot R_{ds,s}$$

$$\begin{aligned} T_b &= KSATIV_i \cdot (V_{gsfbeff} - \psi_s + 2\frac{kT}{q}) \cdot (1 + 3 \cdot WVC_{ox} \cdot R_{ds,s}) + E_{satL} \\ T_c &= KSATIV_i \cdot (V_{gsfbeff} - \psi_s + 2\frac{kT}{q}) \\ &\times \left(E_{satL} + T_a \cdot KSATIV_i \cdot (V_{gsfbeff} - \psi_s + 2\frac{kT}{q}) \right) \end{aligned} \quad (3.227)$$

$$V_{dsat} = \frac{\left(T_b - \sqrt{T_b^2 - 2T_a T_c} \right)}{T_a} \quad (3.228)$$

$$V_{dseff} = \frac{V_{ds}}{\left(1 + \left(\frac{V_{ds}}{V_{dsat}} \right)^{MEXP(T)} \right)^{1/MEXP(T)}} \quad (3.229)$$

3.6 Average Potential, Charge and Related Variables

$$\Delta\psi = \psi_d - \psi_s \quad (3.230)$$

$$q_{ba} = q_{bs} \quad (3.231)$$

If $GEOMOD \neq 3$ then

If $NGATE_i > 0$ then

$$T_{polyd} = \sqrt{1 + \frac{V_{gsfbeff} - \psi_d}{V_{poly0}}} - 1 \quad (3.232)$$

$$V_{polyd} = V_{poly0} \cdot T_{polyd}^2 \quad (3.233)$$

else

$$V_{polyd} = 0 \quad (3.234)$$

$$q_{id} = \begin{cases} V_{gsfbeff} - \psi_d - q_{ba} - V_{polyd} & \text{if } COREMOD = 0 \\ V_{gsfbeff} - \psi_d - V_{polyd} & \text{if } COREMOD = 1 \end{cases} \quad (3.235)$$

$$q_{ia} = 0.5 \cdot (q_{is} + q_{id}) \quad (3.236)$$

$$\Delta q_i = q_{is} - q_{id} \quad (3.237)$$

3.7 Quantum Mechanical Effects

Effects that arise due to structural and electrical confinement in the multi-gate structures are dealt in this section. The threshold voltage shift arising due to bias-dependent ground state sub-band energy is already accounted for in the surface potential calculations. (See the section on 'Surface Potential Calculation'). The reduction in width and bias-dependence in effective oxide thickness due to the inversion charge centroid being away from the interface is taken care of here. The section is evaluated only if $QMTCENIV_i$ or $QMTCENCV_i$ is non-zero. While a single equation with parameters $ETAQM$, $QM0$ and $ALPHAQM$ govern the motion of charge centroid w.r.t. bias, two different quasi-switches are introduced here for the purpose of effective width calculation and effective oxide thickness calculation. $QMTCENIV_i$ uses the above expression to

account for the effective width in $I - V$ calculations and $QMTCENCV_i$ uses the same expression for the effective width and effective oxide thickness for $C - V$ calculations. The pre-calculated factor MTcen is for the geometric dependence (on $TFIN/HFIN/R$) of the charge centroid in sub-threshold region.

Charge Centroid Calculation for Inversion

$$T4 = \frac{q_{ia} + ETAQM \cdot q_{ba}}{QM0} \quad (3.238)$$

$$T5 = 1 + T4^{PQM} \quad (3.239)$$

Charge Centroid Calculation for Accumulation

$$T6 = 1 + \left(\frac{q_{i,acc}}{QM0ACC} \right)^{PQMACC} \quad (3.240)$$

Effective Width Model

If $GEOMOD = 0$ then

$$T_{cen} = TFIN \cdot MTcen \quad (3.241)$$

$$W_{eff} = W_{eff0} \quad (3.242)$$

$$W_{eff,CV} = W_{eff,CV0} \quad (3.243)$$

If $GEOMOD = 1$ then

$$T_{cen} = \min(TFIN, HFIN) \cdot MTcen \quad (3.244)$$

$$W_{eff} = W_{eff0} - 4 \cdot QMTCENIV_i \cdot T_{cen} \quad (3.245)$$

$$W_{eff,CV} = W_{eff,CV0} - 4 \cdot QMTCENCV_i \cdot T_{cen} \quad (3.246)$$

If $GEOMOD = 2$ then

$$T_{cen} = \min(TFIN, HFIN) \cdot MTcen \quad (3.247)$$

$$W_{eff} = W_{eff0} - 8 \cdot QMTCENIV_i \cdot T_{cen} \quad (3.248)$$

$$W_{eff,CV} = W_{eff,CV0} - 8 \cdot QMTCENCV_i \cdot T_{cen} \quad (3.249)$$

If $GEOMOD = 3$ then (3.250)

$$T_{cen} = R \cdot MTcen \quad (3.251)$$

$$W_{eff} = W_{eff0} - 2\pi \cdot QMTCENIV_i \cdot T_{cen} \quad (3.252)$$

$$W_{eff,CV} = W_{eff,CV0} - 2\pi \cdot QMTCENCV_i \cdot T_{cen} \quad (3.253)$$

Effective Oxide Thickness / Effective Capacitance

If $QMTCENCV_i = 0$, then $C_{ox}/C_{ox,acc}$ (with $EOT/EOTACC$) will continue to be used for both $I - V$ and $C - V$. Else the following calculations yield a $C_{ox,eff}$ that shall be used for $C - V$ purposes. However C_{ox} will continue to be used for $I - V$. For calculation of $C_{ox,eff}$, the physical oxide thickness, $TOXP$ scaled appropriately will be added to the inversion charge centroid, T_{cen} calculated above instead of using EOT .

If $QMTCENCV_i \neq 0$ then (3.254)

$$C_{ox,eff} = \begin{cases} \frac{3.9 \cdot \epsilon_0}{TOXP \frac{3.9}{EPSROX} + \frac{T_{cen}}{T5} \cdot \frac{QMTCENCV_i}{\epsilon_{ratio}}} & GEOMOD \neq 3 \\ \frac{3.9 \cdot \epsilon_0}{R \cdot \left[\frac{1}{\epsilon_{ratio}} \ln \left(\frac{R}{R - T_{cen}/T5} \right) + \frac{3.9}{EPSROX} \ln \left(1 + \frac{Toxp}{R} \right) \right]} & GEOMOD = 3 \end{cases} \quad (3.255)$$

$$C_{ox,acc} = \begin{cases} \frac{3.9 \cdot \epsilon_0}{TOXP \frac{3.9}{EPSROX} + \frac{T_{cen}}{T6} \cdot \frac{QMTCENCV_i}{\epsilon_{ratio}}} & GEOMOD \neq 3 \\ \frac{3.9 \cdot \epsilon_0}{R \cdot \left[\frac{1}{\epsilon_{ratio}} \ln \left(\frac{R}{R - T_{cen}/T6} \right) + \frac{3.9}{EPSROX} \ln \left(1 + \frac{Toxp}{R} \right) \right]} & GEOMOD = 3 \end{cases} \quad (3.256)$$

If $QMTCENCV_i = 0$ then (3.257)

$$C_{ox,eff} = C_{ox} \quad (3.258)$$

$$C_{ox,acc} = \frac{3.9 \cdot \epsilon_0}{EOTACC} \quad (3.259)$$

(3.260)

3.8 Mobility degradation and series resistance

Mobility degradation

$$\eta = \begin{cases} \frac{1}{2} \cdot ETAMOB & \text{for NMOS} \\ \frac{1}{3} \cdot ETAMOB & \text{for PMOS} \end{cases} \quad (3.261)$$

$$E_{effa} = 10^{-8} \cdot \left(\frac{q_{ba} + \eta \cdot q_{ia}}{\epsilon_{ratio} \cdot EOT} \right) \quad (3.262)$$

$$D_{mob} = 1 + UA(T) \cdot (E_{effa})^{EU} + \frac{UD(T)}{\left(\frac{1}{2} \cdot \left(1 + \frac{q_{ia}}{q_{ba}} \right) \right)^{UCS(T)}} \quad (3.263)$$

$$D_{mob} = \frac{D_{mob}}{U0MULT} \quad (3.264)$$

Series resistance

The source/drain series resistance is the sum of a bias-independent component and a bias-dependent component. They are described in detail in section 3.13. If RDSMOD=0 the resistance will affect the I_{ds} expressions through a degradation factor D_r .

3.9 Output Conductance

Channel Length Modulation

$$C_{clm} = \begin{cases} PCLM_i + PCLMG_i \cdot q_{ia} & \text{for } PCLMG_i > 0 \\ \frac{1}{\frac{1}{PCLM_i} - PCLMG_i \cdot q_{ia}} & \text{for } PCLMG_i < 0 \end{cases} \quad (3.265)$$

$$M_{clm} = 1 + \frac{1}{C_{clm}} \ln \left[1 + \frac{V_{ds} - V_{dseff}}{VASAT_i} \cdot C_{clm} \right] \quad (3.266)$$

Output Conductance due to DIBL

$$PVAGfactor = \begin{cases} 1 + PVAG_i \cdot \frac{q_{ia}}{E_{sat}L_{eff}} & \text{for } PVAG_i > 0 \\ \frac{1}{1 - PVAG_i \cdot \frac{q_{ia}}{E_{sat}L_{eff}}} & \text{for } PVAG_i < 0 \end{cases} \quad (3.267)$$

$$\theta_{rout} = \frac{0.5 \cdot PDIBL1_i}{\cosh\left(DROUT_i \cdot \frac{L_{eff}}{\lambda}\right) - 1} + PDIBL2_i \quad (3.268)$$

$$V_{ADIBL} = \frac{q_{ia} + 2kT/q}{\theta_{rout}} \cdot \left(1 - \frac{V_{dsat}}{V_{dsat} + q_{ia} + 2kT/q}\right) \cdot PVAGfactor \quad (3.269)$$

$$M_{oc} = \left(1 + \frac{V_{ds} - V_{dseff}}{V_{ADIBL}}\right) \cdot M_{clm} \quad (3.270)$$

M_{oc} is multiplied to I_{ds} in the final drain current expression.

3.10 Velocity Saturation

Current Degradation Due to Velocity Saturation The following formulation models the current degradation factor due to velocity saturation in the linear region. It is adopted from the BSIM5 model [7, 8].

$$E_{sat1} = \frac{2 \cdot VSAT1(T)}{\mu_{eff}} \quad (3.271)$$

$$\delta_{vsat} = DELTAVSAT \quad (3.272)$$

$$D_{vsat} = \frac{1 + \sqrt{\delta_{vsat} + \left(\frac{\Delta q_i}{E_{sat1} L_{eff}}\right)^2}}{1 + \sqrt{\delta_{vsat}}} + \frac{1}{2} \cdot PTWG(T) \cdot q_{ia} \cdot \Delta q_i^2 \quad (3.273)$$

3.11 Drain Current Model

Case: $GEOMOD = 0, 1, 2$ and $COREMOD = 1$

Assume solution to SPE for source and drain side to be β_s and β_d respectively

$$T_0 = \frac{2C_{si}}{C_{ox}} \quad (3.274)$$

$$T_1 = \beta_s \cdot \tan \beta_s \quad (3.275)$$

$$T_2 = \beta_d \cdot \tan \beta_d \quad (3.276)$$

$$T_3 = \begin{cases} T_0 \cdot (T_1 + T_2) + 4 \cdot r2 \cdot \frac{T_1^2 + T_1 T_2 + T_2^2}{3} & NGATE_i > 0 \\ T_0 \cdot (T_1 + T_2) & \text{otherwise} \end{cases} \quad (3.277)$$

$$T_6 = \beta_s^2 + \beta_d^2 \quad (3.278)$$

$$i_{ds0} = \frac{4C_{si}}{C_{ox}} \left(\frac{nkT}{q} \right)^2 \cdot [(T_3 + 2) \cdot (T_1 - T_2) - T_6] \quad (3.279)$$

$$\frac{i_{ds0}}{\Delta q_i} = \frac{nkT}{2q} \cdot (T_3 + 1) \quad (3.280)$$

$$I_{ds} = IDS0MULT \cdot \mu_0(T) \cdot C_{ox} \cdot \frac{W_{eff}}{L_{eff}} \cdot i_{ds0} \cdot \frac{M_{oc}}{D_{vsat} \cdot D_r \cdot D_{mob}} \times NFIN_{total} \quad (3.281)$$

Case: All other cases

If $GEOMOD \neq 3$ then

$$c_{dop} = 1 \quad (3.282)$$

If $NGATE_i > 0$ then

$$T_{poly} = 2 \cdot \chi_{poly} \cdot \frac{T_{com}}{3} \quad (3.283)$$

$$T1 = \kappa_{poly} \cdot q_{ia} \quad (3.284)$$

Else

$$T_{poly} = 0 \quad (3.285)$$

$$T1 = q_{ia} \quad (3.286)$$

$$\eta_{iv} = \frac{q_0}{q_0 + c_{dop}q_{ia}} \quad (3.287)$$

$$T2 = (2 - \eta_{iv}) \cdot \frac{n k T}{q} \cdot \Delta q_i \quad (3.288)$$

$$\frac{i_{ds0}}{\Delta q_i} = T_{poly} + T1 + T2 \quad (3.289)$$

$$i_{ds0} = \frac{i_{ds0}}{\Delta q_i} \cdot \Delta q_i \quad (3.290)$$

$$I_{ds} = IDS0MULT \cdot \mu_0(T) \cdot C_{ox} \cdot \frac{W_{eff}}{L_{eff}} \cdot i_{ds0} \cdot \frac{M_{oc}}{D_{mob} \cdot D_r \cdot D_{vsat}} \times NFIN_{total} \quad (3.291)$$

3.12 Intrinsic Capacitance Model

In BSIM-MG both the intrinsic capacitances and parasitic capacitances are modeled. In this section we describe the formulation of intrinsic capacitances. The formulation of parasitic capacitances will be described in section 3.13

To ensure charge conservation, terminal charges instead of terminal voltages are used as state variables. The terminal charges Q_g , Q_b , Q_s , and Q_d are the charges associated with the gate, bulk, source, and drain terminals, respectively. Please refer to [9] for details of the terminal charge derivation.

Intrinsic (Normalized) Charge

$$q_b = q_{bs}$$

$$i_{ds,CV} = \begin{cases} 2 \cdot \chi_{poly} \cdot \frac{T_{com}}{3} + \kappa_{poly} \cdot q_{ia} + (2 - \eta_{iv}) \frac{nkT}{q} & NGATE_i > 0 \\ q_{ia} + (2 - \eta_{iv}) \frac{nkT}{q} & NGATE_i = 0 \end{cases} \quad (3.292)$$

Calculating q_g

$$T0 = \begin{cases} \kappa_{poly} + 4 \cdot \chi_{poly} \cdot q_{ia} & NGATE_i > 0 \\ 1 & NGATE_i = 0 \end{cases} \quad (3.293)$$

$$q_g = \left[q_{ia} + T0 \cdot \frac{\Delta q_i^2}{12 \cdot i_{ds,CV}} \right] \quad (3.294)$$

Calculating q_d

$$T1 = \begin{cases} 15 \cdot \kappa_{poly} + \chi_{poly} \cdot (32 \cdot q_{id} + 28 \cdot q_{is}) & NGATE_i > 0 \\ 15 & NGATE_i = 0 \end{cases} \quad (3.295)$$

$$T2 = \begin{cases} 63 \cdot \kappa_{poly}^2 + 126 \cdot \chi_{poly} \cdot \kappa_{poly} \cdot q_{ia} + \chi_{poly}^2 \cdot (256 \cdot T_{com} + 240 \cdot q_{is} \cdot q_{id}) & NGATE_i > 0 \\ 63 & NGATE_i = 0 \end{cases} \quad (3.296)$$

$$q_d = \left[0.5 \cdot q_{ia} - \frac{\Delta q_i}{12} \cdot \left(1 - T1 \frac{\Delta q_i}{30 \cdot i_{ds,CV}} - T2 \frac{\Delta q_i^2}{1260 \cdot i_{ds,CV}^2} \right) \right] \quad (3.297)$$

Accumulation Charge

Note: This section is still subject to verification and may be changed or removed in future versions.

The calculation for accumulation region charge are performed only if both the switches CAP-MOD and BULKMOD are set to 1, i.e. for a bulk-substrate device only. This introduces a computational effort equal to the calculation of surface potential on the source side. For calculation of accumulation region charge, the device is treated as intrinsically doped i.e.

NBODY= n_i . However additional flexibility is introduced through a separate effective oxide thickness (EOTACC) and a separate Flatband voltage value (through DELVFBACC) for the accumulation side calculations. The following equations (here written together) are present at appropriate places in the code.

$$r1_{acc} = \begin{cases} \frac{2\epsilon_{sub}}{TFIN \cdot C_{ox,acc}} & GEOMOD \neq 3 \\ \frac{2\epsilon_{sub}}{R \cdot C_{ox,acc}} & GEOMOD = 3 \end{cases} \quad (3.298)$$

If $GEOMOD \neq 3$ then

$$F_{1,acc} = \ln \left(\sqrt{\frac{2\epsilon_{sub} \cdot kT}{q^2 N_c}} \frac{2}{TFIN} \right) \quad (3.299)$$

If $GEOMOD = 3$ then

$$q_{0,acc} = \frac{2 \cdot kT \cdot r1_{acc}}{q} \quad (3.300)$$

$$T0_{acc} = \frac{q \cdot n_i \cdot R}{C_{ox,acc}} \quad (3.301)$$

$$V_{t,dop,acc} = - \left(\frac{kT}{q} \right) \ln \left(\frac{kT}{q \cdot T0_{acc}} \right) - \left(\frac{kT}{q} \right) \ln \left(1 - \exp \left(\frac{q \cdot T0_{acc}}{2 \cdot r1_{acc} \cdot kT} \right) \right) \quad (3.302)$$

$$c_{dop,acc} = 2 \cdot r1_{acc} \cdot \exp \left(- \frac{q \cdot V_{t,dop,acc}}{kT} \right) \quad (3.303)$$

$$V_{t0,acc} = \frac{T0_{acc}}{2} - \left(\frac{kT}{q} \right) \ln \left(\frac{0.5 \cdot q \cdot T0_{acc}}{kT} \right) + V_{t,dop,acc} \quad (3.304)$$

Voltage limiting for $V_{ge} > V_{fb}$ region

$$T1 = -V_{ge} + \Delta\phi - \frac{E_g}{2} + DELVFBACC \quad (3.305)$$

$$V_{gsfbeff,acc} = \begin{cases} \frac{1}{2} \left[T1 + \sqrt{T1^2 + 4 \times 10^{-8}} \right] - \frac{E_g}{2} & GEMOD \neq 3 \\ \frac{1}{2} \left[T1 + \sqrt{T1^2 + 4 \times 10^{-8}} \right] - V_{t0,acc} & GEMOD = 3 \end{cases} \quad (3.306)$$

Surface Potential Evaluation

For $GEMOD \neq 3$, the simplified surface potential calculation outlined for $COREMOD = 1$ case is used with $V_{gsfbeff,acc}$, $F_{1,acc}$ and $r1_{acc}$ calculated above together with $r2 = 0$, $V_{ch} = 0$. Then the normalized charge is evaluated the following way...

$$q_{i,acc} = V_{gsfbeff,acc} - \frac{2kT}{q} [\ln(\beta) - \ln(\cos(\beta)) + F_{1,acc}] \quad (3.307)$$

Similarly for $GEMOD = 3$, the surface potential calculations are performed with $V_{gsfbeff,acc}$ and $r1_{acc}$, with $r2$ and V_{ch} both set to 0. The normalized charge in this case is give by,

$$q_{i,acc} = q_{0,acc} \cdot g \quad (3.308)$$

Terminal Charges

$$Q_{g,intrinsic} = NFIN_{total} \cdot C_{ox,eff} \cdot W_{eff,CV} \cdot L_{eff,CV} \cdot (q_g) \quad (3.309)$$

$$Q_{d,intrinsic} = NFIN_{total} \cdot C_{ox,eff} \cdot W_{eff,CV} \cdot L_{eff,CV} \cdot (-q_d) \quad (3.310)$$

$$Q_{b,intrinsic} = NFIN_{total} \cdot C_{ox} \cdot W_{eff,CV} \cdot L_{eff,CV} \cdot (-q_b) \quad (3.311)$$

$$Q_{s,intrinsic} = -Q_{g,intrinsic} - Q_{d,intrinsic} - Q_{b,intrinsic} \quad (3.312)$$

$$Q_{g,acc} = NFIN_{total} \cdot C_{ox,acc} \cdot W_{eff,CV0} \cdot L_{eff,CV} \cdot (-q_{i,acc}) \quad (3.313)$$

$$Q_{b,acc} = NFIN_{total} \cdot C_{ox,acc} \cdot W_{eff,CV0} \cdot L_{eff,CV} \cdot (-q_{i,acc}) \quad (3.314)$$

3.13 Parasitic resistances and capacitance models

In this section we will describe the models for parasitic resistances and capacitances in BSIM-MG.

BSIM-MG models the parasitic source/drain resistance in two components: a bias dependent extension resistance and a bias independent diffusion resistance. Parasitic gate resistance is modeled as well.

The parasitic capacitance model in BSIM-MG includes a bias-independent fringe capacitance, a bias-dependent overlap capacitance, and substrate capacitances. In the case of MuGFETs on SOI, the substrate capacitances are from source/drain/gate to the substrate

through the buried oxide. For MuGFETs on bulk substrate, an additional junction capacitor is modeled, which we will describe along with the junction current model in section 3.18.

Bias-dependent extension resistance

The bias-dependent extension resistance model is adopted from BSIM4 [10]. There are two options for this bias dependent component. In BSIM3 models $R_{ds}(V)$ is modeled internally through the I-V equation and symmetry is assumed for the source and drain sides. BSIM4 and BSIM-MG keep this option for the sake of simulation efficiency. In addition, BSIM4 and BSIM-MG allow the source extension resistance $R_s(V)$ and the drain extension resistance $R_d(V)$ to be external and asymmetric (i.e. $R_s(V)$ and $R_d(V)$ can be connected between the external and internal source and drain nodes, respectively; furthermore, $R_s(V)$ does not have to be equal to $R_d(V)$). This feature makes accurate RF CMOS simulation possible.

The internal $R_{ds}(V)$ option can be invoked by setting the model selector $RDSMOD = 0$ (internal) and the external one for $R_s(V)$ and $R_d(V)$ by setting $RDSMOD = 1$ (external). The expressions for source/drain series resistances are as follows:

$RDSMOD = 0$ (Internal)

$$R_{ds} = \frac{1}{NFIN_{total} \times W_{eff}0^{WR_i}} \cdot \left(RDSWMIN(T) + \frac{RDSW(T)}{1 + PRWG_i \cdot q_{ia}} \right) \quad (3.315)$$

$$D_r = 1.0 + NFIN_{total} \times \mu_0(T) \cdot C_{ox} \cdot \frac{W_{eff}}{L_{eff}} \cdot \frac{i_{ds0}}{\Delta q_i} \cdot \frac{1}{D_{vsat} \cdot D_{mob}} \\ (R_{ds} + R_{s,geo} + R_{d,geo}) \quad (3.316)$$

D_r goes into the denominator of the final I_{ds} expression.

RDSMOD = 1 (External)

$$V_{gs,eff} = \frac{1}{2} \left[V_{gs} - V_{fbsd} + \sqrt{(V_{gs} - V_{fbsd})^2 + 10^{-4}} \right] \quad (3.317)$$

$$V_{gd,eff} = \frac{1}{2} \left[V_{gd} - V_{fbsd} + \sqrt{(V_{gd} - V_{fbsd})^2 + 10^{-4}} \right] \quad (3.318)$$

$$R_{source} = \frac{1}{Weff0^{WR_i} \cdot NFIN_{total}} \cdot \left(RSWMIN(T) + \frac{RSW(T)}{1 + PRWG_i \cdot V_{gs,eff}} \right) + R_{s,geo} \quad (3.319)$$

$$R_{drain} = \frac{1}{Weff0^{WR_i} \cdot NFIN_{total}} \cdot \left(RDWMIN(T) + \frac{RDW(T)}{1 + PRWG_i \cdot V_{gd,eff}} \right) + R_{d,geo} \quad (3.320)$$

$$D_r = 1.0 \quad (3.321)$$

$R_{s,geo}$ and $R_{d,geo}$ are the source and drain diffusion resistances, which we will describe as follows.

Sheet resistance model

BSIM-MG offers two models for the source/drain diffusion resistance, selected by a parameter $RGEOMOD$. If $RGEOMOD = 0$, the resistance will be simply calculated as the sheet resistance ($RSHS, RSHD$) times the number of squares (NRS, NRD):

$RGEOMOD = 0$ (sheet resistance model)

$$R_{s,geo} = NRS \cdot RSHS \quad (3.322)$$

$$R_{d,geo} = NRD \cdot RSHD \quad (3.323)$$

Diffusion resistance model for variability modeling

If $RGEOMOD = 1$, a diffusion resistance model for variability modeling will be invoked. The physically-derived model captures the complex dependences of resistance on the geometry of FinFETs.

$RGEOMOD = 1$ is derived based on the FinFET structure (single-fin or multi-fin with merged source/drain). Figure 1 shows the cross section of a double-gate FinFET with raised

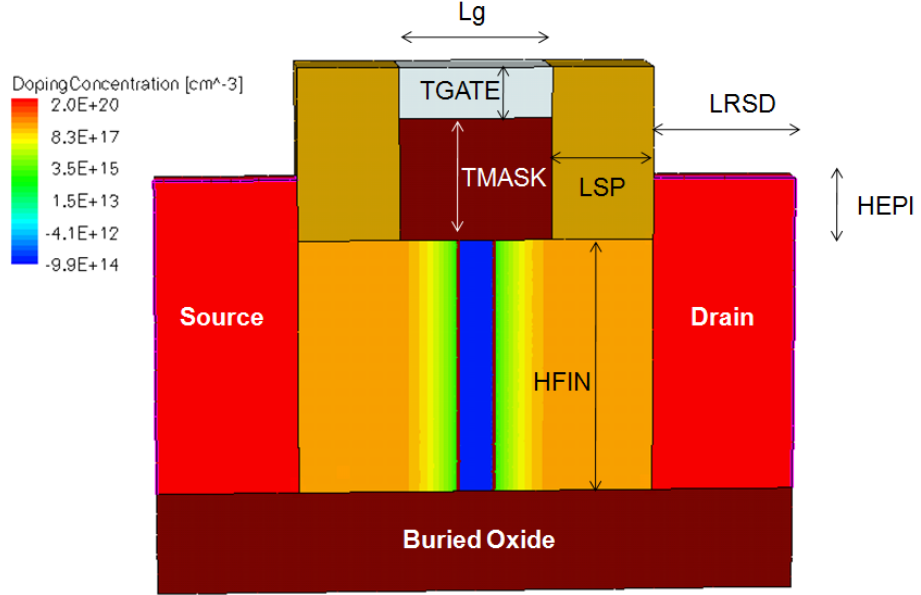


Figure 1: Cross section of a raised source/drain double-gate FinFET and symbol definition

source/drain (RSD) along the source-drain direction. L_g (gate length) and $TOXP$ (physical oxide thickness, not shown in figure 1) are calculated in section 3.1. A hard mask with thickness $TMASK$ often exists on top of the fin. If $TMASK = 0$, the model will assume there is no hard mask and the dielectric thickness on top of the fin is $TOXP$ (triple-gate FinFET). In the figure, LSP is the spacer thickness, $LRSD$ is the length of the raised source/drain, $HFIN$ is the fin height, $TGATE$ is the gate height, and $HEPI$ is the height of the epitaxial silicon above the fin. These parameters are specified by the user.

The resistivity of the raised source/drain can be specified with the parameter $RHORSD$.

If $RHORSD$ is not given the resistivity is calculated using the following expressions [11]:

$$\mu_{MAX} = \begin{cases} 1417 & \text{for NMOS} \\ 470.5 & \text{for PMOS} \end{cases} \quad (3.324)$$

$$\mu_{rsd} = \begin{cases} 52.2 + \frac{\mu_{MAX}-52.2}{1+\left(\frac{NSD}{9.68\times 10^{22} m^{-3}}\right)^{0.680}} - \frac{43.4}{1+\left(\frac{3.41\times 10^{26} m^{-3}}{NSD}\right)^{2.0}} cm^2/V-s & \text{for NMOS} \\ 44.9 + \frac{\mu_{MAX}-44.9}{1+\left(\frac{NSD}{2.23\times 10^{23} m^{-3}}\right)^{0.719}} - \frac{29.0}{1+\left(\frac{6.10\times 10^{26} m^{-3}}{NSD}\right)^{2.0}} cm^2/V-s & \text{for PMOS} \end{cases} \quad (3.325)$$

$$\rho_{RSD} = \frac{1}{q NSD \mu_{RSD}} \quad (3.326)$$

where NSD is the active doping concentration of the raised source/drain. The resistivity of the extension region under the spacer, ρ_{ext} , can be specified with the parameter $RHOEXT$. If $RHOEXT$ is not given, the resistivity is set to ρ_{RSD} .

The diffusion resistance includes three components: the resistance of the extension region under the spacer (R_{ext}), the spreading resistance due to current spreading from the extension region into the raised source/drain (R_{sp}) and the resistance of the raised source/drain region (R_{con}).

To calculate R_{ext} we assume a doping profile as shown in figure 2. The doping concentration at the channel edge is $NSDE$ (default: $2 \times 10^{19} cm^{-3}$) ¹. The doping concentration increases exponentially with position until it reaches NSD . The doping gradient can be specified with the parameter LDG in units of meters per decade. The extension resistance is given by:

$$R_{ext} = \frac{\rho_{RSD}}{A_{fin0}} \left[LSP + \Delta L - LDG \cdot \log \left(\frac{NSD}{NSDE} \right) + \frac{LDG}{\ln(10)} \left(\frac{NSD}{NSDE} - 1 \right) \right] \quad (3.327)$$

where

$$A_{fin0} = HFIN \times TFIN \times NFIN \quad (3.328)$$

The spreading resistance, R_{sp} is derived by assuming the current spreads at a constant angle θ_{RSP} in the raised source/drain. Comparison with numerical simulation shows that θ_{RSP} is

¹the channel edge may be on either side of the gate edge depending of the sign of ΔL

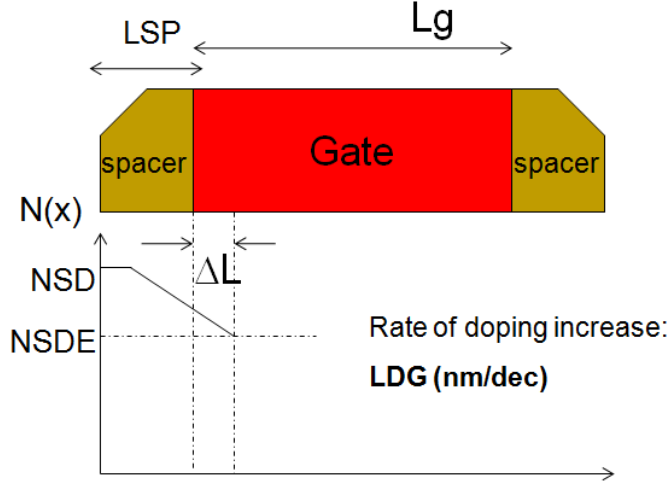


Figure 2: Doping profile considered in $RGEOMOD = 1$.

around 55 degrees. The spreading resistance is given as a function of the cross sectional area of the raised source/drain (A_{rsd}) and the effective fin area (A_{fin}):

$$R_{sp} = \frac{\rho_{RSR} \cdot \cot(\theta_{rsp})}{\sqrt{\pi} \cdot NFIN} \cdot \left[\frac{1}{\sqrt{A_{fin}}} - \frac{2}{\sqrt{A_{rsd}}} + \sqrt{\frac{A_{fin}}{A_{rsd}^2}} \right] \quad (3.329)$$

A_{fin} is given by

$$A_{fin} = \begin{cases} HFIN \times TFIN & \text{for } HEPI \geq 0 \\ (HFIN + HEPI) \times TFIN & \text{for } HEPI < 0 \end{cases} \quad (3.330)$$

Here $HEPI < 0$ is the case where silicidation removes part of the silicon, forming a recessed source/drain (Fig. 3).



Figure 3: Lithography-defined FinFET with a smaller source/drain height compared to the fin height (silicide not shown).

The raised source drain cross sectional area (A_{rsd}) is given by

$$A_{rsd} = \begin{cases} FPITCH \cdot HFIN + \left[TFIN + \right. \\ \left. (FPITCH - TFIN) \cdot CRATIO \right] \cdot HEPI & \text{for } HEPI \geq 0 \\ FPITCH \cdot (HFIN + HEPI) & \text{for } HEPI < 0 \end{cases} \quad (3.331)$$

In the above formula, we have assumed a rectangular geometry for negative $HEPI$ (Figure. 3) and the cross sectional area is simply the fin pitch times the final height of the source/drain. For positive $HEPI$, we have considered a RSD formed by selective epitaxial growth, in which case the RSD may not be rectangular (e.g. fig. 4). In calculating the cross sectional area, we take into account the non-rectangular corner through the parameter $CRATIO$. $CRATIO$ is defined as the ratio of corner area filled with silicon to the total corner area. In the example given in figure 5, $CRATIO$ is 0.5.

The calculation of the contact resistance (R_{con}) is based on the transmission line model [12]. R_{con} is expressed as a function of the total area ($A_{rsd,total}$) and the total perimeter ($P_{rsd,total}$):

$$R_{rsd,TML} = \frac{\rho_{RSD} \cdot l_t}{A_{rsd,total}} \cdot \frac{\cosh(\alpha) + \eta \cdot \sinh(\alpha)}{\sinh(\alpha) + \cdot \cosh(\alpha)} \quad (3.332)$$

$$\alpha = \frac{LRSD}{l_t} \quad (3.333)$$

$$l_t = \sqrt{\frac{RHOC \cdot A_{rsd,total}}{\rho_{RSD} \cdot P_{rsd,total}}} \quad (3.334)$$

where RHOC is the contact resistivity at the silicide/silicon interface.

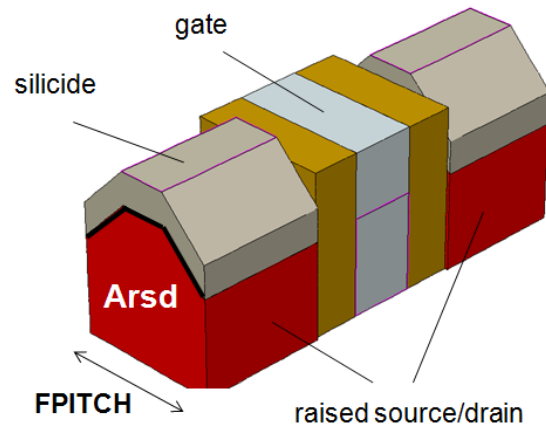


Figure 4: FinFET with non-rectangular epi and top silicide

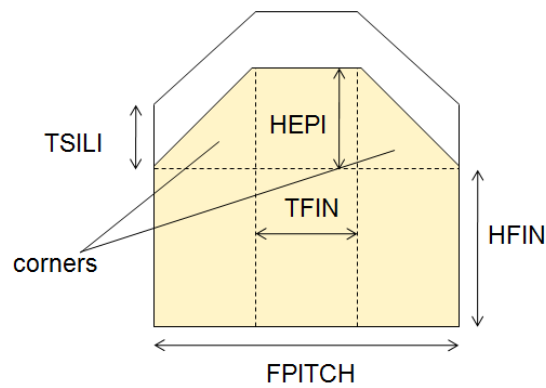


Figure 5: 2-D cross section of a FinFET with non-rectangular epi and top silicide

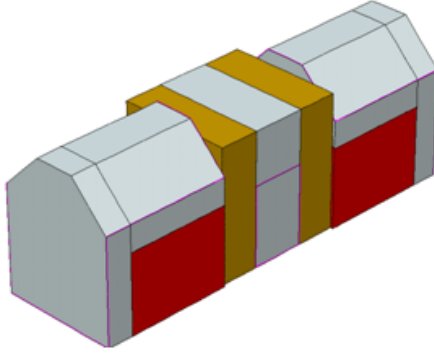


Figure 6: FinFET with a non-rectangular epi and silicide on top and two ends.

The total area and perimeter are given by

$$A_{rsd,total} = A_{rsd} \times NFIN + ARSDEND \quad (3.335)$$

$$P_{rsd,total} = (FPITCH + DELTAPRSD) \times NFIN + PRSSEND \quad (3.336)$$

DELTAPRSD is the per-fin increase in perimeter due to non-rectangular raised source/drains. *ARSDEND* and *PRSSEND* are introduced to model the additional cross-sectional area and the additional perimeter, respectively, at the two ends of a multi-fin FinFET.

SDTERM = 1 indicates the source/drain are terminated with silicide (Fig. 6), while *SDTERM* = 0 indicates they are not. η is given by

$$\eta = \begin{cases} \frac{\rho_{RSD} \cdot l_t}{RHOC} & SDTERM = 1 \\ 0.0 & SDTERM = 0 \end{cases} \quad (3.337)$$

In the case of the recessed source/drain, a side component of the contact resistance must be modeled as well. It is given by

$$R_{rsd,side} = \frac{RHOC}{NFIN \cdot (-HEPI) \cdot TFIN} \quad (3.338)$$

Finally, the total diffusion resistance is given by

$$R_{s,geo} = R_{d,geo} = \frac{R_{rsd} + R_{ext}}{NF} \cdot \left[RGEOA + RGEOB \times TFIN + RGEOC \times FPITCH + RGEOD \times LRSD + RGEOE \times HEPI \right] \quad (3.339)$$

where

$$R_{rsd} = \begin{cases} R_{rsd,TML} + R_{sp} & \text{for } HEPI \geq 0 \\ \frac{(R_{rsd,TML} + R_{sp}) \times R_{rsd,side}}{(R_{rsd,TML} + R_{sp}) + R_{rsd,side}} & \text{for } HEPI < 0 \end{cases} \quad (3.340)$$

Fitting parameters RGEOA, RGEOB, RGEOC, RGEOD and RGEOE are introduced for fitting flexibility.

Gate electrode resistance model

The gate electrode resistance model can be switched on by setting $RGATEMOD = 1$. This introduces an internal node "ge". The gate electrode resistor (R_{geltl}) is placed between the external "g" node and the internal "ge" node.

The gate electrode resistance model takes into account the number of gate contacts, $NGCON$. $NGCON = 1$ indicates single-sided contact; $NGCON = 2$ indicates double-sided contact. R_{geltl} is given by

$$R_{geltl} = \begin{cases} \frac{RGEXT + RGFIN \cdot NFIN}{3 \cdot NF} & \text{for } NGCON = 1 \\ \frac{RGEXT + RGFIN \cdot NFIN}{12 \cdot NF} & \text{for } NGCON = 2 \end{cases} \quad (3.341)$$

Bias-dependent overlap capacitance model

An accurate overlap capacitance model is essential. This is especially true for the drain side where the effect of the capacitance is amplified by the transistor gain. The overlap capacitance changes with gate to source and gate to drain biases. In LDD MOSFETs a substantial portion of the LDD region can be depleted, both in the vertical and lateral directions. This can lead to a large reduction of the overlap capacitance. This LDD region can be in accumulation or depletion. We use a single equation for both regions by using such smoothing parameters as $V_{gs,overlap}$ and $V_{gd,overlap}$ for the source and drain side, respectively. Unlike the case with the

intrinsic capacitance, the overlap capacitances are reciprocal. In other words, $C_{gs,overlap} = C_{sg,overlap}$ and $C_{gd,overlap} = C_{dg,overlap}$.

The bias-dependent overlap capacitance model in BSIM-MG is adopted from BSIM4 [10] for $CGEOMOD = 0$ and $CGEOMOD = 2$. The overlap charge is given by:

$$\frac{Q_{gs,ov}}{NFIN_{total} \cdot WeffCV} = CGSO \cdot V_{gs} + \\ CGSL \cdot \left[V_{gs} - V_{fbsd} - V_{gs,overlap} - \frac{CKAPPAS}{2} \left(\sqrt{1 - \frac{4V_{gs,overlap}}{CKAPPAS}} - 1 \right) \right] \quad (3.342)$$

$$\frac{Q_{gd,ov}}{NFIN_{total} \cdot WeffCV} = CGDO \cdot V_{gd} + \\ CGDL \cdot \left[V_{gd} - V_{fbsd} - V_{gd,overlap} - \frac{CKAPPAD}{2} \left(\sqrt{1 - \frac{4V_{gd,overlap}}{CKAPPAD}} - 1 \right) \right] \quad (3.343)$$

$$V_{gs,overlap} = \frac{1}{2} \left[V_{gs} - V_{fbsd} + \delta_1 - \sqrt{(V_{gs} - V_{fbsd} + \delta_1)^2 + 4\delta_1} \right] \quad (3.344)$$

$$V_{gd,overlap} = \frac{1}{2} \left[V_{gd} - V_{fbsd} + \delta_1 - \sqrt{(V_{gd} - V_{fbsd} + \delta_1)^2 + 4\delta_1} \right] \quad (3.345)$$

$$\delta_1 = 0.02V \quad (3.346)$$

For $CGEOMOD = 1$, the overlap capacitors are bias-independent, as we will discuss in the end of this section.

Substrate parasitics

In multi-gate devices such as the FinFET, there is capacitive coupling from the source/drain to the substrate through the buried oxide. This component is modeled in BSIM-MG and is given by:

$$C_{sbox} = C_{box} \cdot ASEO + C_{box,sw} \cdot (PSEO - FPITCH * NFIN_{total}) \quad (3.347)$$

$$C_{dbox} = C_{box} \cdot ADEO + C_{box,sw} \cdot (PDEO - FPITCH * NFIN_{total}) \quad (3.348)$$

where the side component per width is [13]

$$C_{box,sw} = CSDESW \cdot \ln \left(1 + \frac{HFIN}{EOTBOX} \right) \quad (3.349)$$

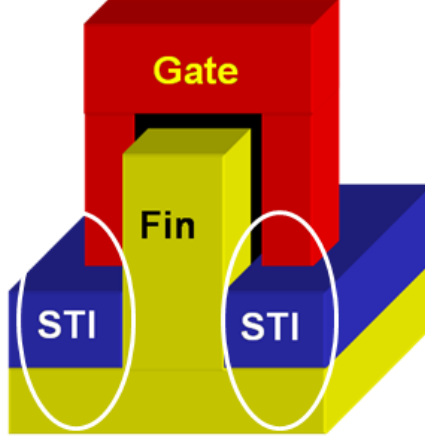


Figure 7: Illustration of the direct gate-to-substrate overlap region in the FinFET.

There is also direct capacitive coupling from the gate to the substrate in FinFETs (Fig. 7). Following BSIM4[10] this component is given by

$$C_{ge,overlap} = CGBO \cdot L_{eff,CV} \quad (3.350)$$

C_{sbox} , C_{dbox} and $C_{ge,overlap}$ are all linear capacitors.

Fringe capacitances and capacitance model selectors

The fringing capacitance consists of a bias-independent outer fringing capacitance and a bias-dependent inner fringing capacitance. Only the bias-independent outer fringing capacitance is modeled.

BSIM-MG offers 3 models for the outer fringe capacitance, selected by $CGEOMOD$.

For $CGEOMOD = 0$, the fringe and overlap capacitances are proportional to the number of fins and the effective width. The fringe capacitance is given by:

$$\underline{CGEOMOD = 0}$$

$$C_{gs,fr} = NFIN_{total} \cdot W_{eff,CV} \cdot CFS_i \quad (3.351)$$

$$C_{gd,fr} = NFIN_{total} \cdot W_{eff,CV} \cdot CFD_i \quad (3.352)$$

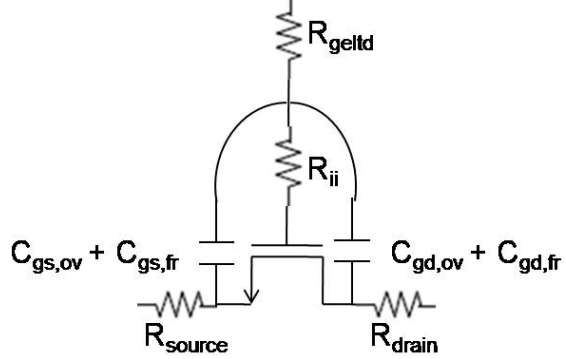


Figure 8: R-C network for $CGEOMOD=0$, $NQSMOD=1$, $RGATEMOD=1$ and $RDSMOD=1$. If $NQSMOD$, $RGATEMOD$ or $RDSMOD$ is 0, then the corresponding resistances become 0 and the nodes collapse.

Fig. 8 illustrates the parasitic resistance and capacitance network used for $CGEOMOD = 0$.

In some multi-gate applications the parasitic capacitances are not directly proportional to the width of the device. BSIM-MG offers $CGEOMOD = 1$ so that the fringe and overlap capacitance values can be directly specified without assuming any width dependencies. The simple expressions for fringe and overlap capacitances in $CGEOMOD = 1$ are:

$$\underline{CGEOMOD = 1}$$

$$C_{gs,ov} = COVS_i \quad (3.353)$$

$$C_{gd,ov} = COVD_i \quad (3.354)$$

$$C_{gs,fr} = CGSP \quad (3.355)$$

$$C_{gd,fr} = CGDP \quad (3.356)$$

$$C_{ds,fr} = CDSP \quad (3.357)$$

The parasitic resistance and capacitance network for $CGEOMOD = 1$ is illustrated in Fig. 9.

If $CGEOMOD = 2$, an outer fringe capacitance model for variability modeling which address the complex dependencies on the FinFET geometry will be invoked. $RGEOMOD = 1$ and $CGEOMOD = 2$ share the same set of input parameters and can be used at the same

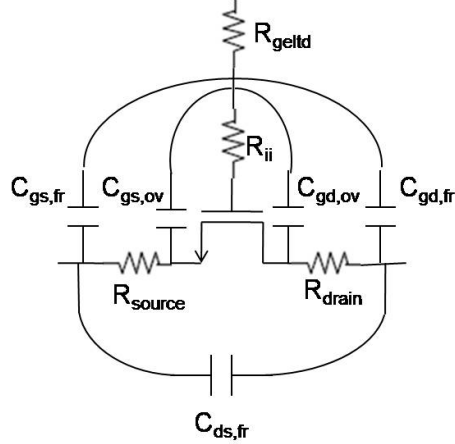


Figure 9: R-C network for CGEOMOD=1, NQSMOD=1, RGATEMOD=1 and RDMSMOD=1. If NQSMOD, RGATEMOD or RDMSMOD is 0, then the corresponding resistances become 0 and the nodes collapse.

time. Both models are derived based on the FinFET structure (single-fin or multi-fin with merged source/drain).

In $CGEOMOD = 2$ the fringe capacitance is partitioned into a top component, a corner component and a side component (Fig. 10). The top and side components are calculated based on a 2-D fringe capacitance model, which has been derived and calibrated to numerical simulation in [14]. The corner component is calculated based on the formula of parallel plate capacitors.

$$C_{fr,top} = C_{fringe,2D}(H_g, H_{rsd}, LRSD) \times TFIN \times NFIN \quad (3.358)$$

$$C_{fr,side} = 2 \times C_{fringe,2D}(W_g, T_{rsd}, LRSD) \times HFIN \times NFIN \quad (3.359)$$

$$C_{corner} = \frac{\epsilon_{sp}}{LSP} \cdot [A_{corner} \times NFIN + ARSDEND + ASILIEND] \quad (3.360)$$

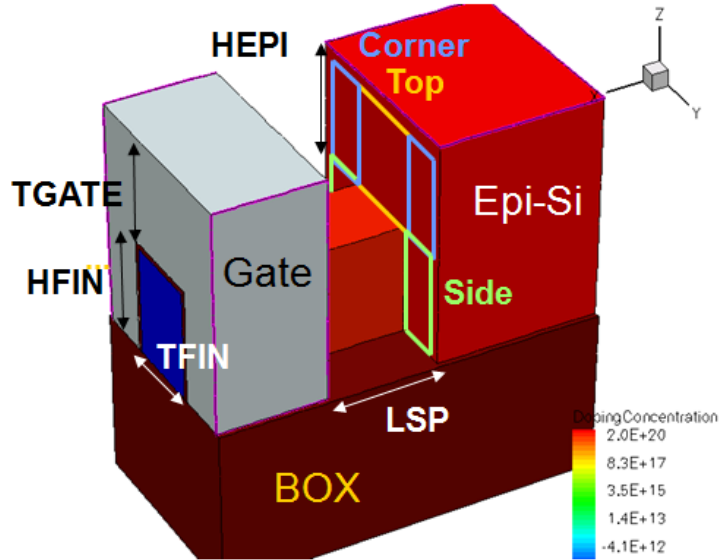


Figure 10: Illustration of top, corner and side components of the outer fringe capacitance

where

$$H_g = TGATE + TMASK \quad (3.361)$$

$$T_{rsd} = \frac{1}{2}(FPITCH - TFIN) \quad (3.362)$$

$$W_g = T_{rsd} - TOXP \quad (3.363)$$

$$H_{rsd} = HEPI + TSILI \quad (3.364)$$

ARSDEND and ASILIEND are the additional area of silicon and silicide, respectively, at the two ends of a multi-fin FinFET.

The three components are summed up to give the total fringe capacitance. Several fitting

parameters are added to aid fitting. The final expression is:

$$\underline{CGEOMOD = 2}$$

$$C_{fr,geo} = (C_{corner} + C_{fr,top} + CGEOE \cdot C_{fr,side}) \times NF \times [CGEOA + CGEOB \cdot TFIN + CGEOC \cdot FPITCH + CGEOD \cdot LRSD] \quad (3.365)$$

For the case of $TMASK > 0$ the fringe capacitances are calculated a little differently, since the 2D model is valid only for a thin T_{ox} . C_{corner} is set to 0. $C_{fr,top}$ is proportional to $FPITCH$ and is given by

$$C_{fr,top} = \left\{ 3.467 \times 10^{-11} \cdot \ln \left(\frac{EPSRSP \cdot 10^{-7}}{3.9 \cdot LSP} \right) + 0.942 \cdot H_{rsd} \cdot \frac{\epsilon_{sp}}{LSP} \right\} \cdot ([TFIN + (FPITCH - TFIN) \cdot CRATIO] \cdot NFIN \quad (3.366)$$

3.14 Impact Ionization and GIDL/GISL Model

Impact Ionization Current

I_{ii} can be switched off by setting $IIMOD = 0$

$$\underline{\text{Case: } IIMOD = 1} \quad (3.367)$$

$$I_{ii} = \frac{ALPHA0_i + ALPHA1_i \cdot L_{eff}}{L_{eff}} (V_{ds} - V_{dseff}) \cdot e^{\frac{BETA0(T)}{V_{ds} - V_{dseff}}} \cdot I_{ds} \quad (3.368)$$

Case: $IIMOD = 2$

$$I_{ii} = \text{ALPHAI}i \cdot I_{ds} \cdot \exp \left(\frac{V_{diff}}{\text{BETAII}2_i + \text{BETAII}1_i V_{diff} + \text{BETAII}0_i V_{diff}^2} \right) \quad (3.369)$$

$$V_{diff} = V_{ds} - V_{dsatii} \quad (3.370)$$

$$V_{dsatii} = V_{gsStep} \cdot \left(1 - \frac{LII_i}{L_{eff}} \right) \quad (3.371)$$

$$V_{gsStep} = \left(\frac{ESATII_i L_{eff}}{1 + ESATII_i L_{eff}} \right) \left(\frac{1}{1 + SII1_i V_{gsfbeff}} + SII2_i \right) \left(\frac{SII0(T) \cdot V_{gsfbeff}}{1 + SIID_i V_{ds}} \right) \quad (3.372)$$

Gate-Induced-Drain/Source-Leakage Current

GIDL/GISL are calculated only for $GIDLMod = 1$

$$T0 = AGIDL_i \cdot W_{eff0} \cdot \left(\frac{V_{ds} - V_{gs} - EGIDL_i + V_{fbsd}}{\epsilon_{ratio} \cdot EOT} \right)^{PGIDL_i} \times \exp \left(-\frac{\epsilon_{ratio} \cdot EOT \cdot BGIDL(T)}{V_{ds} - V_{gs} - EGIDL_i + V_{fbsd}} \right) \times NFIN_{total} \quad (3.373)$$

$$I_{gidl} = \begin{cases} T0 \cdot \frac{V_{de}^3}{CGIDL_i + V_{de}^3} & \text{for } BULKMOD = 1 \\ T0 \cdot V_{ds} & \text{for } BULKMOD = 0 \end{cases} \quad (3.374)$$

$$T1 = AGISL_i \cdot W_{eff0} \cdot \left(\frac{-V_{ds} - V_{gd} - EGISL_i + V_{fbsd}}{\epsilon_{ratio} \cdot EOT} \right)^{PGISL_i} \times \exp \left(-\frac{\epsilon_{ratio} \cdot EOT \cdot BGISL(T)}{-V_{ds} - V_{gd} - EGISL_i + V_{fbsd}} \right) \times NFIN_{total} \quad (3.375)$$

$$I_{gisl} = \begin{cases} T1 \cdot \frac{V_{se}^3}{CGISL_i + V_{se}^3} & \text{for } BULKMOD = 1 \\ T1 \cdot V_{sd} & \text{for } BULKMOD = 0 \end{cases} \quad (3.376)$$

3.15 Gate Tunneling Current

$$T_{ox,ratio} = \frac{1}{TOXP^2} \quad (3.377)$$

Gate to body current I_{gbinv} and I_{gbacc} calculated only if $IGBMOD = 1$

$$A = 3.75956 \times 10^{-7} \quad (3.378)$$

$$B = 9.82222 \times 10^{11} \quad (3.379)$$

$$V_{aux,igbinv} = NIGBINV_i \cdot \frac{kT}{q} \cdot \ln \left(1 + \exp \left(\frac{q_{ia} - EIGBINV_i}{NIGBINV_i \cdot kT/q} \right) \right) \quad (3.380)$$

$$\begin{aligned} I_{gbinv} = & W_{eff0} \cdot L_{eff} \cdot A \cdot T_{ox,ratio} \cdot V_{ge} \cdot V_{aux,igbinv} \cdot Igtemp \cdot NFIN_{total} \\ & \times \exp(-B \cdot TOXP \cdot (AIGBINV_i - BIGBINV_i \cdot q_{ia}) \cdot (1 + CIGBINV_i \cdot q_{ia})) \end{aligned} \quad (3.381)$$

$$A = 4.97232 \times 10^{-7} \quad (3.382)$$

$$B = 7.45669 \times 10^{11} \quad (3.383)$$

$$V_{fbzb} = \Delta\Phi - E_g/2 - \phi_B \quad (3.384)$$

$$T0 = V_{fbzb} - V_{ge} \quad (3.385)$$

$$T1 = T0 - 0.02; \quad (3.386)$$

$$V_{aux,igbacc} = NIGBACC_i \cdot \frac{kT}{q} \cdot \ln \left(1 + \exp \left(\frac{T0}{NIGBACC_i \cdot kT/q} \right) \right) \quad (3.387)$$

$$V_{oxacc} = \begin{cases} q_{i,acc} & \text{for BULKMOD=1 and CAPMOD=1} \\ 0.5 \cdot [T1 + \sqrt{(T1)^2 - 0.08 \cdot V_{fbzb}}] & \text{for CAPMOD } \neq 1 \text{ and } V_{fbzb} \leq 0 \\ 0.5 \cdot [T1 + \sqrt{(T1)^2 + 0.08 \cdot V_{fbzb}}] & \text{for CAPMOD } \neq 1 \text{ and } V_{fbzb} > 0 \end{cases} \quad (3.388)$$

$$\begin{aligned} I_{gbacc} = & W_{eff0} \cdot L_{eff} \cdot A \cdot T_{ox,ratio} \cdot V_{ge} \cdot V_{aux,igbacc} \cdot Igtemp \cdot NFIN_{total} \\ & \times \exp(-B \cdot TOXP \cdot (AIGBACC_i - BIGBACC_i \cdot V_{oxacc}) \cdot (1 + CIGBACC_i \cdot V_{oxacc})) \end{aligned} \quad (3.389)$$

For BULKMOD=1, I_{gb} simply flows from the gate into the substrate. For BULKMOD=0, I_{gb} mostly flows into the source because the potential barrier for holes is lower at the source, which has a lower potential. To ensure continuity when V_{ds} switches sign, I_{gb} is partitioned into a source component, I_{gbs} and a drain component, I_{gbd} using a partition function:

$$I_{gbs} = (I_{gbinv} + I_{gbacc}) \cdot W_f \quad (3.390)$$

$$I_{gbd} = (I_{gbinv} + I_{gbacc}) \cdot W_r \quad (3.391)$$

Gate to channel current I_{gc} is calculated only for $IGCMOD = 1$

$$A = \begin{cases} 4.97232 \times 10^{-7} & \text{for NMOS} \\ 3.42536 \times 10^{-7} & \text{for PMOS} \end{cases} \quad (3.392)$$

$$B = \begin{cases} 7.45669 \times 10^{11} & \text{for NMOS} \\ 1.16645 \times 10^{12} & \text{for PMOS} \end{cases} \quad (3.393)$$

$$T0 = q_{ia} \cdot (V_{ge} - 0.5 \cdot V_{dsx} + 0.5 \cdot V_{es} + 0.5 \cdot V_{ed}) \quad (3.394)$$

$$\begin{aligned} I_{gc0} = & W_{eff0} \cdot L_{eff} \cdot A \cdot T_{ox,ratio} \cdot Igtemp \cdot NFIN_{total} \cdot T0 \\ & \times \exp(-B \cdot TOXP \cdot (AIGC_i - BIGC_i \cdot q_{ia}) \cdot (1 + CIGC_i \cdot q_{ia})) \end{aligned} \quad (3.395)$$

$$V_{dseffx} = \sqrt{V_{dseffx}^2 + 0.01} - 0.1 \quad (3.396)$$

$$I_{gcs} = I_{gc0} \cdot \frac{PIGCD_i \cdot V_{dseffx} + \exp(PIGCD_i \cdot V_{dseffx}) - 1.0 + 1.0E - 4}{PIGCD_i^2 \cdot V_{dseffx}^2 + 2.0E - 4} \quad (3.397)$$

$$I_{gcd} = I_{gc0} \cdot \frac{1.0 - (PIGCD_i \cdot V_{dseffx} + 1.0) \exp(-PIGCD_i \cdot V_{dseffx}) + 1.0E - 4}{PIGCD_i^2 \cdot V_{dseffx}^2 + 2.0E - 4} \quad (3.398)$$

Gate to source/drain current I_{gs}, I_{gd} are calculated only for $IGCMOD = 1$

$$A = \begin{cases} 4.97232 \times 10^{-7} & \text{for NMOS} \\ 3.42536 \times 10^{-7} & \text{for PMOS} \end{cases} \quad (3.399)$$

$$B = \begin{cases} 7.45669 \times 10^{11} & \text{for NMOS} \\ 1.16645 \times 10^{12} & \text{for PMOS} \end{cases} \quad (3.400)$$

$$V'_{gs} = \sqrt{V_{gs}^2 + 10^{-4}} \quad (3.401)$$

$$V'_{gd} = \sqrt{V_{gd}^2 + 10^{-4}} \quad (3.402)$$

$$i_{gsd,mult} = Igtemp \cdot \frac{W_{eff0} \cdot A}{(TOXP \cdot POXEDGE_i)^2} \cdot \left(\frac{TOXREF}{TOXP \cdot POXEDGE_i} \right)^{NTOXi} \quad (3.403)$$

$$\begin{aligned} I_{gs} = & i_{gsd,mult} \cdot DLCIGS \cdot V_{gs} \cdot V'_{gs} \cdot NFIN_{total} \\ & \times \exp(-B \cdot TOXP \cdot POXEDGE_i \cdot (AIGS_i - BIGS_i \cdot V'_{gs}) \cdot (1 + CIGS_i \cdot V'_{gs})) \end{aligned} \quad (3.404)$$

$$\begin{aligned} I_{gd} = & i_{gsd,mult} \cdot DLCIGD \cdot V_{gd} \cdot V'_{gd} \cdot NFIN_{total} \\ & \times \exp(-B \cdot TOXP \cdot POXEDGE_i \cdot (AIGD_i - BIGD_i \cdot V'_{gd}) \cdot (1 + CIGD_i \cdot V'_{gd})) \end{aligned} \quad (3.405)$$

3.16 Non Quasi-static Models

This version offers three different Non quasi-static (NQS) models. Each of these can be turned on/off using the $NQSMOD$ switch. Setting $NQSMOD = 0$ turns off all NQS models and switches to plain quasi-static calculations.

Gate Resistance Model ($NQSMOD = 1$)

NQS effects for $NQSMOD = 1$ is modeled through an effective intrinsic input resistance, R_{ii} [15]. This would introduce a gate node in between the intrinsic gate and the physical gate electrode resistance (RGATEMOD). This node collapses to the intrinsic gate if the user turns

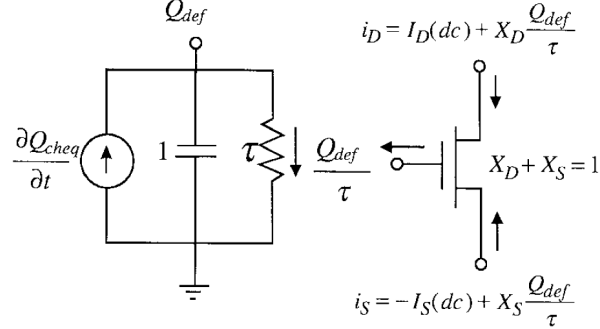


Figure 11: R-C network for calculating deficient charge Q_{def} and the instantaneous charge, Q_{def}/τ is used in place of the quasi-static charges. [17]

off this model.

$$I_{dovVds} = \mu_0(T)C_{ox}\frac{W_{eff}}{L_{eff}}q_{ia} \cdot \frac{M_{oc}}{D_{vsat}} \quad (3.406)$$

$$\frac{1}{R_{ii}} = \frac{NF}{NFIN} \cdot XRCRG1_i \cdot \left(I_{dovVds} + XRCRG2 \cdot \frac{\mu_{eff}C_{oxe}W_{eff}kT}{qL_{eff}} \right) \quad (3.407)$$

Charge Deficit Model ($NQSMOD = 2$)

The charge-deficit model from BSIM4 has been adopted here [16]. Based on a relaxation time approach, the deficient charge (equilibrium quasi-static charge minus the instantaneous channel charge) is kept track through a R-C sub-circuit [17]. An extra node whose voltage is equal to the deficient charge is introduced for this purpose. The instantaneous channel charge that is obtained from the self-consistent solution of the MOSFET and R-C sub-circuit is then split between the source and drain using a partition ratio ($X_{d,part}$) calculated from the quasi-static charges. A capacitance of 1 Farad is used for this purpose, while the resistance is give by the inverse of the relaxation time constant, $1/\tau$.

$$X_{d,part} = \frac{qd}{qg} \quad (3.408)$$

$$I_{dovVds} = \mu_0(T)C_{ox}\frac{W_{eff}}{L_{eff}}q_{ia}\frac{M_{oc}}{D_{vsat}} \quad (3.409)$$

$$\frac{1}{R_{ii}} = \frac{NF}{NFIN} \cdot XRCRG1_i \cdot \left(I_{dovVds} + XRCRG2 \cdot \frac{\mu_{eff}C_{oxe}W_{eff}kT}{qL_{eff}} \right) \quad (3.410)$$

$$\frac{1}{\tau} = \frac{1}{R_{ii} \cdot C_{ox} \cdot W_{eff} \cdot L_{eff}} \quad (3.411)$$

Charge Segmentation Model ($NQSMOD = 3$)

Note: This model is not supported for $COREMOD = 1 \&& GEOMOD \neq 3$, i.e. for double gate and likes together with the simplified surface potential solution.

The charge segmentation approach is a simplified form of a full-fledged segmentation where a long channel transistor is divided into N number of segments each of length $\frac{L}{N}$. The approach used here takes advantage of the fact that the core I-V and the C-V model can be broken down and expressed into separate functions of the source end and the drain end channel charge (q_{is} and q_{id} respectively), i.e. a certain $F(q_{is})-F(q_{id})$ for some functional form $F()$. Based on the value for the parameter NSEG (minimum 4 and a maximum of 10), selecting $NQSMOD = 3$ would introduce NSEG-1 number of internal nodes ($q_1, q_2, \dots, q_{NSEG-1}$) in the channel. From the bias-independent calculation up until the surface potential solutions including calculations pertaining to mobility degradation, velocity saturation, channel length modulation are all performed only once for a given transistor. However the core I-V and C-V calculations are repeated NSEG number of times with varying boundary conditions. The calculations for the n -th segment would look something like $F(q_{n-1}) - F(q_n)$. The continuity of current together with the boundary conditions imposed by the quasi-static solutions to the surface potential at source and drain ends (q_{is} and q_{id}) would yield a self-consistent result where the voltage at each of nodes, $V(q_n)$ would end up being the channel charge at that position. The leakage currents and other effects are also evaluated only once. The computational effort is far less compared to a full-fledged segmentation as the core I-V and C-V calculations take up only a fraction of the time compared to a full transistor model. There is no non quasi-static effect for the body charge, as the channel is assumed to be fully-depleted. This model does not extend

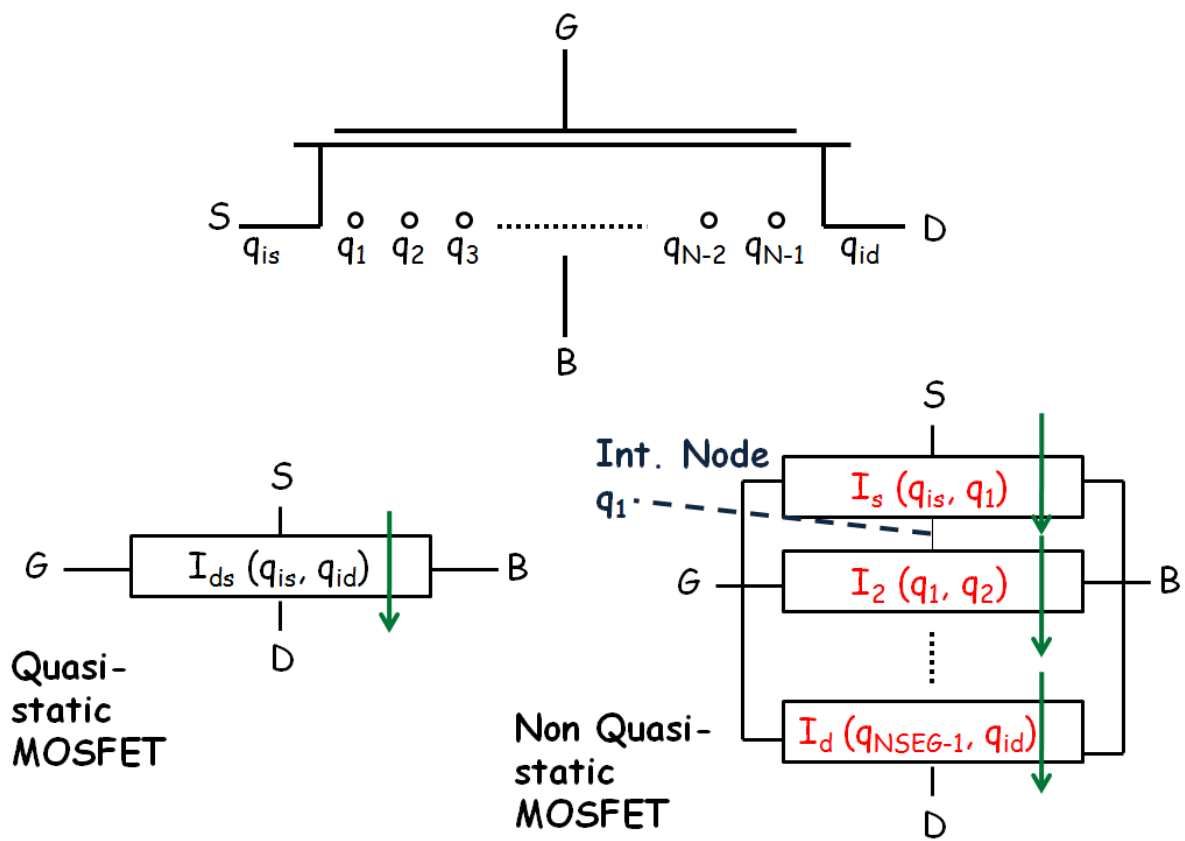


Figure 12: A N-segment charge-segmented MOSFET with N-1 internal nodes

to accumulation region where we assume the holes are supplied quickly from the body contact for the BULKMOD=1 case.

This model introduces no new parameters, and hence does not require any additional fitting / measurements to be performed. The DC and AC results for NQSMOD=3 and NSEG number of segments are also self-consistent with the quasi-static results. We are still investigating a metric to identify the best number of segments, NSEG that would suit your accuracy while balancing the additional computational effort introduced with each additional segment.

3.17 Generation-recombination Component

$$I_{ds,gen} = HFIN \cdot TFIN \cdot (L_{eff} - LINTIGEN) \cdot (AIGEN_i \cdot V_{ds} + BIGEN_i \cdot V_{ds}^3) \\ \cdot \exp \left[\frac{qE_g}{NTGEN_i \cdot kT} \left(\frac{T}{TNOM} - 1 \right) \right] \times NFIN_{total} \quad (3.412)$$

3.18 Junction Current and capacitances

The junction current and capacitances are only calculated for bulk multi-gate devices (*BULKMOD = 1*).

Source side junction current

Bias Independent Calculations

$$I_{sbs} = ASEJ \cdot J_{ss}(T) + PSEJ \cdot J_{sswgs}(T) + W_{eff0} \cdot NFIN_{total} \cdot J_{sswgs}(T) \quad (3.413)$$

$$NV_{tms} = \frac{kT}{q} \cdot NJS \quad (3.414)$$

$$XExpBVS = \exp\left(-\frac{BVS}{NV_{tms}}\right) \cdot XJBVS \quad (3.415)$$

$$T_b = 1 + \frac{IJTHSFWD}{I_{sbs}} - XExpBVS \quad (3.416)$$

$$V_{jsmFwd} = NV_{tms} \cdot \ln\left(\frac{T_b + \sqrt{T_b^2 + 4 \cdot XExpBVS}}{2}\right) \quad (3.417)$$

$$T_0 = \exp\left(\frac{V_{jsmFwd}}{NV_{tms}}\right) \quad (3.418)$$

$$IV_{jsmFwd} = I_{sbs} \left(T_0 - \frac{XExpBVS}{T_o} + XExpBVS - 1 \right) \quad (3.419)$$

$$S_{slpFwd} = \frac{I_{sbs}}{NV_{tms}} \cdot \left(T_0 + \frac{XExpBVS}{T_0} \right) \quad (3.420)$$

$$V_{jsmRev} = -BVS - NV_{tms} \cdot \ln\left(\frac{\frac{IJTHSREV}{I_{sbs}} - 1}{XJBVS}\right) \quad (3.421)$$

$$T_1 = XJBVS \cdot \exp\left(-\frac{BVS + V_{jsmRev}}{NV_{tms}}\right) \quad (3.422)$$

$$IV_{jsmRev} = I_{sbs} \cdot (1 + T_1) \quad (3.423)$$

$$S_{slpRev} = -I_{sbs} \cdot \frac{T_1}{NV_{tms}} \quad (3.424)$$

Bias Dependent Calculations

If $V_{es} < V_{jsmRev}$

$$I_{es} = \left(\exp\left(\frac{V_{es}}{NV_{tms}}\right) - 1 \right) \cdot (IV_{jsmRev} + S_{slpRev}(V_{es} - V_{jsmRev})) \quad (3.425)$$

Else If $V_{jsmRev} \leq V_{es} \leq V_{jsmFwd}$

$$I_{es} = I_{sbs} \cdot \left(\exp\left(\frac{V_{es}}{NV_{tms}}\right) + XExpBVS - 1 - XJBVS \cdot \exp\left(-\frac{BVS + V_{es}}{NV_{tms}}\right) \right) \quad (3.426)$$

Else $V_{es} > V_{jsmFwd}$

$$I_{es} = IV_{jsmFwd} + S_{slpFwd}(V_{es} - V_{jsmFwd}) \quad (3.427)$$

Drain side junction current

Bias Independent Calculations

$$I_{sbd} = ADEJ \cdot J_{sd}(T) + PDEJ \cdot J_{sswd}(T) + W_{eff0} \cdot NFIN_{total} \cdot J_{sswgd}(T) \quad (3.428)$$

$$NV_{tmd} = \frac{kT}{q} \cdot NJD \quad (3.429)$$

$$XExpBVD = \exp\left(-\frac{BVD}{NV_{tmd}}\right) \cdot XJBVD \quad (3.430)$$

$$T_b = 1 + \frac{IJTHDFWD}{I_{sbd}} - XExpBVD \quad (3.431)$$

$$V_{jdmFwd} = NV_{tmd} \cdot \ln\left(\frac{T_b + \sqrt{T_b^2 + 4 \cdot XExpBVD}}{2}\right) \quad (3.432)$$

$$T_0 = \exp\left(\frac{V_{jdmFwd}}{NV_{tmd}}\right) \quad (3.433)$$

$$IV_{jdmFwd} = I_{sbd} \left(T_0 - \frac{XExpBVD}{T_o} + XExpBVD - 1 \right) \quad (3.434)$$

$$D_{slpFwd} = \frac{I_{sbd}}{NV_{tmd}} \cdot \left(T_0 + \frac{XExpBVD}{T_0} \right) \quad (3.435)$$

$$V_{jdmRev} = -BVD - NV_{tmd} \cdot \ln\left(\frac{\frac{IJTHDREV}{I_{sbd}} - 1}{XJBVD}\right) \quad (3.436)$$

$$T_1 = XJBVD \cdot \exp\left(-\frac{BVD + V_{jdmRev}}{NV_{tmd}}\right) \quad (3.437)$$

$$IV_{jdmRev} = I_{sbd} \cdot (1 + T_1) \quad (3.438)$$

$$D_{slpRev} = -I_{sbd} \cdot \frac{T_1}{NV_{tmd}} \quad (3.439)$$

Bias Dependent Calculations

If $V_{ed} < V_{jdmRev}$

$$I_{ed} = \left(\exp\left(\frac{V_{ed}}{NV_{tmd}}\right) - 1 \right) \cdot (IV_{jdmRev} + D_{slpRev}(V_{ed} - V_{jdmRev})) \quad (3.440)$$

Else If $V_{jdmRev} \leq V_{ed} \leq V_{jdmFwd}$

$$I_{ed} = I_{sbd} \cdot \left(\exp\left(\frac{V_{ed}}{NV_{tmd}}\right) + XExpBVD - 1 - XJBVD \cdot \exp\left(-\frac{BVD + V_{ed}}{NV_{tmd}}\right) \right) \quad (3.441)$$

Else $V_{ed} > V_{jdmFwd}$

$$I_{ed} = IV_{jdmFwd} + D_{slpFwd}(V_{ed} - V_{jdmFwd}) \quad (3.442)$$

Source side junction capacitance

Bias Independent Calculations

$$C_{zbs} = CJS(T) \cdot ASEJ \quad (3.443)$$

$$C_{zbssw} = CJWS(T) \cdot PSEJ \quad (3.444)$$

$$C_{zbsswg} = CJWGS(T) \cdot W_{eff0} \cdot NFIN_{total} \quad (3.445)$$

Bias Dependent Calculations

$$Q_{es1} = \begin{cases} C_{zbs} \cdot PBS(T) \cdot \frac{1 - \left(1 - \frac{V_{es}}{PBS(T)}\right)^{1-MJS}}{1-MJS} & V_{es} < 0 \\ V_{es} \cdot C_{zbs} + V_{es}^2 \cdot \frac{MJS \cdot C_{zbs}}{2 \cdot PBS(T)} & V_{es} > 0 \end{cases} \quad (3.446)$$

$$Q_{es2} = \begin{cases} C_{zbssw} \cdot PBSWS(T) \cdot \frac{1 - \left(1 - \frac{V_{es}}{PBSWS(T)}\right)^{1-MJSWS}}{1-MJSWS} & V_{es} < 0 \\ V_{es} \cdot C_{zbssw} + V_{es}^2 \cdot \frac{MJSWS \cdot C_{zbssw}}{2 \cdot PBSWS(T)} & V_{es} > 0 \end{cases} \quad (3.447)$$

$$Q_{es3} = \begin{cases} C_{zbsswg} \cdot PBSWGS(T) \cdot \frac{1 - \left(1 - \frac{V_{es}}{PBSWGS(T)}\right)^{1-MJSWGS}}{1-MJSWGS} & V_{es} < 0 \\ V_{es} \cdot C_{zbsswg} + V_{es}^2 \cdot \frac{MJSWGS \cdot C_{zbsswg}}{2 \cdot PBSWGS(T)} & V_{es} > 0 \end{cases} \quad (3.448)$$

$$Q_{es} = Q_{es1} + Q_{es2} + Q_{es3} \quad (3.449)$$

Two-Step Source side junction capacitance

In some cases, the depletion edge in the channel/ substrate edge might transition into a region

with a different doping (for ex. in a NMOS device: $[n^+ \text{ (source)}, p_1 \text{ (channel/substrate)}, p_2 \text{ (substrate)}]$, where p_1 and p_2 are regions with different doping levels). The following could be used to capture such a situation. In what follows, $V_{escn} (< 0)$ can be interpreted as the transition voltage at which the depletion region switches from p_1 to p_2 region. It is calculated assuming parameters SJxxx (proportionality constant for second region) and MJxxx2 (gradient of second region's doping) are given, to give a continuous charge and capacitance.

For $V_{es} < V_{esc1}$

$$Q_{es1} = C_{zbs} \cdot \left(PBS(T) \cdot \frac{1 - \left(1 - \frac{V_{esc1}}{PBS(T)}\right)^{1-MJS}}{1 - MJS} + SJS \cdot Pbs2 \cdot \frac{1 - \left(1 - \frac{V_{es}-V_{esc1}}{Pbs2}\right)^{1-MJS2}}{1 - MJS2} \right) \quad (3.450)$$

Else use the Q_{es1} of single junction above for $V_{es} > V_{esc1}$ where,

$$V_{esc1} = PBS(T) \cdot \left(1 - \left(\frac{1}{SJS}\right)^{\frac{1}{MJS}}\right) \quad (3.451)$$

$$Pbs2 = \frac{PBS(T) \cdot SJS \cdot MJS2}{MJS \cdot \left(1 - \frac{V_{esc1}}{PBS(T)}\right)^{-1-MJS}} \quad (3.452)$$

For $V_{es} < V_{esc2}$

$$Q_{es2} = C_{zbssw} \cdot PBSWS(T) \cdot \frac{1 - \left(1 - \frac{V_{esc2}}{PBSWS(T)}\right)^{1-MJSWS}}{1 - MJSWS} \quad (3.453)$$

$$+ C_{zbssw} \cdot SJSWS \cdot Pbsws2 \cdot \frac{1 - \left(1 - \frac{V_{es}-V_{esc2}}{Pbsws2}\right)^{1-MJSWS2}}{1 - MJSWS2} \quad (3.454)$$

Else use the Q_{es2} of single junction above for $V_{es} > V_{esc2}$ where,

$$V_{esc2} = PBSWS(T) \cdot \left(1 - \left(\frac{1}{SJSWS}\right)^{\frac{1}{MJSWS}}\right) \quad (3.455)$$

$$Pbsws2 = \frac{PBSWS(T) \cdot SJSWS \cdot MJSWS2}{MJSWS \cdot \left(1 - \frac{V_{esc2}}{PBSWS(T)}\right)^{-1-MJSWS}} \quad (3.456)$$

For $V_{es} < V_{esc3}$

$$Q_{es3} = C_{zbsswg} \cdot PBSWGS(T) \cdot \frac{1 - \left(1 - \frac{V_{esc3}}{PBSWGS(T)}\right)^{1-MJSWGS}}{1 - MJSWGS} \quad (3.457)$$

$$+ C_{zbsswg} \cdot SJSWGS \cdot Pbswgs2 \cdot \frac{1 - \left(1 - \frac{V_{es}-V_{esc3}}{Pbswgs2}\right)^{1-MJSWGS2}}{1 - MJSWGS2} \quad (3.458)$$

Else use the Q_{es3} of single junction above for $V_{es} > V_{esc3}$ where,

$$V_{esc3} = PBSWGS(T) \cdot \left(1 - \left(\frac{1}{SJSWGS}\right)^{\frac{1}{MJSWGS}}\right) \quad (3.459)$$

$$Pbswgs2 = \frac{PBSWGS(T) \cdot SJSWGS \cdot MJSWGS2}{MJSWGS \cdot \left(1 - \frac{V_{esc3}}{PBSWGS(T)}\right)^{-1-MJSWGS}} \quad (3.460)$$

Drain side junction capacitance

Bias Independent Calculations

$$C_{zbd} = CJD(T) \cdot ADEJ \quad (3.461)$$

$$C_{zbds} = CJSWD(T) \cdot PDEJ \quad (3.462)$$

$$C_{zbds} = CJSWGD(T) \cdot W_{eff0} \cdot NFIN_{total} \quad (3.463)$$

Bias Dependent Calculations

$$Q_{ed1} = \begin{cases} C_{zbd} \cdot PBD(T) \cdot \frac{1 - \left(1 - \frac{V_{ed}}{PBD(T)}\right)^{1-MJD}}{1-MJD} & V_{ed} < 0 \\ V_{ed} \cdot C_{zbd} + V_{ed}^2 \cdot \frac{MJD \cdot C_{zbd}}{2 \cdot PBD(T)} & V_{ed} > 0 \end{cases} \quad (3.464)$$

$$Q_{ed2} = \begin{cases} C_{zbds} \cdot PBSWWD(T) \cdot \frac{1 - \left(1 - \frac{V_{ed}}{PBSWWD(T)}\right)^{1-MJSWD}}{1-MJSWD} & V_{ed} < 0 \\ V_{ed} \cdot C_{zbds} + V_{ed}^2 \cdot \frac{MJSWD \cdot C_{zbds}}{2 \cdot PBSWWD(T)} & V_{ed} > 0 \end{cases} \quad (3.465)$$

$$Q_{ed3} = \begin{cases} C_{zbds} \cdot PBSWGD(T) \cdot \frac{1 - \left(1 - \frac{V_{ed}}{PBSWGD(T)}\right)^{1-MJSWGD}}{1-MJSWGD} & V_{ed} < 0 \\ V_{ed} \cdot C_{zbds} + V_{ed}^2 \cdot \frac{MJSWGD \cdot C_{zbds}}{2 \cdot PBSWGD(T)} & V_{ed} > 0 \end{cases} \quad (3.466)$$

$$Q_{ed} = Q_{ed1} + Q_{ed2} + Q_{ed3} \quad (3.467)$$

Two-Step Drain side junction capacitance

Refer to the description made for the source side.

For $V_{ed} < V_{edc1}$

$$Q_{ed1} = C_{zbd} \cdot \left(PBD(T) \cdot \frac{1 - \left(1 - \frac{V_{edc1}}{PBD(T)}\right)^{1-MJD}}{1 - MJD} + SJD \cdot Pbd2 \cdot \frac{1 - \left(1 - \frac{V_{ed}-V_{edc1}}{Pbd2}\right)^{1-MJD2}}{1 - MJD2} \right) \quad (3.468)$$

Else use the Q_{ed1} of single junction above for $V_{ed} > V_{edc1}$ where,

$$V_{edc1} = PBD(T) \cdot \left(1 - \left(\frac{1}{SJD}\right)^{\frac{1}{MJD}}\right) \quad (3.469)$$

$$Pbd2 = \frac{PBD(T) \cdot SJD \cdot MJD2}{MJD \cdot \left(1 - \frac{V_{edc1}}{PBD(T)}\right)^{-1-MJD}} \quad (3.470)$$

For $V_{ed} < V_{edc2}$

$$Q_{ed2} = C_{zbds_w} \cdot PBSWD(T) \cdot \frac{1 - \left(1 - \frac{V_{edc2}}{PBSWD(T)}\right)^{1-MJSWD}}{1 - MJSWD} \quad (3.471)$$

$$+ C_{zbds_w} \cdot SJSWD \cdot Pbswd2 \cdot \frac{1 - \left(1 - \frac{V_{ed}-V_{edc2}}{Pbswd2}\right)^{1-MJSWD2}}{1 - MJSWD2} \quad (3.472)$$

Else use the Q_{ed2} of single junction above for $V_{ed} > V_{edc2}$ where,

$$V_{edc2} = PBSWD(T) \cdot \left(1 - \left(\frac{1}{SJSWD}\right)^{\frac{1}{MJSWD}}\right) \quad (3.473)$$

$$Pbswd2 = \frac{PBSWD(T) \cdot SJSWD \cdot MJSWD2}{MJSWD \cdot \left(1 - \frac{V_{edc2}}{PBSWD(T)}\right)^{-1-MJSWD}} \quad (3.474)$$

For $V_{ed} < V_{edc3}$

$$Q_{ed3} = C_{zbds_wg} \cdot PBSWGD(T) \cdot \frac{1 - \left(1 - \frac{V_{edc3}}{PBSWGD(T)}\right)^{1-MJSWGD}}{1 - MJSWGD} \quad (3.475)$$

$$+ C_{zbds_wg} \cdot SJSWGD \cdot Pbswgd2 \cdot \frac{1 - \left(1 - \frac{V_{ed}-V_{edc3}}{Pbswgd2}\right)^{1-MJSWGD2}}{1 - MJSWGD2} \quad (3.476)$$

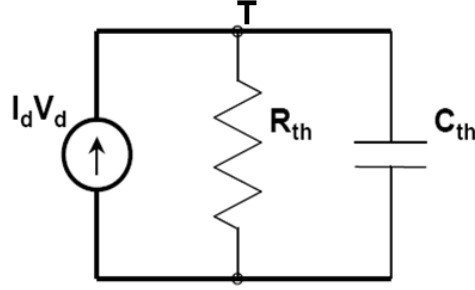


Figure 13: R-C network for self-heating calculation [13]

Else use the Q_{ed3} of single junction above for $V_{ed} > V_{edc3}$ where,

$$V_{edc3} = PBSWGD(T) \cdot \left(1 - \left(\frac{1}{SJSWGD} \right)^{\frac{1}{MJSWGD}} \right) \quad (3.477)$$

$$Pbswgd2 = \frac{PBSWGD(T) \cdot SJSWGD \cdot MJSWGD2}{MJSWGD \cdot \left(1 - \frac{V_{edc3}}{PBSWGD(T)} \right)^{-1-MJSWGD}} \quad (3.478)$$

3.19 Self-heating model

The self-heating effect is modeled using an R-C network approach (based on BSIMSOI [13]), as illustrated in figure 13. The voltage at the temperature node (T) is used for all temperature-dependence calculations in the model.

Thermal resistance and capacitance calculations

The thermal resistance (R_{th}) and capacitance (C_{th}) are modified from BSIMSOI to capture the fin pitch ($FPITCH$) dependence.

$$\frac{1}{R_{th}} = G_{th} = \frac{WTH0 + FPITCH \cdot NFIN_{total}}{RTH0} \quad (3.479)$$

$$C_{th} = CTH0 + FPITCH \cdot NFIN_{total} \quad (3.480)$$

Table 1: Origin of noise models in BSIM-CMG

Model in BSIM-CMG 106.0.0	Origin
Flicker noise model	BSIM4 Unified Model (FNOIMOD=1)
Thermal noise	BSIM4 TNOIMOD=0
Gate current shot noise	BSIM4 gate current noise
Noise associated with parasitic resistances	BSIM4 parasitic resistance noise

3.20 Noise Models

Noise models in BSIM-CMG are based on BSIM4 [10]. Table 1 lists the origin of each noise model:

Flicker noise model

$$E_{sat,noi} = \frac{2VSAT_i}{\mu_{eff}} \quad (3.481)$$

$$L_{eff,noi} = L_{eff} - 2 \cdot LINTNOI \quad (3.482)$$

$$\Delta L_{clm} = l \cdot \ln \left[\frac{1}{E_{sat,noi}} \cdot \left(\frac{V_{ds} - V_{dseff}}{l} + EM \right) \right] \quad (3.483)$$

$$N_0 = \frac{C_{oxe} \cdot q_{is}}{q} \quad (3.484)$$

$$N_l = \frac{C_{oxe} \cdot q_{id}}{q} \quad (3.485)$$

$$N^* = \frac{kT}{q^2} (C_{oxe} + CIT) \quad (3.486)$$

$$FN1 = NOIA \cdot \ln \left(\frac{N_0 + N^*}{N_l + N^*} \right) + NOIB \cdot (N_0 - N_l) + \frac{NOIC}{2} (N_0^2 - N_l^2) \quad (3.487)$$

$$FN2 = \frac{NOIA + NOIB \cdot N_l + NOIC \cdot N_l^2}{(N_l + N^*)^2} \quad (3.488)$$

$$S_{si} = \frac{kTq^2\mu_{eff}I_{ds}}{C_{oxe}L_{eff,noi}^2f^{EF} \cdot 10^{10}} \cdot FN1 + \frac{kTI_{ds}^2\Delta L_{clm}}{W_{eff} \cdot NFIN_{total} \cdot L_{eff,noi}^2f^{EF} \cdot 10^{10}} \cdot FN2 \quad (3.489)$$

$$S_{wi} = \frac{NOIA \cdot kT \cdot I_{ds}^2}{W_{eff} \cdot NFIN_{total} \cdot L_{eff,noi} f^{EF} \cdot 10^{10} \cdot N^{*2}} \quad (3.490)$$

$$S_{id,flicker} = \frac{S_{wi}S_{si}}{S_{wi} + S_{si}} \quad (3.491)$$

Thermal noise model ($TNOIMOD = 0$)

$$Q_{inv} = |Q_{s,intrinsic} + Q_{d,intrinsic}| \times NFIN_{total} \quad (3.492)$$

$$\overline{i_d^2} = \begin{cases} NTNOI \cdot \frac{4kT\Delta f}{L_{eff}^2} & \text{if RDSMOD} = 0 \\ NTNOI \cdot \frac{4kT\Delta f}{L_{eff}^2} \cdot \mu_{eff}Q_{inv} & \text{if RDSMOD} = 1 \end{cases} \quad (3.493)$$

Gate current shot noise

$$\overline{i_{gs}^2} = 2q(I_{gcs} + I_{gs}) \quad (3.494)$$

$$\overline{i_{gd}^2} = 2q(I_{gcd} + I_{gd}) \quad (3.495)$$

$$\overline{i_{gb}^2} = 2qI_{gbinv} \quad (3.496)$$

Resistor noise The noise associated with each parasitic resistors in BSIM-MG are calculated

If $RDSMOD = 1$ then

$$\frac{\overline{i_{RS}^2}}{\Delta f} = 4kT \cdot \frac{1}{R_{source}} \quad (3.497)$$

$$\frac{\overline{i_{RD}^2}}{\Delta f} = 4kT \cdot \frac{1}{R_{drain}} \quad (3.498)$$

If $RGATEMOD = 1$ then

$$\frac{\overline{i_{RG}^2}}{\Delta f} = 4kT \cdot \frac{1}{R_{geltl}} \quad (3.499)$$

Table 2: Sample input decks for BSIM-CMG

Netlist	Description
idvgnmos.sp	$I_d - V_{gs}$ characteristics for n-FETs ($25^\circ C$)
idvgpmos.sp	$I_d - V_{gs}$ characteristics for p-FETs ($25^\circ C$)
idvdnmos.sp	$I_d - V_{ds}$ characteristics for n-FETs ($25^\circ C$)
idvdpmos.sp	$I_d - V_{ds}$ characteristics for p-FETs ($25^\circ C$)
ac.sp	AC simulation example
noise.sp	Noise simulation example
gummel_n.sp	Gummel symmetry test for nFET
gummel_p.sp	Gummel symmetry test for pFET
inv_dc.sp	Inverter DC simulation
rdsgeo.sp	Test for RGEOMOD=1
cfrgeo.sp	Test for CGEOMOD=2
inverter_transient.sp	Inverter transient response simulation example
ringosc_17stg.sp	17-stage ring oscillator simulation example

4 Simulation Outputs

Sample input decks for BSIM-CMG are listed in Table 2

Table 4: Examples of parameters that are measured or specified by the user

Parameter Name	Description
EOT	Gate oxide thickness
HFIN	Fin Height
TFIN	Fin Thickness
L	Fin Length Drawn
NFIN	Number of Fins
NF	Number of Fingers in parallel
NBODY	Channel Doping Concentration
BULKMOD	0: SOI 1: bulk
GIDLMOD	0: off 1:on
GEOMOD	0: double gate 1: triple gate 2: quadruple gate
RDSMOD	0: internal 1: external
DEVTYPE	0: PMOS 1:NMOS
NGATE	0: metal gate > 0: Poly Gate doping

5 Parameter Extraction Procedure

5.1 Global Parameter Extraction

5.1.1 Basic Device Parameter List

The objective of this procedure is to find one global set of parameters for BSIM-CMG to fit experimental data for devices with channel length ranging from short to long dimensions. The original work is published in [18].

Some parameters are measured or specified by user, and need not be extracted, such as those given in Table 4.

Parameters that are going to be extracted are divided into two categories. Category One parameters are presented as the coefficients in a set of length dependent intermedi-

ate quantities. These intermediate quantities are introduced to facilitate the extraction procedure. To keep the procedure simple, these quantities are not visible to the end user. Category Two parameters don't appear in these intermediate quantities.

The length dependent intermediate quantities, 9 in total, are summarized below.

Group 1: $U0[L]$, $\Delta L[L]$, $UA[L]$, $UD[L]$, $RDSW[L]$ [Relates to Mobility and R_{series}]

Group 2: $VSAT[L]$, $VSAT1[L]$, $PTWG[L]$ [Relates to Velocity Saturation]

Group 3: $MEXP[L]$ [Relates to Smoothing Functions]

$U0[L]$ and $\Delta L[L]$ and the associated Category One parameters are

$$U0[L] = U0_0 \times (1 - UP \times L_{eff}^{-LPA}) \dots \text{Eq (1); (Here, } L_{eff} = L - 2 \times \Delta L[L])$$

$$\Delta L[L] = LINT + LL \times e^{-\frac{(L+XL)}{LLN}} \dots \text{Eq (2);}$$

The other length dependent quantities $UA[L]$, $UD[L]$, $RDSW[L]$, $MEXP[L]$, $VSAT[L]$, $VSAT1[L]$, $PTWG[L]$. These 8 length dependent variables have identical functional form, and are represented as $Param[L]$:

$$Param[L] = Param_0 + AParam \times e^{-\frac{L_{eff}}{BParam}} \dots \text{Eq(4);}$$

$$\text{Example: } UA[L] = UA_0 + AU A \times e^{-\frac{L_{eff}}{BUA}}$$

Here, $Param[L] = Param_0$ when L_{eff} is large, while $AParam$, $BParam$ are geometry scaling parameters which add necessary correction to $Param_0$ when the L_{eff} shrinks. $Param_0$, $AParam$, $BParam$ belong to Category One.

Category Two parameters which don't appear in the length dependent functions are:

PHIG, CIT, EU, ETAMOB, DVT0, DVT1, CDSC, DVT2, ETA0, DSUB, CDSCL, AGIDL, BGIDL, EGIDL, VTL, XN, LC,MM, PCLM, PDIBL1, PDIBL2, DROUT, PVAG, etc

Since Category One parameters can only manifest themselves by first yielding the 9 length dependent intermediate quantities, determining the value of these intermediate quantities is inevitable if we want to extract them. Category Two parameters, however, can be extracted from experimental data directly.

Now we start extracting all the global parameters in both categories.

The extraction procedure can be divided into 8 stages:

- Parameter initialization
- Linear region: Step 1-6

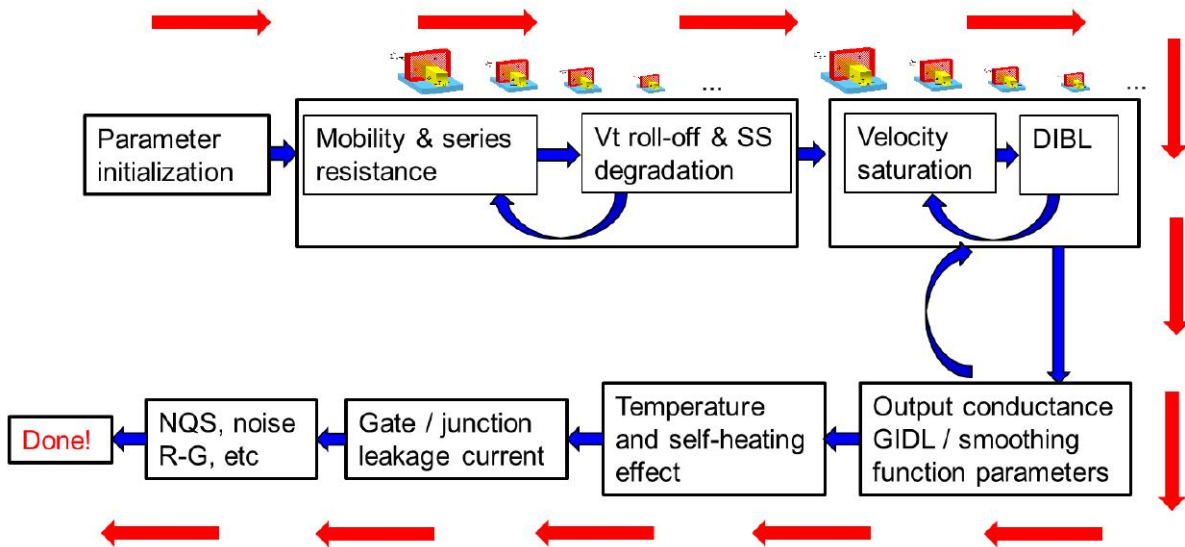


Figure 14: Extraction Flow Chart

- Saturation region: Step 7-11
- GIDL and Output Conductance: Step 12-13
- Smoothing between linear and saturation regions: Step 14
- Parameters for temperature effect and self-heating effect: Step 15
- Gate / Junction leakage current : Step 16
- Other important physical effects : Step 17

See the extraction overview flow chart for details.

5.1.2 Parameter Initialization

- Determine $V_{th}(L)$ by strong inversion region data using maximum slope extrapolation algorithm.
- Plot $\frac{V_d(\sim 0.05V)}{I_d(V_g, L)}$ v.s. L for different
- Make linear fitting to the curve set above, extrapolate each straight line and find the intersection (ΔL , R_{series}), Initialize $LINT = \frac{\Delta L}{2}$, $RDSW = R_{series}$ as shown in the Fig. 15.

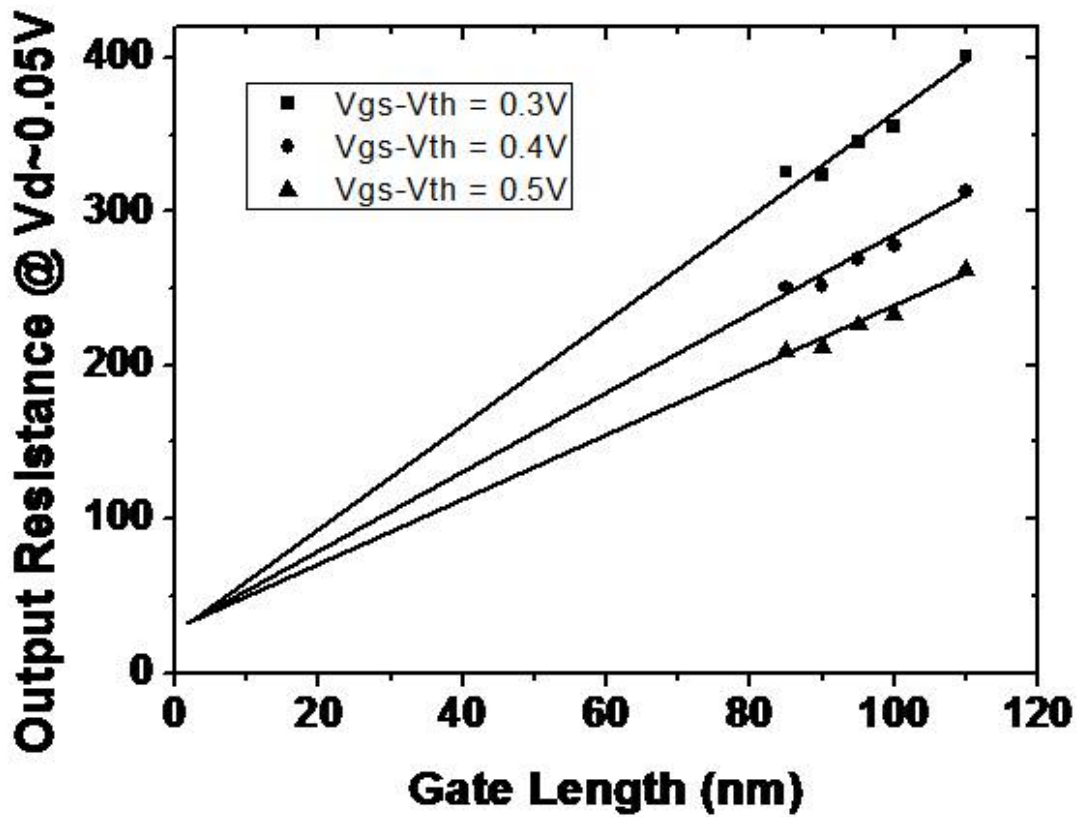


Figure 15: Initialize ΔL and R_{series}

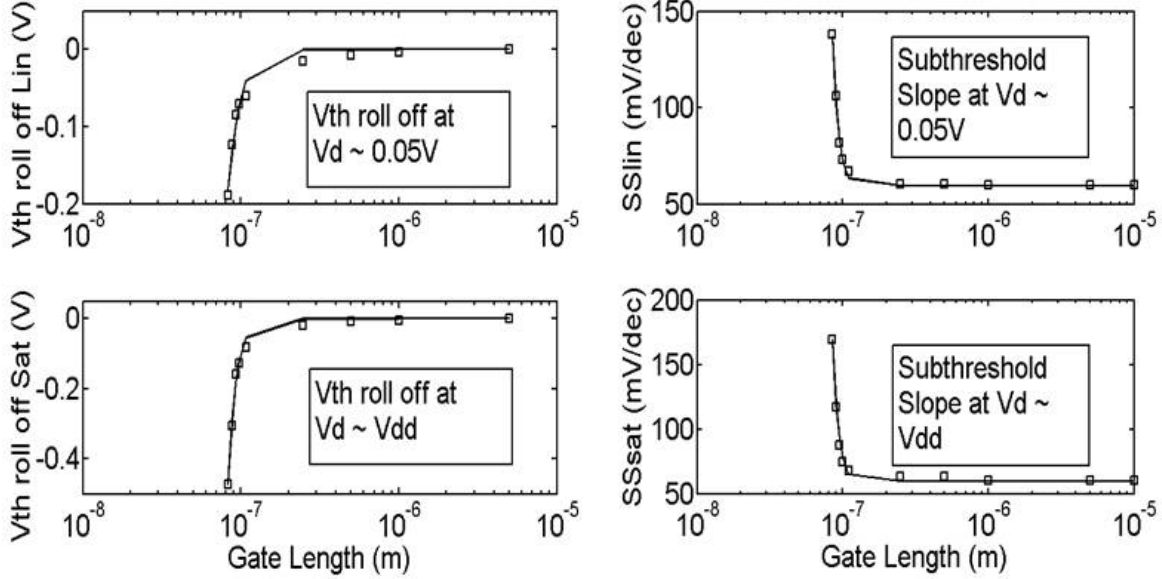


Figure 16: Initialize SCE and RSCE Parameters

- Use Constant-Current method to extract $V_{th}(L)$ by using sub-threshold region data.
- Plot $\Delta V_{th}(L)$ v.s. $@V_d \sim 0.05V$ and V_{dd} respectively. Extract short channel effect(SCE) and Reverse SCE parameters DVT0, DVT1, ETA0, DSUB, K1RSCE, LPE0 as shown in Figure 16 left.
- Plot $2.3n(L) \times \frac{kT}{q}$ v.s. $L @ V_d \sim 0.05V$ and V_{dd} . Extract CDSC, CDSRD, DVT2 as shown in Figure 16 right.
- Set all other parameters in Category One and Two as default value as the manual shows.

5.1.3 Linear region

Step 1: Extract work function, interface charge and mobility model parameters for long gate length. [Note: Larger length is better, as it will minimize the short channel effect and emphasize carrier mobility, work function and interface charge related parameters.]

Extracted Parameters	Device & Experimental Data	Extraction Methodology
PHIG, CIT	A long device I_d v.s. V_g @ $V_d \sim 0.05V$	Observe sub-threshold region offset and slope.
U_{00} , U_{A0} , U_{D0} , EU, ETAMOB	A long device I_d v.s. V_g @ $V_d \sim 0.05V$	Observe strong inversion region I_{dlin} and G_{mlin} .

Step 2: Refine Vth roll-off, DIBL and SS degradation parameters.

Extracted Parameters	Device & Experimental Data	Extraction Methodology
DVT0, DVT1, CDSC, DVT2	Both short and medium devices I_d v.s. V_g @ $V_d \sim 0.05V$	Observe sub-threshold region of all devices in the same plot. Optimize DVT0, DVT1, CDSC, DVT2.

Note: need not very accurate fitting because mobility, series resistance parameters are not determined yet.

Step 3: Extract low field mobility $U_0[L]$ for long and medium gate lengths.

So far, we have good fit with data in sub-threshold regions from long to short channel devices, and strong inversion for long channel devices. We need good fit for strong inversion in medium and short channel devices.

In linear region, current is to the first order, governed by low field mobility. So we start by tuning low field mobility values.

In short channel devices series resistance, coulombic scattering and enhanced mobility degradation effects are pronounced. To avoid the influence of these effects, long and medium channel length devices are selected to especially extract low field mobility parameters.

Extracted Parameters	Device & Experimental Data	Extraction Methodology
UP,LPA	Long and medium devices I_d v.s. $V_g @ V_d \sim 0.05V$ $U_0[L] = U_{00} \times (1 - UP \times L_{eff}^{-LPA})$	Observe strong inversion region $Idlin$ and G_mlin , extract $U0[L]$ to get UP,LPA. i.e. for each L_i , find Y_i corresponding to L_i , fit (L_i, Y_i) by Eq(1) to extract UP,LPA). Refer to Figure 17 for instance.

Step 4: Extract mobility model and series resistance parameters for short gate lengths.

Extracted Parameters	Device & Experimental Data	Extraction Methodology
$Param_0, AParam,$ $BParam, LINT, LL, LLN$	Short and medium devices I_d v.s. $V_g @ V_d \sim 0.05V$	<ul style="list-style-type: none"> a. Observe strong inversion region $Idlin$ and G_mlin. Similar to Step 3, find values of $UA[L]$, $UD[L]$, $RDSW[L]$ and $DeltaL[L]$ that gives good fit to experimental data, varying them simultaneously. UA_0, UD_0 are provided from Step 1 and $RDSW_0$, $LINT$ are provided from parameter Initialization. b. Variation of each parameter with respect to L should be kept minimal with smooth continuous trend. c. From the length dependence of $UA[L]$, $UD[L]$, $RDSW[L]$ and $L[L]$, find AUA, BUA; AUD, BUD; $ARDSW$, $BRDSW$; LL, LLN.

Note: Step 3 parameters are extracted from long and medium channel lengths,

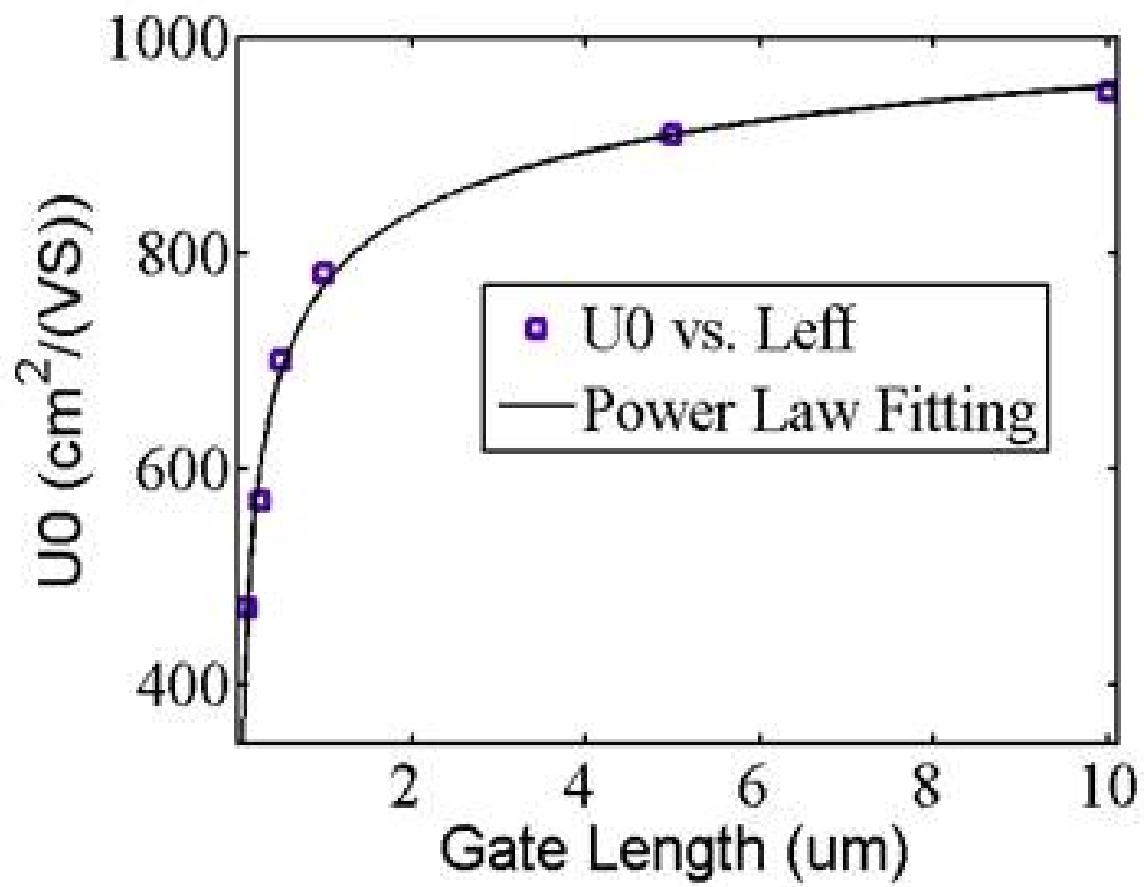


Figure 17: Fit low field electron mobility with L_g

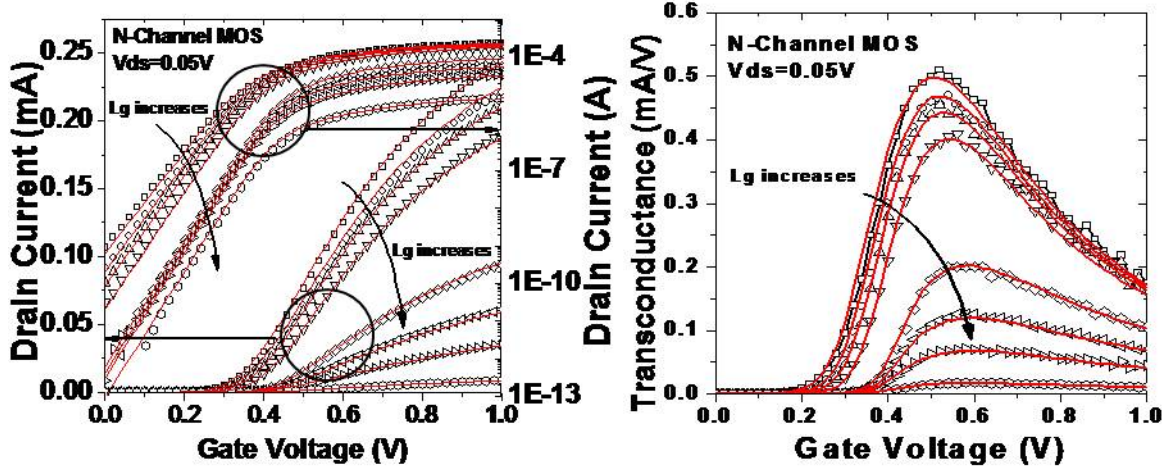


Figure 18: $I_d v.s. V_g$ and $G_m v.s. V_g$ @ $V_d \sim 0.05V$

whereas, Step 4 involves short and medium channel lengths. As in Step 4 'exponential' corrections are particularly pronounced for small L (short channel). Its Taylor expansion when L_{eff} is medium can give appropriate modifications when power functions alone don't fit very well for medium lengths. Thus, the extracted parameters remain valid for all channel lengths to bring forth the intended length dependence in effect.

Step 5: Refine geometry scaling parameters for mobility degradation parameters.

Refined Parameters	Device & Experimental Data	Extraction Methodology
AUA,AUD,ARDSW,LL	Short and medium devices I_d v.s. V_g @ $V_d \sim 0.05V$	Observe strong inversion region of all devices in the same plot; optimize AUA, AUD, ARDSW, LL.

Step 6: Refine all Group 1 scaling parameters.

Further optimize the parameters by repeating step 5 and 2. If not getting good fitting, tune LLN, BUA, BUD, BRDSW. If still not good, tune other parameters in Group 1 as appropriate. Iteration ends in step 5 and then proceeds to step 7. A sample fitting result up till this step is shown in Figure 18.

5.1.4 Saturation region

Step 7: Refine DIBL parameters.

Extracted Parameters	Device & Experimental Data	Extraction Methodology
ETA0, DSUB, CDSCD	Short and long devices I_d v.s. V_g @ $V_d \sim V_{dd}$	Observe sub-threshold region of all devices in the same plot. Optimze ETA0, DSUB, CDSCD.

Note: need not very accurate fitting because velocity saturation, smoothing function and output conductance parameters are not determined yet.

Step 8: Extract velocity saturation parameters for long and medium gate lengths

Extracted Parameters	Device & Experimental Data	Extraction Methodology
$VSAT_0$, $VSAT1_0$, $PTWG_0$, $KSATIV_0$, $MEXP_0$	long device and medium devices I_d v.s. V_g @ $V_d \sim V_{dd}$	Observe strong inversion region I_{dsat} , G_{msat} , I_dV_d .

Note: long channel alone is not enough to accurately extract velocity saturation parameters.

Step 9: Extract velocity saturation parameters for short and medium gate lengths

Extracted Parameters	Device & Experimental Data	Extraction Methodology
AVSAT, AVSAT1, APTWG, BVSAT, BVSAT1, BPTWG	short and medium devices I_d v.s. V_g @ $V_d \sim V_{dd}$	<ul style="list-style-type: none"> a. Observe strong inversion region of I_{dsat} and G_{msat}. Find $VSAT1[L_i]=X_i$, $VSAT[L_i]=Y_i$, $PTWG[L_i]=Z_i$ to fit data. b. Extract AVSAT1, BVSAT1 from (L_i, X_i); AVSAT,BVSAT from (L_i, Y_i); APTWG, BPTWG from (L_i, Z_i).

Step 10: Refine geometry scaling parameters for velocity saturation, over the range from short to long channel devices.

Refined Parameters	Device & Experimental Data	Extraction Methodology
--------------------	----------------------------	------------------------

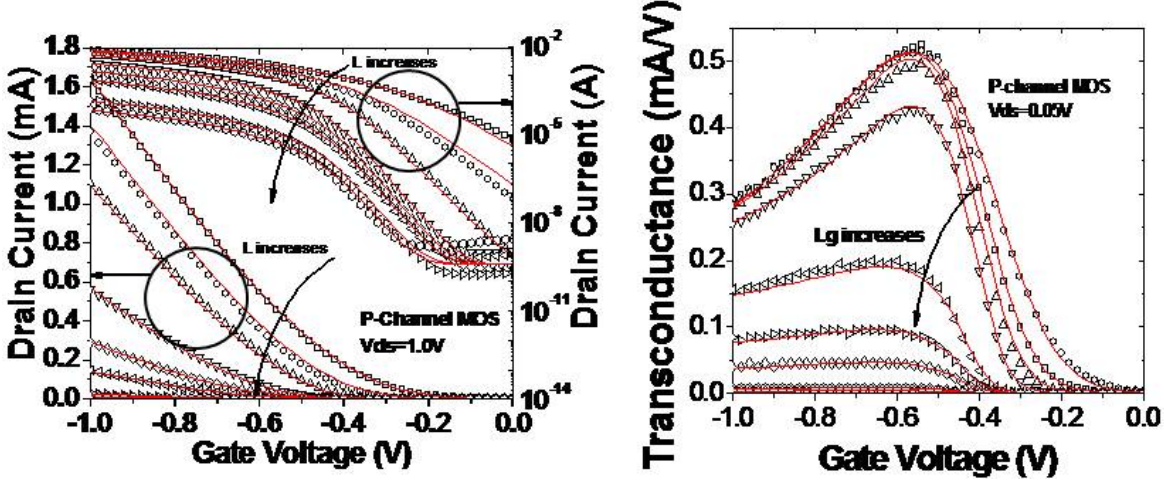


Figure 19: $I_d v.s. V_g$ and $G_m v.s. V_g$ @ $V_d \sim V_{dd}$

AVSAT, AVSAT1, APTWG	medium and short devices I_d v.s. V_g @ $V_d \sim V_{dd}$	Observe strong inversion region of all devices in the same plot. Optimize AVSAT, AVSAT1, APTWG.
----------------------	--	---

Step 11: Refine Group 2 scaling parameters.

Further refine the geometry scaling parameters by repeating step 10 and 7. If not getting good fitting, tune BVSAT, BVSAT1, BPTWG. If still not good, tune other parameters in Group 2 as appropriate. Iteration ends in step 10 and then proceeds to step 13. A sample fitting result up till this step is shown in Figure 19.

5.1.5 Other Parameters representing important physical effects

Step 12: Extract GIDL current model parameters.

Extracted Parameters	Device & Experimental Data	Extraction Methodology
AGIDL, BGIDL, EGIDL	long and short devices I_d v.s. V_d @ different V_g	Observe sub-threshold region I_d v.s. V_g @ $V_d \sim V_{dd}$ & R_{out} v.s. V_d @ $V_g \sim 0V$.

Step 13: Extract output conductance parameters.

Extracted Parameters	Device & Experimental Data	Extraction Methodology
MEXP[L], PCLM, PDIBL1, PDIBL2, DROUT, PVAG	Long and short devices I_d v.s. V_d @ different V_g	Observe strong inversion region I_d v.s. V_d & G_d v.s. V_d @ different V_g .

$MEXP_0$, AMEXP, BMEXP	MEXP[L] v.s. L from Step 14, i.e. (L_i, X_i)	Observe data trend; extract AM- EXP and BMEXP. An example is shown in Figure 20.
-------------------------	---	--

A sample global fitting result for $L_g=90\text{nm}$ N-Channel MOS is shown in Figure 21 as below.

5.1.7 Other Effects

Step 15: Temperature and Self-Heating Effects.

Extracted Parameters	Device & Experimental Data	Extraction Methodology
Thermal resistance (RTH0) and capacitances (CTH0) for the self-heating model and etc.	I_{ds} v.s. V_{gs} @ $V_d V_{dd}$ under different temperatures.	Observe data trend and tune RTH0, CTH0, TNOM, TBGASUB, TBGBSUB, etc.

Step 16: Gate / Junction leakage current

Extracted Parameters	Device & Experimental Data	Extraction Methodology
Gate tunneling current and junction current parameters.	I_{gb} v.s. V_{gs} @ $V_d 0V$.	Observe data trend and tune NIGBINV, AIGBINV, BIGBINV, CIGBINV, EIGBINV, AS, PS1, PS2, NJS, IJTHSFWD, BVS, XJBVS, AD, PD1, PD2, NJD, IJTHDFWD, BVD, XJBVD, etc.

Step 17: Advanced Feature

Extracted Parameters	Device & Experimental Data	Extraction Methodology
Non quasi static effect, noise model, poly depletion, generation recombination etc.	S-parameters, noise figure, CV measurement, etc.	Extract XRCRG1, XRCRG2, NOIA, NOIB, NOIC, FN1, FN2, AIGEN, BIGEN, etc.

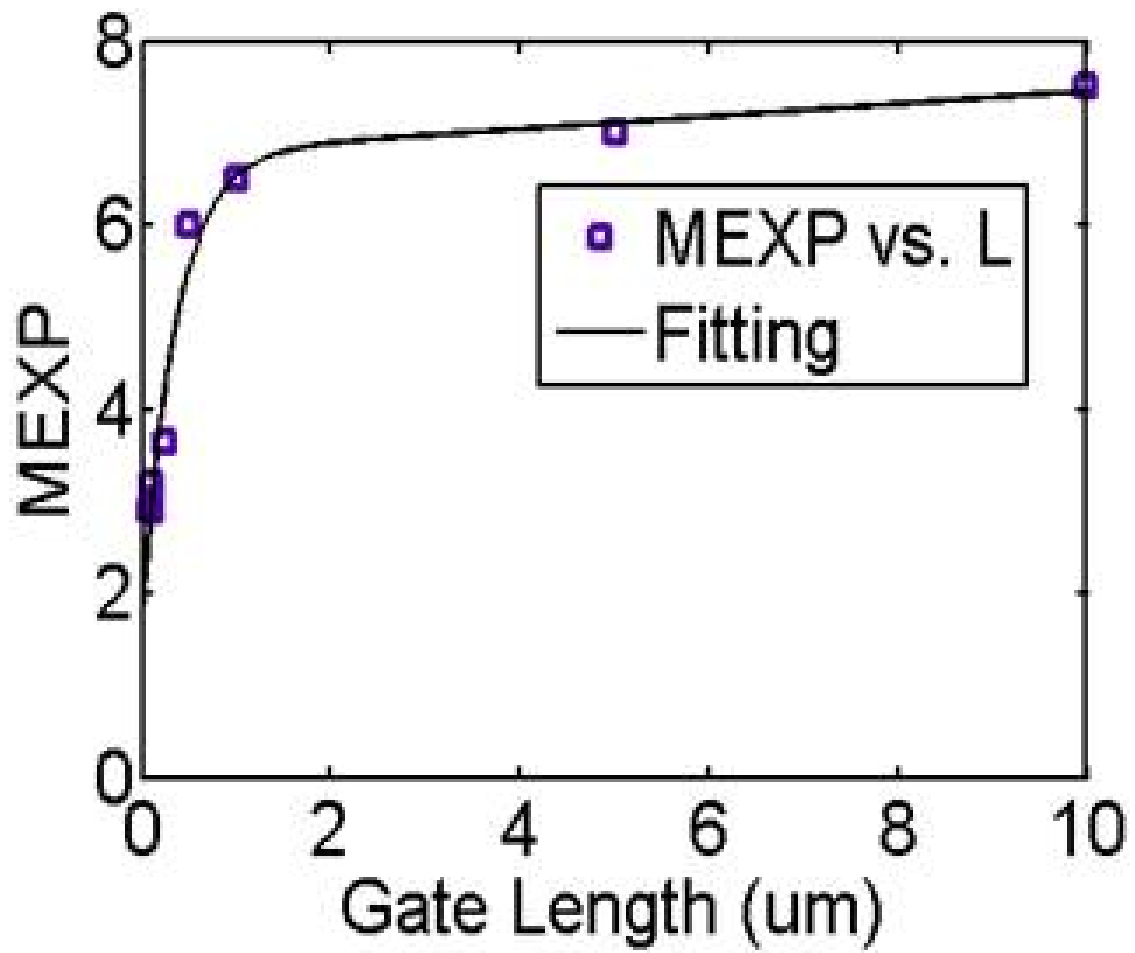


Figure 20: MEXP v.s. L_g

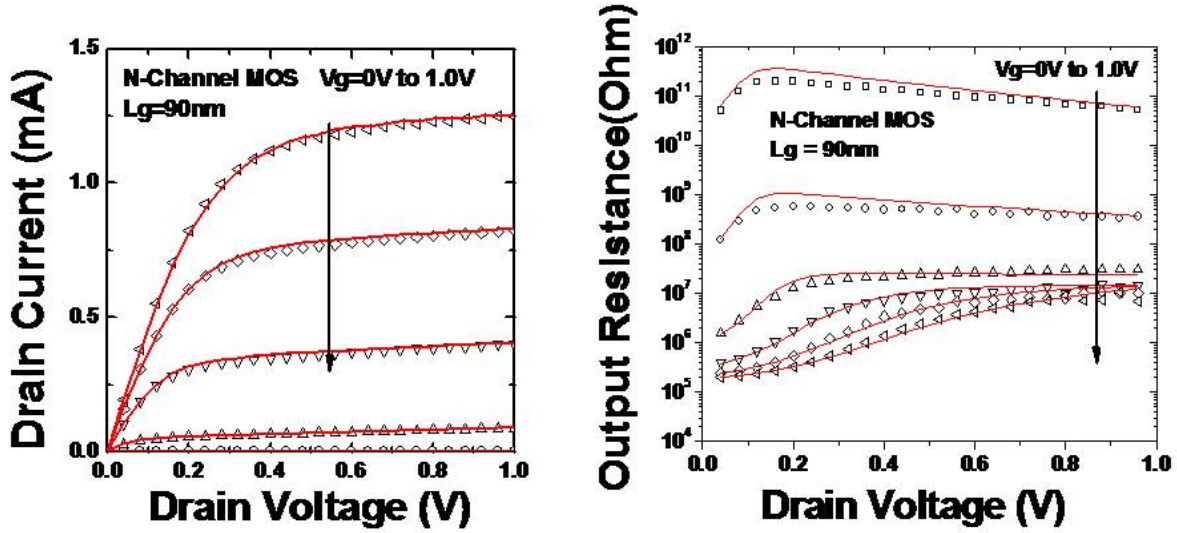


Figure 21: $I_{dv.s}V_d$ and $R_{out}v.s.V_d$

6 Complete Parameter List

6.1 Instance Parameters

Note: Instance parameters with superscript ^(m) are also model parameters

Name	Unit	Default	Min	Max	Description
L ^(m)	m	30n	1n	-	Designed Gate Length
D ^(m)	m	40n	1n	-	Diameter of cylinder (for GEOMOD = 3)
TFIN ^(m)	m	15n	1n	-	Body (fin) thickness
FPICTH ^(m)	m	80n	TFIN	-	Fin Pitch
NF	-	1	1	-	Number of fingers
NFIN ^(m)	-	1	1	-	Number of fins per finger
NGCON ^(m)	-	1	1	2	Number of gate contacts
ASEO ^(m)	m ²	0	0	-	Source to substrate overlap area through oxide (all fingers)

ADEO ^(m)	m^2	0	0	-	Drain to substrate overlap area through oxide (all fingers)
PSEO ^(m)	m	0	0	-	Perimeter of source to substrate overlap region through oxide (all fingers)
PDEO ^(m)	m	0	0	-	Perimeter of drain to substrate overlap region through oxide (all fingers)
ASEJ ^(m)	m^2	0	0	-	Source junction area (all fingers; for bulk MuGFETs, <i>BULKMOD</i> = 1)
ADEJ ^(m)	m^2	0	0	-	Drain junction area (all fingers; for bulk MuGFETs, <i>BULKMOD</i> = 1)
PSEJ ^(m)	m	0	0	-	Source junction perimeter (all fingers; for bulk MuGFETs, <i>BULKMOD</i> = 1)
PDEJ ^(m)	m	0	0	-	Drain junction perimeter (all fingers; for bulk MuGFETs, <i>BULKMOD</i> = 1)
CGSP ^(m)	F	0	0	-	Constant gate to source fringe capacitance (for <i>CGEOMOD</i> = 1)
CGDP ^(m)	F	0	0	-	Constant gate to drain fringe capacitance (for <i>CGEOMOD</i> = 1)
CDSP ^(m)	F	0	0	-	Constant drain to source fringe capacitance (for <i>CGEOMOD</i> = 1)
NRS ^(m)	-	0	0	-	Number of source diffusion squares (for <i>RGEOMOD</i> = 0)
NRD ^(m)	-	0	0	-	Number of drain diffusion squares (for <i>RGEOMOD</i> = 0)
LRSD ^(m)	m	L	0	-	Length of the source/drain

6.2 Model Controllers and Process Parameters

Note: binnable parameters are marked as: ^(b)

Name	Unit	Default	Min	Max	Description
DEVTYPE	-	NMOS	PMOS	NMOS	NMOS=1, PMOS=0

BULKMOD	-	0	0	1	Substrate model selector. 0 = multi-gate on SOI substrate, 1 = multi-gate on bulk substrate.
COREMOD	-	0	0	1	simplified surface potential selector ; 0=turn off, 1=turn on (lightly-doped or undoped)
GEOMOD	-	1	0	3	structure selector; 0 = double gate, 1 = triple gate, 2 = quadruple gate, 3 = cylindrical gate
RDSMOD	-	0	0	1	bias-dependent source/drain resistance model selector (controls <i>si</i> and <i>di</i> nodes); 0 = internal, 1 = external
IGCMOD	-	0	0	1	model selector for <i>Igc</i> , <i>Igs</i> and <i>Igd</i> ; 1=turn on, 0=turn off
IGBMOD	-	0	0	1	model selector for <i>Igb</i> ; 1=turn on, 0=turn off
GIDLMOD	-	0	0	1	GIDL/GISL current switcher; 1=turn on, 0=turn off
IIMOD	-	0	0	2	impact ionization model switch; 0 = OFF, 1 = BSIM4 based, 2 = BSIMSOI based
NQSMOD	-	0	0	1	NQS gate resistor and <i>gi</i> node switcher; 1=turn on, 0=turn off
SHMOD	-	0	0	1	Self-heating and <i>T</i> node switcher; 1=turn on, 0=turn off
RGATEMOD	-	0	0	1	Gate electrode resistor and <i>ge</i> node switcher ; 1=turn on, 0=turn off
RGEOMOD	-	0	0	1	bias independent parasitic resistance model selector (see sec. 3.13)
CGEOMOD	-	0	0	2	parasitic capacitance model selector (see sec. 3.13)
CAPMOD	-	0	0	1	accumulation region capacitance model selector; 0=no accumulation capacitance, 1=accumulation capacitance included
XL	<i>m</i>	0	-	-	L offset for channel length due to mask/etch effect

LINT	m	0.0	-	-	Length reduction parameter (dopant diffusion effect)
LL	$m^{(LLN+1)}$	0.0	-	-	Length reduction parameter (dopant diffusion effect)
LLN	-	1.0	-	-	Length reduction parameter (dopant diffusion effect)
DLC	m	0.0	-	-	Length reduction parameter for CV (dopant diffusion effect)
LLC	$m^{(LLN+1)}$	0.0	-	-	Length reduction parameter for CV (dopant diffusion effect)
DLBIN	m	0.0	-	-	Length reduction parameter for binning
EOT	m	1.0n	0.1n	-	SiO_2 equivalent gate dielectric thickness (including inversion layer thickness)
TOXP	m	1.2n	0.1n	-	Physical oxide thickness
EOTBOX	m	140n	1n	-	SiO_2 equivalent buried oxide thickness (including substrate depletion)
HFIN	m	30n	1n	-	fin height
FECH	-	1.0	0	-	end-channel factor, for different orientation/shape (Mobility difference between the side channel and the top channel is handled by this parameter)
DELTAW	m	0.0	-	-	reduction of effective width due to shape of fin
FECHCV	-	1.0	0	-	CV end-channel factor, for different orientation/shape
DELTAWCV	m	0.0	-	-	CV reduction of effective width due to shape of fin
NBODY ^(b)	m^{-3}	1e22	1e18	5e24	channel (body) doping concentration ²
NSD	m^{-3}	2e26	2e25	1e27	S/D doping concentration
PHIG ^(b)	eV	4.61	0	-	workfunction of gate
EPSROX	-	3.9	1	-	relative dielectric constant of the gate insulator

²Model currently supports $NBODY < 5 \times 10^{24} m^{-3}$. For larger values, we recommend the use of BSIM4 or BSIM4SOI.

EPSRSUB	-	11.9	1	-	relative dielectric constant of the channel material
EASUB	<i>eV</i>	4.05	0	-	electron affinity of the substrate material
NI0SUB	m^{-3}	1.1e16	-	-	intrinsic carrier concentration of channel at 300.15K
BG0SUB	<i>eV</i>	1.12	-	-	band gap of the channel material at 300.15K
NC0SUB	m^{-3}	2.86e25	-	-	conduction band density of states at 300.15K
NGATE ^(b)	m^{-3}	0	-	-	parameter for Poly Gate doping. Set $NGATE = 0$ for metal gates

6.3 Basic Model Parameters

Note: binnable parameters are marked as: ^(b)

Name	Unit	Default	Min	Max	Description
CIT ^(b)	F/m^2	0.0	-	-	parameter for interface trap
CDSC ^(b)	F/m^2	7e-3	0.0	-	coupling capacitance between S/D and channel
CDSCD ^(b)	F/m^2	7e-3	0.0	-	drain-bias sensitivity of CDSC
DVT0 ^(b)	-	0.0	0.0	-	SCE coefficient
DVT1 ^(b)	-	0.60	> 0	-	SCE exponent coefficient
PHIN ^(b)	V	0.05	-	-	nonuniform vertical doping effect on surface potential
ETA0 ^(b)	-	0.60	0.0	-	DIBL coefficient
DSUB ^(b)	-	1.06	> 0	-	DIBL exponent coefficient
K1RSCE ^(b)	$V^{1/2}$	0.0	-	-	prefactor for reverse short channel effect
LPE0 ^(b)	m	5e-9	$-L_{eff}$	-	equivalent length of pocket region at zero bias
DVTSHIFT	V	-	0.0	-	Additional Vth shift handle
QMFACTOR ^(b)	-	0.0	-	-	prefactor for QM V_{th} shift correction
QMTCENIV	-	0.0	-	-	prefactor/switch for QM effective width correction for IV
QMTCENCV	-	0.0	-	-	prefactor/switch for QM effective width and oxide thickness correction for CV
ETAQM	-	0.54	-	-	body-charge coefficient for QM charge centroid
QM0	V	1e-3	> 0	-	normalization parameter for QM charge centroid (inversion)
PQM	-	0.66	-	-	Fitting parameter for QM charge centroid (inversion)
QM0ACC	V	1e-3	> 0	-	normalization parameter for QM charge centroid (accumulation)
PQMACC	-	0.66	-	-	Fitting parameter for QM charge centroid (accumulation)

VSAT ^(b)	<i>m/s</i>	85000	-	-	saturation velocity for the saturation region
VSAT1 ^(b)	<i>m/s</i>	VSAT	-	-	saturation velocity for the linear region
DELTAVSAT ^(b)	-	1.0	0.01	-	velocity saturation parameter in the linear region
KSATIV ^(b)	-	1.0	-	-	parameter for long channel Vdsat
MEXP ^(b)	-	4	2	-	smoothing function factor for Vdsat
PTWG ^(b)	V^{-2}	0.0	-	-	Correction factor for velocity saturation
U0 ^(b)	$m^2/V - s$	3e-2	-	-	low field mobility
ETAMOB ^(b)	-	2.0	-	-	effective field parameter
UP ^(b)	μm^{LPA}	0.0	-	-	mobility L coefficient
LPA	-	1.0	-	-	mobility L power coefficient
UA ^(b)	$(cm/MV)^{EU}$	0.3	> 0.0	-	phonon / surface roughness scattering parameter
EU ^(b)	cm/MV	2.5	> 0.0	-	phonon / surface roughness scattering parameter
UD ^(b)	cm/MV	0.0	> 0.0	-	columbic scattering parameter
UCS ^(b)	-	1.0	> 0.0	-	columbic scattering parameter
PCLM ^(b)	-	0.013	> 0.0	-	Channel Length Modulation (CLM) parameter
PCLMG ^(b)	-	0	-	-	Gate bias dependent parameter for channel Length Modulation (CLM)
VASAT ^(b)	V	0.2	-	-	Channel Length Modulation (CLM) parameter
RDSWMIN	$\Omega - \mu_m^{WR}$	0.0	0.0	-	<i>RDSMOD = 0</i> S/D extension resistance per unit width at high V_{gs}
RDSW ^(b)	$\Omega - \mu_m^{WR}$	100	0.0	-	<i>RDSMOD = 0</i> zero bias S/D extension resistance per unit width
RSWMIN	$\Omega - \mu_m^{WR}$	0.0	0.0	-	<i>RDSMOD = 1</i> source extension resistance per unit width at high V_{gs}
RSW ^(b)	$\Omega - \mu_m^{WR}$	50	0.0	-	<i>RDSMOD = 1</i> zero bias source extension resistance per unit width

RDWMIN	$\Omega - \mu_m^{WR}$	0.0	0.0	-	$RDSMOD = 1$ drain extension resistance per unit width at high V_{gs}
RDW ^(b)	$\Omega - \mu_m^{WR}$	50	0.0	-	$RDSMOD = 1$ zero bias drain extension resistance per unit width
PRWG ^(b)	V^{-1}	0.0	0.0	-	gate bias dependence of S/D extension resistance
WR ^(b)	-	1.0	-	-	W dependence parameter of S/D extension resistance
RGEXT	Ω	0.0	0.0	-	Effective gate electrode external resistance (Experimental)
RGFIN	Ω	1.0e-3	1.0e-3	-	Effective gate electrode resistance per fin per finger
RSHS	Ω	0.0	0.0	-	Source-side sheet resistance
RSHD	Ω	RSHS	0.0	-	Drain-side sheet resistance
PDIBL1 ^(b)	-	1.30	0.0	-	parameter for DIBL effect on Rout
PDIBL2 ^(b)	-	2e-4	0.0	-	parameter for DIBL effect on Rout
DROUT ^(b)	-	1.06	> 0.0	-	L dependence of DIBL effect on Rout
PVAG ^(b)	-	1.0	-	-	V_{gs} dependence on early voltage
AIGBINV ^(b)	$(Fs^2/g)^{0.5}m^{-1}$	1.11e-2	-	-	parameter for Igb in inversion
BIGBINV ^(b)	$(Fs^2/g)^{0.5}m^{-1}V^{-1}$	9.49e-4	-	-	parameter for Igb in inversion
CIGBINV ^(b)	V^{-1}	6.00e-3	-	-	parameter for Igb in inversion
EIGBINV ^(b)	V	1.1	-	-	parameter for Igb in inversion
NIGBINV ^(b)	-	3.0	> 0.0	-	parameter for Igb in inversion
AIGBACC ^(b)	$(Fs^2/g)^{0.5}m^{-1}$	1.36e-2	-	-	parameter for Igb in accumulation
BIGBACC ^(b)	$(Fs^2/g)^{0.5}m^{-1}V^{-1}$	1.71e-3	-	-	parameter for Igb in accumulation
CIGBACC ^(b)	V^{-1}	7.5e-2	-	-	parameter for Igb in accumulation
NIGBACC ^(b)	-	1.0	> 0.0	-	parameter for Igb in accumulation
AIGC ^(b)	$(Fs^2/g)^{0.5}m^{-1}$	1.36e-2	-	-	parameter for Igc in inversion
BIGC ^(b)	$(Fs^2/g)^{0.5}m^{-1}V^{-1}$	1.71e-3	-	-	parameter for Igc in inversion
CIGC ^(b)	V^{-1}	0.075	-	-	parameter for Igc in inversion
NIGC ^(b)	-	1.0	> 0.0	-	parameter for Igc in inversion
PIGCD ^(b)	-	1.0	> 0.0	-	V_{ds} dependence of Igcs and Igcd
DLCIGS	m	0.0	-	-	Delta L for Igs model.

AIGS ^(b)	$(Fs^2/g)^{0.5}m^{-1}$	1.36e-2	-	-	parameter for Igs in inversion
BIGS ^(b)	$(Fs^2/g)^{0.5}m^{-1}V^{-1}$	1.71e-3	-	-	parameter for Igs in inversion
CIGS ^(b)	V^{-1}	0.075	-	-	parameter for Igs in inversion
DLCIGD	m	DLCIGS	-	-	Delta L for Ig model.
AIGD ^(b)	$(Fs^2/g)^{0.5}m^{-1}$	AIGS	-	-	parameter for Ig in inversion
BIGD ^(b)	$(Fs^2/g)^{0.5}m^{-1}V^{-1}$	BIGS	-	-	parameter for Ig in inversion
CIGD ^(b)	V^{-1}	CIGS	-	-	parameter for Ig in inversion
POXEDGE ^(b)	-	1	> 0.0	-	Factor for the gate edge Tox
AGIDL ^(b)	Ω^{-1}	6.055e-12	-	-	pre-exponential coeff. for GIDL
BGIDL ^(b)	V/m	0.3e9	-	-	exponential coeff. for GIDL
CGIDL ^(b)	V^3	0.2	-	-	parameter for body bias effect of GIDL
EGIDL ^(b)	V	0.2	-	-	band bending parameter for GIDL
PGIDL ^(b)	-	1.0	-	-	Exponent of electric field for GIDL
AGISL ^(b)	Ω^{-1}	AIGDL	-	-	pre-exponential coeff for GISL.
BGISL ^(b)	V/m	BGIDL	-	-	exponential coeff. for GISL
CGISL ^(b)	V^3	0.2	-	-	parameter for body bias effect of GISL
EGISL ^(b)	V	EGIDL	-	-	band bending parameter for GISL
PGISL ^(b)	-	1.0	-	-	Exponent of electric field for GISL
ALPHA0 ^(b)	$m \cdot V^{-1}$	0.0	-	-	first parameter of Iii (IIMOD=1)
ALPHA1 ^(b)	V^{-1}	0.0	-	-	L scaling parameter of Iii (IIMOD=1)
BETA0 ^(b)	V^{-1}	0.0	-	-	Vds dependent paramter of Iii (IIMOD=1)
ALPHAI ^(b)	-	0.0	-	-	Pre-exponential constant for Iii (IIMOD=2)
BETAI ^(b)	V^{-1}	0.0	-	-	Vds dependent paramter of Iii (IIMOD=2)
BETAI ^(b)	-	0.0	-	-	Vds dependent paramter of Iii (IIMOD=2)
BETAI ^(b)	V	0.1	-	-	Vds dependent paramter of Iii (IIMOD=2)
ESATII ^(b)	V/m	1.0e7	-	-	Saturation channel E-Field for Iii (IIMOD=2)

LII ^(b)	$V - m$	0.5e-9	-	-	Channel length dependent parameter of Iii (IIMOD=2)
SII0 ^(b)	V^{-1}	0.5	-	-	Vgs dependent paramter of Iii (IIMOD=2)
SII1 ^(b)	-	0.1	-	-	Vgs dependent paramter of Iii (IIMOD=2)
SII2 ^(b)	V	0.0	-	-	Vgs dependent paramter of Iii (IIMOD=2)
SIID ^(b)	V	0.0	-	-	Vds dependent paramter of Iii (IIMOD=2)
EOTACC	m	EOT	0.1n	-	SiO_2 equivalent gate dielectric thickness for accumulation region
DELVFBACC	V	0.0	-	-	Additional V_{fb} shift required for accumulation region
CFS ^(b)	F/m	2.5e-11	0.0	-	source-side outer fringe cap (for CGEOMOD = 0)
CFD ^(b)	F/m	CFS	0.0	-	drain-side outer fringe cap (for CGEOMOD = 0)
CGSO	F/m	calculated	0.0	-	Non LDD region source-gate overlap capacitance per unit channel width (for CGEOMOD = 0, 2)
CGDO	F/m	calculated	0.0	-	Non LDD region drain-gate overlap capacitance per unit channel width (for CGEOMOD = 0, 2)
CGSL ^(b)	F/m	0	0.0	-	Overlap capacitance between gate and lightly-doped source region (for CGEOMOD = 0, 2)
CGDL ^(b)	F/m	CGSL	0.0	-	Overlap capacitance between gate and lightly-doped drain region (for CGEOMOD = 0, 2)
CKAPPAS ^(b)	V	0.6	0.02	-	Coefficient of bias-dependent overlap capacitance for the source side (for CGEOMOD = 0, 2)

CKAPPAD ^(b)	V	CKAPPAS	0.02	-	Coefficient of bias-dependent overlap capacitance for the drain side (for $CGEOMOD = 0, 2$)
CGBO	F/m	0	0.0	-	Gate-substrate overlap capacitance per unit channel length
CSDESW	F/m	0	0.0	-	Source/drain sidewall fringing capacitance per unit length
COVS ^(b)	F/m	2.5e-11	0.0	-	Constant gate-to-source overlap cap (for $CGEOMOD = 1$)
COVD ^(b)	F/m	COVS	0.0	-	Constant gate-to-drain overlap cap (for $CGEOMOD = 1$)
CJS	F/m^2	0.0005	0.0	-	Unit area source-side junction capacitance at zero bias
CJD	F/m^2	CJS	0.0	-	Unit area drain-side junction capacitance at zero bias
CJSWS	F/m	5.0e-10	0.0	-	Unit length sidewall junction capacitance at zero bias (source-side)
CJSWD	F/m	CJSWS	0.0	-	Unit length sidewall junction capacitance at zero bias (drain-side)
CJSWGS	F/m	0.0	0.0	-	Unit length gate sidewall junction capacitance at zero bias (source-side)
CJSWGD	F/m	CJSWGS	0.0	-	Unit length gate sidewall junction capacitance at zero bias (drain-side)
PBS	V	1.0	0.01	-	Bottom junction built-in potential (source-side)
PBD	V	PBS	0.01	-	Bottom junction built-in potential (drain-side)
PBSWS	V	1.0	0.01	-	Isolation-edge sidewall junction built-in potential (source-side)
PBSWD	V	PBSWS	0.01	-	Isolation-edge sidewall junction built-in potential (drain-side)
PBSWGS	V	PBSWS	0.01	-	Gate-edge sidewall junction built-in potential (source-side)

PBSWGD	V	PBSWGS	0.01	-	Gate-edge sidewall junction built-in potential (drain-side)
MJS	—	0.5	-	-	Source bottom junction capacitance grading coefficient
MJD	—	MJS	-	-	Drain bottom junction capacitance grading coefficient
MJSWS	—	0.33	-	-	Isolation-edge sidewall junction capacitance grading coefficient (source-side)
MJSWD	—	MJSWS	-	-	Isolation-edge sidewall junction capacitance grading coefficient (drain-side)
MJSWGS	—	MJSWS	-	-	Gate-edge sidewall junction capacitance grading coefficient (source-side)
MJSWGD	—	MJSWGS	-	-	Gate-edge sidewall junction capacitance grading coefficient (drain-side)
SJS	—	0.0	0.0	-	Constant for source-side two-step second junction capacitance
SJD	—	SJS	0.0	-	Constant for drain-side two-step second junction capacitance
SJSWS	—	0.0	0.0	-	Constant for sidewall two-step second junction capacitance (source-side)
SJSWD	—	SJSWS	0.0	-	Constant for sidewall two-step second junction capacitance (drain-side)
SJSWGS	—	0.0	0.0	-	Constant for gate sidewall two-step second junction capacitance (source-side)
SJSWGD	—	SJSWGS	0.0	-	Constant for gate sidewall two-step second junction capacitance (drain-side)
MJS2	—	0.125	-	-	Source bottom two-step second junction capacitance grading coefficient
MJD2	—	MJS2	-	-	Drain bottom two-step second junction capacitance grading coefficient
MJSWS2	—	0.083	-	-	Isolation-edge sidewall two-step second junction capacitance grading coefficient (source-side)

MJSWD2	-	MJSWS2	-	-	Isolation-edge sidewall two-step second junction capacitance grading coefficient (drain-side)
MJSWGS2	-	MJSWS2	-	-	Gate-edge sidewall two-step second junction capacitance grading coefficient (source-side)
MJSWGD2	-	MJSWGS2	-	-	Gate-edge sidewall two-step second junction capacitance grading coefficient (drain-side)
JSS	A/m^2	1.0e-4	0.0	-	Bottom source junction reverse saturation current density
JSD	A/m^2	JSS	0.0	-	Bottom drain junction reverse saturation current density
JSWS	A/m	0	0.0	-	Unit length reverse saturation current for isolation-edge source sidewall junction
JSWD	A/m	JSWS	0.0	-	Unit length reverse saturation current for isolation-edge drain sidewall junction
JSWGS	A/m	0	0.0	-	Unit length reverse saturation current for gate-edge source sidewall junction
JSWGD	A/m	JSWGS	0.0	-	Unit length reverse saturation current for gate-edge drain sidewall junction
NJS	-	1.0	0.0	-	Source junction emission coefficient
NJD	-	NJS	0.0	-	Drain junction emission coefficient
IJTHSFWD	A	0.1	$10I_{sbs}$	-	Forward source diode breakdown limiting current
IJTHDFWD	A	IJTHSFWD	$10I_{sbd}$	-	Forward drain diode breakdown limiting current
IJTHSREV	A	0.1	$10I_{sbs}$	-	Reverse source diode breakdown limiting current
IJTHDREV	A	IJTHSREV	$10I_{sbd}$	-	Reverse drain diode breakdown limiting current

BVS	V	10.0	-	-	Source diode breakdown voltage
BVD	V	BVS	-	-	Drain diode breakdown voltage
XJBVS	-	1.0	-	-	Fitting parameter for source diode breakdown current
XJBVD	-	XJBVS	-	-	Fitting parameter for source diode breakdown current
LINTIGEN	m	0.0	-	$L_{eff}/2$	L_{int} offset for R/G current
NTGEN ^(b)	-	1.0	> 0.0	-	parameter for R/G current (Experimental)
AIGEN ^(b)	$m^{-3}V^{-1}$	0.0	-	-	parameter for R/G current (Experimental)
BIGEN ^(b)	$m^{-3}V^{-3}$	0.0	-	-	parameter for R/G current (Experimental)
XRCRG1 ^(b)	-	12.0	0.0 or $\geq 10^{-3}$	-	parameter for non quasi-static gate resistance (NQSMOD=1) and NQSMOD=2
XRCRG2 ^(b)	-	1.0	-	-	parameter for non quasi-static gate resistance (NQSMOD=1) and NQSMOD=2
NSEG	-	5	4	10	Number of channel segments for NQSMOD=3
EF	-	1.0	> 0.0	2.0	Flicker noise frequency exponent
LINTNOI	m	0.0	-	$L_{eff}/2$	L_{int} offset for flicker noise calculation
EM	V/m	4.1e7	-	-	Flicker noise parameter
NOIA	$eV^{-1}s^{1-EF}m^{-3}$	6.250e39	-	-	Flicker noise parameter
NOIB	$eV^{-1}s^{1-EF}m^{-1}$	3.125e24	-	-	Flicker noise parameter
NOIC	$eV^{-1}s^{1-EF}m$	8.750e7	-	-	Flicker noise parameter
NTNOI	-	1.0	0.0	-	Thermal noise parameter

6.4 Parameters for geometry-dependent parasitics

The parameters listed in this section are for RGEOMOD=1 and CGEOMOD=2.

Name	Unit	Default	Min	Max	Description
HEPI	m	10n	-	-	Height of the raised source/drain on top of the fin
TSILI	m	10n	-	-	Thickness of the silicide on top of the raised source/drain
RHOC	$\Omega - m^2$	1p	10^{-18}	10^{-9}	Contact resistivity at the silicon/silicide interface
RHORSD	$\Omega - m$	calculated	0	-	Average resistivity of silicon in the raised source/drain region
RHOEXT	$\Omega - m$	RHORSD	0	-	Average resistivity of silicon in the fin extension region
CRATIO	-	0.5	0	1	Ratio of the corner area filled with silicon to the total corner area
DELTAPRSD	m	0.0	- FPITCH	-	Change in silicon/silicide interface length due to non-rectangular epi
SDTERM	-	0	0	1	Indicator of whether the source/drain are terminated with silicide
LSP	m	0.2(L+XL)	0	-	Thickness of the gate sidewall spacer
LDG	m	5n	0	-	Lateral diffusion gradient in the fin extension region
EPSRSP	-	3.9	1	-	Relative dielectric constant of the gate sidewall spacer material
TGATE	m	30n	0	-	Gate height on top of the hard mask
TMASK	m	30n	0	-	Height of the hard mask on top of the fin
ASILIEND	m^2	0	0	-	Extra silicide cross sectional area at the two ends of the FinFET
ARSDEND	m^2	0	0	-	Extra raised source/drain cross sectional area at the two ends of the FinFET
PRSDEND	m	0	0	-	Extra silicon/silicide interface perimeter at the two ends of the FinFET

NSDE	m^{-3}	2×10^{25}	10^{25}	10^{26}	Active doping concentration at the channel edge
RGEOA	-	1.0	-	-	Fitting parameter for RGEOMOD=1
RGEOB	m^{-1}	0	-	-	Fitting parameter for RGEOMOD=1
RGEOC	m^{-1}	0	-	-	Fitting parameter for RGEOMOD=1
RGEOD	m^{-1}	0	-	-	Fitting parameter for RGEOMOD=1
RGEOE	m^{-1}	0	-	-	Fitting parameter for RGEOMOD=1
CGEOA	-	1.0	-	-	Fitting parameter for CGEOMOD=2
CGEOB	m^{-1}	0	-	-	Fitting parameter for CGEOMOD=2
CGEOC	m^{-1}	0	-	-	Fitting parameter for CGEOMOD=2
CGEOD	m^{-1}	0	-	-	Fitting parameter for CGEOMOD=2
CGEOE	-	1.0	-	-	Fitting parameter for CGEOMOD=2

6.5 Parameters for Temperature Dependence and Self-heating

Note: binnable parameters are marked as: ^(b)

Name	Unit	Default	Min	Max	Description
TNOM	C	27	0.0	-	Temperature at which the model is extracted (in Celcius)
TBGASUB	eV/K	7.02e-4	-	-	Bandgap Temperature Coefficient
TBGBSUB	K	1108.0	-	-	Bandgap Temperature Coefficient
KT1	V	0.0	-	-	V_{th} Temperature Coefficient
KT1L	$V \cdot m$	0.0	-	-	V_{th} Temperature Coefficient
UTE ^(b)	-	0.0	-	-	Mobility Temperature Coefficient
UTL ^(b)	-	-1.5e-3	-	-	Mobility Temperature Coefficient
UA1 ^(b)	-	1.032e-3	-	-	Mobility Temperature Coefficient
UD1 ^(b)	-	0.0	-	-	Mobility Temperature Coefficient
UCSTE ^(b)	-	-4.775e-3	-	-	Mobility Temperature Coefficient
AT ^(b)	$1/K$	-0.00156	-	-	Saturation Velocity Temperature Coefficient
TMEXP ^(b)	$1/K$	0	-	-	Temperature Coefficient for V_{dseff} smoothing
PTWGT ^(b)	$1/K$	0.004	-	-	PTWG Temperature Coefficient
PRT ^(b)	-	0.001	-	-	Series Resistance Temperature Coefficient
IIT ^(b)	-	-0.5	-	-	Impact Ionization Temperature Coefficient (IIMOD=1)
TII ^(b)	-	0.0	-	-	Impact Ionization Temperature Coefficient (IIMOD=2)
TGIDL ^(b)	$1/K$	-0.003	-	-	GISL/GIDL Temperature Coefficient
IGT ^(b)	-	2.5	-	-	Gate Current Temperature Coefficient
TCJ	$1/K$	0.0	-	-	Temperature coefficient for CJS/CJD
TCJSW	$1/K$	0.0	-	-	Temperature coefficient for CJSWS/CJSWD
TCJSWG	$1/K$	0.0	-	-	Temperature coefficient for CJSWGS/CJSWGD
TPB	$1/K$	0.0	-	-	Temperature coefficient for PBS/PBD

TPBSW	$1/K$	0.0	-	-	Temperature coefficient for PB-SWS/PBSWD
TPBSWG	$1/K$	0.0	-	-	Temperature coefficient for PB-SWGS/PBSWGD
XTIS	-	3.0	-	-	Source junction current temperature exponent
XTID	-	XTIS	-	-	Drain junction current temperature exponent
RTH0	Ω	0.01	0.0	-	Thermal resistance for self-heating calculation
CTH0	F	1.0e-5	0.0	-	Thermal capacitance for self-heating calculation
WTH0	m	0.0	0.0	-	Width-dependence coefficient for self-heating calculation

6.6 Parameters for Variability Modeling

A set of parameters causing variability in device behavior are identified. Users can associate appropriate variability function as appropriate. The list is open to modification with users feedbacks and suggestions. Other than DTEMP, DELVTRAND, UOMULT and IDS0MULT, the parameters listed here were already introduced previously as either instance parameters or model parameters. All of the following parameters should be elevated to instance parameter status if required for variability modeling or should be delegated to a model parameter status (unless introduced before as an instance parameter). **Note: parameters already introduced as instance parameters are marked: (i) and model parameters are marked: $(model)$**

Name	Unit	Default	Min	Max	Description
DELVTRAND	V	0.0	-	-	Threshold voltage shift handle
U0MULT	-	1.0	-	-	Multiplier to mobility (or more precisely divides D_{mob}, D_{mobs})
IDS0MULT	-	1.0	-	-	Multiplier to source-drain channel current
DTEMP	K	0.0	-	-	Temperature shift handle
TFIN (i)	m	15n	1n	-	Body (fin) thickness
FPICTH (i)	m	80n	TFIN	-	Fin Pitch
XL (mod)	m	0	-	-	L offset for channel length due to mask/etch effect
NBODY (mod)	m^{-3}	1e22	1e18	5e24	channel (body) doping concentration
EOT (mod)	m	1.0n	0.1n	-	SiO_2 equivalent gate dielectric thickness (including inversion layer thickness)
TOXP (mod)	m	1.2n	0.1n	-	Physical oxide thickness
RSHS (mod)	Ω	0.0	0.0	-	Source-side sheet resistance
RSHD (mod)	Ω	RSHS	0.0	-	Drain-side sheet resistance
RHOC (mod)	$\Omega - m^2$	1p	10^{-18}	10^{-9}	Contact resistivity at the silicon/silicide interface
RHORSD (mod)	$\Omega - m$	calculated	0	-	Average resistivity of silicon in the raised source/drain region
RHOEXT (mod)	$\Omega - m$	RHORSD	0	-	Average resistivity of silicon in the fin extension region

7 History of BSIM-MG Models

October, 2006 BSIM-CMG 1.0 alpha version released.

August, 2007 BSIM-CMG 1.0 released.

January 2008 BSIM-CMG 1.0.1 released with several bug fixes compared with BSIM-CMG1.0.

March, 2008 BSIM-IMG 1.0 alpha version released.

November 2008 BSIM-CMG 1.1.0 alpha version released. Temperature effects, noise models (flicker noise, thermal noise and shot noise), junction current, intrinsic input resistance (R_{ii}) are added. Both $RDSMOD = 0$ and $RDSMOD = 1$ in BSIM4 are now supported in BSIM-CMG. $MOBMOD = 0$ (based on BSIM4[10]) is added and set as the default mobility model.

May 2009 BSIM-CMG 102.0 released. This release is essentially the official release of 1.1.0 alpha. $Gmin$ ³ is added for improved convergence.

Oct 2009 BSIM-CMG 103.0 released. This release now supports a Cylindrical gate geometry through $GEOMOD = 3$ with an associated short channel scale length and quantum effects model. The existing I-V have been enhanced to model Poly-depletion accurately. Self-heating is now supported with addition of a Temperature node. Junction Capacitance and Junction Current equations were revamped with source-drain asymmetry supported. The asymmetry is now also in GIDL/GISL currents. Length dependent equations have been added for a Global Parameter Extraction without binning. SHMOD, RGATEMOD, NQSMOD and RDSMOD also control the number of internal nodes for faster simulations. Many bug-fixes were implemented too.

Feb 2010 BSIM-CMG 104.0 released. A new channel length modulation model adopted from BSIM4 is added. This release also supports the impact ionization model similar to one in BSIMSOI. NRS/NRD parameter and its associated equations have been added. $Gmin$ implementation has been removed with consensus among various EDA vendors. The suggested value for simulator side $Gmin$ (between source/drain to body node) is 1E-18 S. Lots of bug-fixes were implemented too.

November, 2010 BSIM-IMG 101.0 alpha version released.

³A very large resistor between the bulk node and the intrinsic source/drain node.

References

- [1] M. V. Dunga, C.-H. Lin, D. D. Lu, W. Xiong, C. R. Cleavelin, P. Patruno, J.-R. Huang, F.-L. Yang, A. M. Niknejad, and C. Hu, “BSIM-MG: A Versatile Multi-Gate FET Model for Mixed-Signal Design,” in *2007 Symposium on VLSI Technology*, 2007.
- [2] D. Lu, M. V. Dunga, C.-H. Lin, A. M. Niknejad, and C. Hu, “A multi-gate MOSFET compact model featuring independent-gate operation,” in *IEDM Technical Digest*, 2007, p. 565.
- [3] Y. Cheng and C. Hu, *MOSFET Modeling and BSIM3 User’s Guide*. Kluwer Academic Publishers, 1999.
- [4] M. V. Dunga, *Ph.D. Dissertation: Nanoscale CMOS Modeling*. UC Berkeley, 2007.
- [5] A. S. Householder, *The Numerical Treatment of a Single Nonlinear Equation*. McGraw-Hill, New York, 1970.
- [6] X. Gourdon and P. Sebah, *Newton’s method and high order iterations*. [Online]. Available: <http://numbers.computation.free.fr/Constants/constants.html>
- [7] J. He, J. Xi, M. Chan, H. Wan, M. Dunga, B. Heydari, A. M. Niknejad, and C. Hu, “Charge-Based Core and the Model Architecture of BSIM5,” in *International Symposium on Quality Electronic Design*, 2005, pp. 96–101.
- [8] *BSIM5.0.0 MOSFET Model*, BSIM Group, The Regents of the University of California, February 2005.
- [9] S. Venugopalan, “A Compact Model of Cylindrical Gate MOSFET for Circuit Simulations,” *UC Berkeley Master’s Report*, december 2009.
- [10] *BSIM Models*. Department of Electrical Engineering and Computer Science, UC Berkeley. [Online]. Available: <http://www-device.eecs.berkeley.edu/~bsim3/>
- [11] G. Masetti, M. Severi, and S. Solmi, “Modeling of Carrier Mobility Against Carrier Concentration in Arsenic-, Phosphorus-, and Boron-Doped Silicon,” *IEEE Transaction on Electron Devices*, vol. 30, no. 7, pp. 764–769, july 1983.
- [12] H. H. Berger, “Model for contacts to planar devices,” *Solid-State Electronics*, vol. 15, pp. 145–158, 1972.

- [13] *BSIM-SOI Model*. University of California, Berkeley. [Online]. Available: <http://www-device.eecs.berkeley.edu/~bsimsoi/>
- [14] W.-M. Lin, F. Li, D. D. Lu, A. M. Niknejad, and C. Hu, “A Compact Fringe Capacitance Model for FinFETs,” unpublished.
- [15] X. Jin, J.-J. Ou, C.-H. Chen, W. Liu, M. J. Deen, P. R. Gray, and C. Hu, “An Effective Gate Resistance Model for CMOS RF and Noise Modeling,” in *IEDM Technical Digest*, 1998, p. 961.
- [16] *BSIM Models*. Department of Electrical Engineering and Computer Science, UC Berkeley. [Online]. Available: <http://www-device.eecs.berkeley.edu/~bsim3/bsim4/>
- [17] M. Chan, K. Y. Hui, C. Hu, and P. K. Ko, “A robust and physical BSIM3 non-quasi-static transient and AC small-signal model for circuit simulation,” *IEEE Transaction on Electron Devices*, vol. 45, no. 4, pp. 834–841, April 1998.
- [18] S. Yao, T. H. Morshed, D. D. Lu, S. Venugopalan, W. Xiong, C. R. Cleavelin, A. M. Niknejad, and C. Hu, “A Global Parameter Extraction Procedure for Multi-gate MOSFETs,” in *International Conference on Microelectronic Test Structures*, Mar. 2010, pp. 194–197.

Acknowledgments

We deeply appreciate the feedback we received from (in alphabetical order by last name):

Brian Chen (Accelicon)
Wei-Hung Chen (UC Berkeley)
Jung-Suk Goo (GlobalFoundries)
Keith Green (TI)
Ben Gu (Freescale)
Wilfried Haensch (IBM)
Min-Chie Jeng (TSMC)
Yeung Gil Kim (Proplus Solutions)
Wai-Kit Lee (TSMC)
Dayong Li (Cadence)
Hancheng Liang (Proplus Solutions)
Sally Liu (TSMC)
Weidong Liu (Synopsys)
James Ma (Proplus Solutions)
Colin C. McAndrew (Freescale)
Slobodan Mijalkovic (Silvaco)
Andrei Pashkovich (Silvaco)
S. C. Song (Qualcomm)
Ke-wei Su (TSMC)
Niraj Subba (GlobalFoundries)
Charly Sun (Synopsys)
Sushant Suryagandh (GlobalFoundries)
Lawrence Wagner (IBM)

Joddy Wang (Synopsys)

Qingxue Wang (Synopsys)

Josef Watts (IBM)

Richard Williams (IBM)

Dehuang Wu (Synopsys)

Jane Xi (Synopsys)

Jushan Xie (Cadence)

Wade Xiong (TI)

Wenwei Yang (Proplus Solutions)

Fulong Zhao (Cadence)

Manual created: March 13, 2012